SUSTAINABLE WATER SOLUTIONS: EVALUATING WATER PRACTICES AND WATERMELON RIND-MEDIATED Ag/TiO_2 NANOCOMPOSITE MODIFIED SOLAR DISINFECTION EFFICACY IN OBUNGA SLUM, KISUMU COUNTY

GATHIRU MARYLYN MUGURE

I56/37610/2017

A THESIS SUBMITTED IN PARTIAL FULFILMENT OF THE REQUIREMENTS FOR THE AWARD OF THE DEGREE OF MASTER OF SCIENCE (APPLIED ANALYTICAL CHEMISTRY) IN THE SCHOOL OF PURE AND APPLIED SCIENCES, KENYATTA UNIVERSITY

NOVEMBER, 2024

DECLARATION

This thesis is my original work and has not been presented for a degree or award in any other institutions of higher learning.

Signature ..... Date...17th November...2024

Gathiru Marylyn Mugure

Supervisors

This thesis has been submitted with our approval as University supervisors

Signature ..... Date...18.11.2024

Dr. Eric Masika
Department of Chemistry,
Kenyatta University

Signature ..... Date...18:11:2024

Prof. Naumih Noah
School of Pharmacy and Health Sciences,
United States International University-Africa

Signature ..... Date.17th November 2024

Prof. Emilly Obuya
Faculty of Chemistry and Biochemistry
Russell Sage College

DEDICATION

I dedicate this work to my parents, Josphat and Irene Gathiru, and siblings, James and JoyGrace Gathiru. Their love and support have motivated me throughout this journey.

ACKNOWLEDGEMENTS

First and foremost, I would like to thank God for His grace, mercies, and provision throughout this journey. His favour has brought me people of kind words and great actions. In line with this, I would like to acknowledge my family, especially my parents, Irene Gathiru and Josphat Gathiru, for their prayers and words of encouragement. I am immensely grateful for my supervisors: Dr. Eric Masika, Prof. Naumih Noah, and Prof Emilly Obuya. Their patience, encouragement, guidance, support, and understanding have inspired me. I notably thank Prof Anastasiah Ngigi for her mentorship, training, inspiration, and support. My special thanks to Mr Anthony Mwangi of the National Phytotherapeutics Research Centre at Kenyatta University for his invaluable training on UV-Vis, FTIR, and XRF characterization. I also wish to thank Dr Sharon Kiprotich of the Department of Physical and Biological Sciences at Murang'a University for her guidance with XRD characterization analysis. Finally, I express my special gratitude to Mr. James Gathiru and Mr Simon Mburu for their guidance and unconditional assistance. To everyone whose name I have not highlighted, your help is highly appreciated.

TABLE OF CONTENTS

LIST OF FIGURES

LIST OF TABLES

ABBREVIATIONS AND ACRONYMS

Ag	Silver
Ag/TiO_2	Silver/ Titanium dioxide
BPA	Bisphenol A
EDS	Energy dispersive spectroscopy
FTIR	Fourier Transform Infrared Spectroscopy
$NaBH_4$	Sodium borohydride
PET	Polyethylene terephthalate
POU	Point-of-use
SEM	Scanning electron microscopy
SODIS	Solar disinfection
TEM	Transmission electron microscopy
TiO_2	Titanium dioxide
WMRE	Watermelon rind extract
XRD	X-ray diffraction spectroscopy
XRF	X-ray fluorescence spectroscopy

ABSTRACT

Approximately 2 billion people worldwide lack access to safe drinking water, leading to 4 billion reported waterborne diarrheal diseases annually. The situation in Obunga slum, located in Kisumu County, with its poor sanitation standards and lack of safe water, highlights the urgent need for a sustainable scientific water treatment solution. Solar disinfection (SODIS) of water, a point-of-use water treatment method that utilizes ultraviolet (UV) radiation and the thermal effects of solar radiation to kill pathogens, is a potential solution. However, its efficiency is influenced by weather conditions. The incorporation of a visible light active photocatalyst has been proposed to enhance its efficiency. This visible light active photocatalyst was synthesized using a green synthesis method, using *Citrullus lanatus* (watermelon) rind extract (WMRE). This research, with its potential to significantly improve water treatment, aimed to evaluate the water and sanitation practices of Obunga slum residents, validate the application of SODIS in the slum, and increase the effectiveness of SODIS by incorporating WMRE-synthesized silver/ titanium dioxide (Ag/TiO_2) nanocomposite. The water and sanitation survey was done using structured questionnaires randomly administered to individual household heads; SODIS was performed on common ground sources within Obunga slum; synthesis of Ag/TiO_2 nanocomposite followed, and the effectiveness of SODIS modified with Ag/TiO_2 nanocomposite was analysed. The green synthesis of Ag/TiO_2 nanocomposite was done using WMRE, and the operating conditions were optimized, while the control synthesis was done using sodium borohydride ($NaBH_4$). The Ag/TiO_2 nanocomposite powders were coated on 3-4 mm glass beads and incorporated into SODIS, and effectiveness was assessed. The water and sanitation survey revealed that all Obunga slum residents lacked access to improved sanitation facilities, which demands immediate attention and action. Only 34.65% were accessing safe water sources, highlighting the pressing need for improved sanitation. SODIS for the recommended 6 hours resulted in > 99.99% kill rate for *E. coli* bacteria and only 82.36% kill rate for non-*E. coli* coliform bacteria, supporting the need to incorporate a visible light-active photocatalyst. Synthesis of Ag/TiO_2 using WMRE was optimal at a reaction time of 45 minutes, temperature of 100 ℃, and pH 12 and yielded spherical Ag nanoparticles with an average diameter of 7.48 nm ± 4.06 nm modified on the surface of TiO_2 nanoparticles, yielding improved Ag nanoparticles monodispersity. An absorption peak displayed the visible light activity of WMRE-synthesized Ag/TiO_2 at 425 nm and was comparable to the control's. SODIS modified with Ag/TiO_2 nanocomposite resulted in a > 99.99% *E. coli* and coliform bacteria kill rate statistically similar to the > 99.98% kill rate achieved when treatment was performed without modification, indicating no improved effectiveness upon modification. Ag/TiO_2 nanocomposite is a widely studied and utilized anti-microbial agent; this lack of enhanced efficiency was attributed to an interaction error between the glass beads and contaminated water. Despite the lack of significant improvement in SODIS, the assessment of the water and sanitation standards of Obunga slum and the successful synthesis of visible light active Ag/TiO_2 nanocomposite using WMRE provide hope for the future of water treatment.

CHAPTER ONE: INTRODUCTION

1.1 Background of the study

Access to water is a human right. Article I.1 of the General Comment No. 15 implemented by the Commission on Economic, Social and Cultural Rights in November 2002 states, "The human right to water is indispensable for leading a life in human dignity. It is a prerequisite for the realization of other human rights" (Oliveira, 2017). This right to accessing water was defined as everyone's right to "sufficient, safe, physically accessible and affordable water; for personal and domestic uses" (Arun and Ashok, 2016).

The 2030 Sustainable Development Goal (SDG) 6 aims to have the entire global population access to water and sanitation. However, third-world countries have lagged due to the cost of safe water access and improved sanitation. Furthermore, the COVID-19 pandemic and consequent financial stresses have stalled progress toward achieving this goal. In 2020, only 74% of the global population accessed safe drinking water, leaving 2 billion people lacking safe water. Therefore, it is estimated that by 2030, 1.6 billion people will still be without access to safe water. In the same year, only 54% of the global population had access to improved sanitation services, leaving 3.5 billion people lacking access to safely managed sanitation. It is, therefore, estimated that by the year 2030, 2.8 billion people will still be without access to improved sanitation (ONU, 2022).

Progress towards meeting the SDGs is slower in developing countries. These countries failed to achieve the Millennium Development Goals (MDG) 7 for water and sanitation. This goal aimed to ensure that at least half of the population had access to safe water and

improved sanitation, serving as a foundation for the Sustainable Development Goals (SDGs) (Satterthwaite, 2016). In Kenya, only 68.6% of residents have access to safe water, and 59.3% access safely managed sanitation services. This marks less than 50% of the progress towards the entire population's access to safe water and improved sanitation by 2030. Furthermore, this progress rate has been categorized as stagnant by the SDG report for the year 2022 and is indicative of an expected failure to meet this goal (GoK, 2019; ONU, 2022).

The source and storage determine the safety of drinking water. Water sources are categorized either as improved or unimproved. Improved water sources are characterized by construction and design that guarantees the safety of delivered water and include household connections, protected springs, boreholes, public standpipes, and controlled rainwater collection. Unimproved water sources, therefore, do not guarantee the safety of delivered water and include unprotected wells and springs, surface water, and vendor-supplied water (JMP for Water Supply Sanitation and Hygiene, 2018). Poor water handling after delivery can result in contamination; therefore, user behaviour is essential to ensuring water safety. Proper water storage involves the usage of clean containers having a single outlet, a fitted lid, and easy handling (Slavik *et al*., 2020).

Sanitation standards are judged based on the protection and improvement of the health and well-being of people. Sanitation has various aspects: management of solid waste, safe collection, storage and treatment of human excreta, drainage of storm water, disposal and treatment of sewage effluents, and management of industrial and hazardous waste (Letema

et al., 2014). Improved sanitation requires that all these aspects are fulfilled. Where one or more of these aspects is not met, a risk is created to the health and well-being of people and is therefore considered unimproved sanitation (JMP for Water Supply Sanitation and Hygiene, 2018).

Poor sanitation standards risk drinking water's safety and determine a community's quality of life. As a result of poor sanitation standards, 5 out of 10 people in developing countries are exposed to sanitation-related diseases, resulting in 828,651 annual deaths (UNICEF and WHO, 2020). Improved sanitation would break the cycle of diseases, enhancing the quality of life. Various initiatives have therefore been undertaken to improve the standards of life worldwide. The World Bank's Independent Evaluation Group found that good hand-washing practices, proper sanitation, and water treatment at the point of use (POU) resulted in a decrease in disease occurrence (Venis, 2023).

The creation and growth of slums increase the general population of people whose quality of life is poor. According to the UN-HABITAT, a slum is "an area with a dense population per household and lacking sufficient living space, durable housing, easy access to safe drinking water, proper sanitation and security of tenancy" (UN-HABITAT, 2018). The creation and growth of slums are attributed to the continued rise in the cost of living, resulting in rural-urban migration (Simiyu, 2016). In the year 2020, 1 billion of the global population lived in slums, with a majority of this population being in Central, Eastern, Southern and South-Eastern Asia and sub-Saharan Africa (ONU, 2022).

Urban cities, even when well-planned, are challenged by the growth of slum areas. This growth results from the overwhelming and unexpected increase in population, which exceeds already established and sustainable plans to provide amenities in these cities. All Kenyan cities have been recorded as having informal settlements. Kisumu City, a lakeside town, has been challenged by the creation and growth of slums. Obunga, Nyalenda, Bandani, Kaloleni, Manyatta, and Kibos slums have been studied and documented in Kisumu city (Maoulidi, 2010).

Obunga slum meets all the requirements for an area to be considered a slum, with residents lacking access to most if not all, social amenities and having no education and medical facilities. Their living setup involves congested buildings made from mud and old metallic sheets. Their major sources of water are standing pipes shared within homes, unprotected springs and wells, water vendors, and kiosks supplied either by Kisumu Water and Sanitation Company Limited (KIWASCO) or other projects (Ananga, 2015). Their economic activities are low ranging, with a monthly income ranging between 10,000-15,000 Ksh, and include running small kiosks selling second-hand clothes, fish, charcoal, vegetables, and ready-made food. Obunga residents are not well educated, with their highest formal education level being high school (Herman, 2017).

The slum is characterized by very poor sanitation standards, with sewer lines often bursting and left to flow openly, sometimes reaching the residents' doorsteps. Further, about 40% of the residents lack access to proper latrines, with some opting to defecate in the open. Kisumu County Government, which is mandated to offer waste solutions to

Kisumu city residents, does not do so for this slum, and the residents, therefore, have to dispose of domestic waste in the open (Gerryshom, 2015).

Poor sanitation conditions challenge the quality of safe water sources in Obunga slum. For the few Obunga residents with access to tap water, faecal contamination challenges their water quality. This faecal contamination results from the proximity of pit latrines to water sources and the vandalization of tap water pipes, which exposes them to the open sewer system (Maoulidi, 2010). Use and awareness of the need for POU water treatment methods are indispensable for improving the residents' quality of life. Solutions to clean water from all sources should be offered with significant consideration for the financial constraints experienced by Obunga slum residents (Gerryshom, 2015).

Solar disinfection (SODIS) of water is a naturally occurring process and can be harnessed for household use. This water treatment method is simple, low cost, and effective against faecal bacteria. SODIS was first observed on the surface of water bodies and later utilized for disinfection of contaminated drinking water by Professor Aftim Acra of the American University in Beirut in 1984 (Luzi *et al.,* 2016). Household use of this water treatment method utilizes the sun and polyethylene terephthalate (PET) bottles, which are readily and easily accessible. Contaminated water is placed into 2-L clear PET bottles and exposed to the sun for 6-48 hours, after which the microbes are inactivated, yielding clean drinking water, as shown in Figure 1.1 (McGuigan *et al*., 2012).

Figure 1.1 Overview of SODIS showing its household application.

The climatic conditions of Obunga slum are expected to favour SODIS. Obunga slum experiences temperatures ranging from 20 °C to 35 °C throughout the year, high humidity due to the influence of Lake Victoria, and two rainy seasons ranging from March to May and August to October (Herman, 2017). All these conditions meet the climatic conditions requirement for the application of SODIS.

The utilization of the sun during SODIS water treatment, which makes it attractive, also limits its effectiveness. Due to this dependence, it cannot be utilized in regions and seasons without sufficient sun exposure. Modifying the treatment conditions has effectively increased efficiency by incorporating nano-photocatalysts (Danwittayakul *et al.*, 2020). This incorporation is done either by coating them on support systems or onto the surface of the treatment medium. Low-cost photocatalyst support such as glass rings, glass beads, glass rods, and porcelain beads have been explored (Joseph and Vijayanandan, 2023).

Contamination of the water under treatment by leaching of components of the bottle material is one of the challenges encountered during SODIS. Bisphenol A (BPA) contamination is of great concern due to its recorded respiratory irritation effects and endocrine disruption, resulting in hormonal imbalance complications in both men and women (Ohore and Songhe, 2019). Solutions to degrade BPA in water have been suggested and include the use of visible light active photocatalysts (Subagio *et al*., 2010). Incorporation of a photocatalyst into SODIS is, therefore, expected to counter chemical contamination during treatment.

Photocatalysts have been applied in environmental remediation for the removal of chemical contaminants and improvement of the microbial quality of water (R. Javed *et al*., 2022). Materials used as photocatalysts have to be chemically and thermally stable semiconductors activated by photoirradiation. Zinc oxide (ZnO), zinc sulphide (ZnS), titanium dioxide (TiO_2), iron (II)oxide (Fe_2O_3), and cadmium sulphide (CdS) are the most researched and utilized photocatalysts (Dalrymple and Goswami, 2017).

The most utilized photocatalyst is TiO_2. This is because it offers the advantage of low toxicity and high availability, hence reduced cost, low susceptibility to photocorrosion, and lower dependence on pH (Dalrymple and Goswami, 2017). The nano-TiO_2 application offers the added benefit of a small surface area. Though the application of TiO_2 in photocatalysis is highly effective, it is challenged by its low quantum yield and absorbance of only Ultraviolet (UV) radiation (Peiris *et al*., 2021). To overcome these challenges, noble metal modification has been done (Pelaez *et al*., 2012; Peiris *et al*., 2021).

The need for overall effectiveness guides the selection of a nanoparticle synthesis approach. There are two synthesis approaches: the top-down approach, which involves breaking down the bulk material to the desired nano-size, and the bottom-up approach, which involves nucleation and growth. The top-down approach is very harsh, often producing defective nanoparticles, and is therefore not preferred. The bottom-up approach is preferred since it produces nanoparticles with the desired shape, size, and stability (Ramsden, 2013).

Metallic nanoparticles can be prepared and stabilized by chemical, physical, and biological methods. Chemical methods include electrochemical techniques, pyrolysis, photochemical, and chemical reduction. Physical methods include physical vapor condensation and arc discharge. Biological methods involve using plants and microorganisms (green synthesis) instead of some chemicals used during synthesis. Chemical and physical methods are costly, energy and chemical-intensive, making biological methods desirable. The focus is specifically on the utilization of plant extracts (green synthesis) since the use of microorganisms is slower and requires extraction and recovery mechanisms for the microorganisms (Ramteke *et al*., 2013; Faried *et al*., 2016; Sorescu *et al*., 2016).

1.2 Problem statement

One of the biggest challenges encountered by Obunga slum residents is the lack of safe drinking water. Faecal contamination with *E. coli* has been highly recorded in Obunga slum water sources (Opisa *et al*., 2012; Herman, 2017). Therefore, its inactivation would

influence the selection of a water treatment method. Common water treatment methods used in the slum are boiling, cloth filtration, and sedimentation (Maoulidi, 2010). Boiling is the only effective water treatment method against *E. coli* bacteria. However, it is energy-intensive and detrimental to the environment due to the use of firewood and charcoal (Brown and Sobsey, 2012; Carratalà *et al*., 2016). For this reason, a water treatment method offering an effective and sustainable scientific solution should be introduced.

Application of SODIS as a POU water treatment method in Obunga slum would favour them because it is highly effective against *E. coli* bacteria, simple to use, and low-cost (Luzi *et al*., 2016). SODIS is limited by its dependence on climatic conditions and use of only the UV component of solar radiation, making it time-consuming and less efficient than other water treatment methods. The incorporation of a nano-photocatalyst in the water treatment process has been proven to make SODIS more efficient (Luzi *et al*., 2016).

The application of pure TiO_2 nanoparticles in photocatalysis is challenged by its low quantum yield resulting from a fast recombination rate and activity only in the UV-radiation range owing to its large bandgap energy of 3.26 eV (Guo *et al*., 2019). Surface modification of TiO_2 using noble metals has been preferred since it overcomes both challenges without altering its crystal structure. The interaction between the TiO_2 surface and modified metal results in a Schottky barrier that acts as an electron trap, slowing down recombination (Ola and Maroto-Valer, 2015). Additionally, the surface plasmon resonance (SPR) of noble metals results in visible light activity (Ramasamy *et al*., 2012).

Common surface modification methods involve the use of hazardous chemicals, making the process costly and detrimental to the environment (Mekprasart *et al*., 2013). In agreement with the green chemistry principles 3 and 9 of chemical synthesis that is non-hazardous and improved catalysis (Ivanković, 2017); a green method of modification using watermelon rind extract (WMRE) as the reducing agent has been proposed.

1.3 Justification

SODIS field tests performed in Cambodia, Pakistan, Kenya, Bolivia, and Bangladesh have shown this water treatment method to be effective in microbial inactivation and reduction of waterborne diarrhoea occurrence in children (Du Preez *et al*., 2011; McGuigan *et al*., 2011; Atikul *et al*., 2015; Martínez *et al*., 2020). Even though challenges have been encountered in the household acceptance of SODIS, use in rural Cambodia resulted in an effective and communally acceptable water treatment (McGuigan *et al*., 2011). This is indicative of its potential for use in low-income households.

Visible light active SODIS is highly efficient, with the photocatalyst incorporation involving the use of photocatalyst support (Chong *et al*., 2010; Keane *et al*., 2014). Glass beads are preferred over other forms of support since they increase the surface area to volume ratio and reduce the mean distance between the target microorganisms and the photocatalyst surface (Keane *et al*., 2014). Additionally, BPA, which is not a component used in the synthesis of PET, has been reported in water packaged in PET bottles due to leaching. Although monitoring BPA contamination during SODIS was not part of this study, it was anticipated that using a photocatalyst in SODIS would also lead to the

degradation of BPA during the water treatment process. This degradation utilizes the electron-hole (e^-/h^{+}) pairs and ROS. Therefore, the photocatalyst can be reused.

1.4 Research questions

i) What are the water and sanitation standards of Obunga slum residents?

ii) What is the efficiency of SODIS as a POU water treatment method for the residents of Obunga slum?

iii) What are the optimal operating conditions for synthesizing Ag/TiO_2 using WMRE?

iv) What is the effectiveness of SODIS modified with glass beads coated with Ag/TiO_2 nanocomposite?

1.5 Hypotheses

i. The residents of Obunga slum demonstrate poor water and sanitation practices, emphasizing the need for a practical and cost-effective point-of-use (POU) water treatment method.

ii. Solar disinfection (SODIS) is a viable and effective water treatment method for the residents of Obunga slum.

iii. Optimizing the operating conditions during the synthesis of Ag/TiO_2 nanocomposites using WMRE will improve nanoparticle monodispersity.

iv. Incorporating Ag/TiO_2 nanocomposites synthesized using WMRE into the SODIS process using glass beads will improve water treatment efficiency.

1.6 Objectives

1.6.1 General objective

The general objective of this research was to evaluate the water quality and the watermelon rind-mediated Ag/TiO_2 nanocomposite-modified solar disinfection efficacy in Obunga slum, Kisumu County**.**

1.6.2 Specific objectives

i) To assess the water and sanitation practices of the residents of Obunga slum.

ii) To evaluate the efficacy of SODIS as a POU water treatment method for Obunga slum residents.

iii) To determine the optimal operating time, temperature, and pH for the synthesis of Ag/TiO_2 nanocomposite using WMRE

iv) To evaluate the efficiency of SODIS modified with Ag/TiO_2 nanocomposite for water treatment for Obunga slum residents.

1.7 Significance of study

SODIS is a relatively simple water treatment technique that can be applied at the household level without external control. Its implementation in Obunga slum is expected to provide an effective solution for improving drinking water safety. Furthermore, by incorporating WMRE-synthesized Ag/TiO_2 nanocomposite, the dependence of the SODIS water treatment method on the availability of the sun's ultraviolet radiation would be reduced, allowing for the use of the more readily available visible radiation. This improvement would enhance water treatment effectiveness, reduce time consumption and water safety, and result in fewer waterborne diseases among children in

Obunga slum. Furthermore, WMRE synthesis will offer a sustainable method due to the availability and low cost of watermelon rind while also helping reduce green waste and, consequently, global warming.

CHAPTER TWO: LITERATURE REVIEW

2.1 Solar disinfection (SODIS) of water

The earth's surface receives solar radiation in the form of infrared radiation, visible light, ultraviolet (UV) light, X-rays, and gamma rays. SODIS uses sunlight's heat and light effects to inactivate waterborne pathogens. The light effects of sunlight utilized during SODIS are due to UV-radiation, which is categorized into three groups: UV-A, whose wavelength ranges from 320-400 nm, UV-B whose wavelength ranges from 290-320 nm; and UV-C, whose wavelength ranges from 250-290 nm. The heat effects of sunlight utilized during SODIS are due to infra-red radiation (IR) (McGuigan *et al*., 2012).

UV-radiation interactions with biological systems and processes result in inactivation of microorganisms. These interactions cause DNA structure alteration, suppressed physiological processes, and extreme physiological stress, causing cell division and stunted growth. DNA structure alterations lead to mutation and cell death and are accredited for microbial inactivation during SODIS (Rastogi *et al.*, 2010). These mechanisms of disinfection are discussed below.

2.1.1 Mechanism of water disinfection

Inactivation of microorganisms due to DNA damage occurs mainly through UV-A radiations. The ozone layer allows no UV-C, only about 10% of UV-B and all UV-A to reach the earth's surface; therefore, no inactivation results from UV-C, and very little is attributed to UV-B (McGuigan *et al*., 2012). DNA has a maximum UV absorbance of 260 nm, beyond which mutation and cell death occur (Olson and Morrow, 2012). As a result,

only UV-B directly damages DNA, while UV-A inactivation involves the formation of reactive oxygen species (ROS) that interact with the microorganisms (Gandhi and Prakash, 2023).

UV-B radiation damages DNA strands in microorganisms by causing the formation of thymine dimers, where adjacent thymine bases bond together, as shown in Figure 2.1 (Rastogi, 2015). This interference disrupts base pairing with complementary purines, hindering DNA replication by polymerase enzymes, which may skip the dimers, omit bases, or insert incorrect ones. The result, regardless of the path followed by the polymerase enzyme, is DNA damage (McGuigan *et al*., 2012). Repairing pyridine dimers can lead to mutations and cell death. Even when repair is possible, it consumes all the cell's energy, disrupting essential processes and eventually resulting in cell death (McGuigan *et al*., 2012). DNA damage from these structural alterations is irreversible.

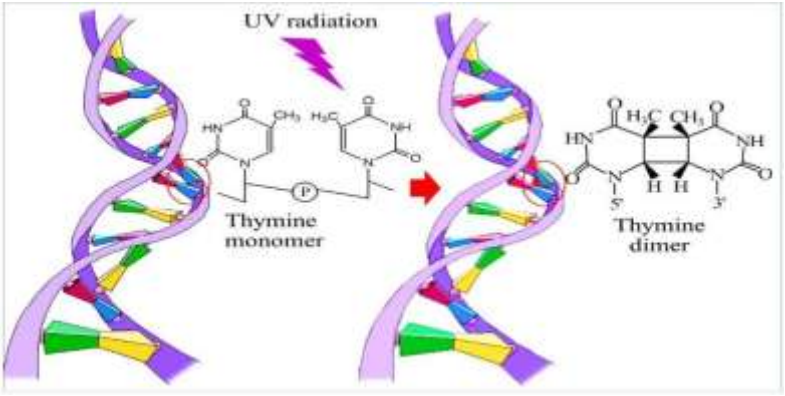

Figure 2.1 Thymine dimer isomerization due to UV-B.

Inactivation of microorganisms by UV-A involves a chain of chemical reactions. The first step is the excitation of the photosensitizer (S), which either directly interacts with cell

components or reacts with dissolved oxygen, forming Reactive Oxygen Species (ROS), which include superoxide (O_2^-), hydrogen peroxide (H_2O_2) and hydroxyl radical ($OH^{\cdot}$). Photosensitization reactions resulting in the formation of ROS and organic free radicals occur in two ways as shown in Equation 2.1 and Equation 2.2 (Giannakis *et al*., 2022). The second step is the oxidation of the cell components owing to the high oxidizing power of the ROS. The final step is ROS attenuation, during which the microorganism reduces or eliminates its effects (McGuigan *et al*., 2012).

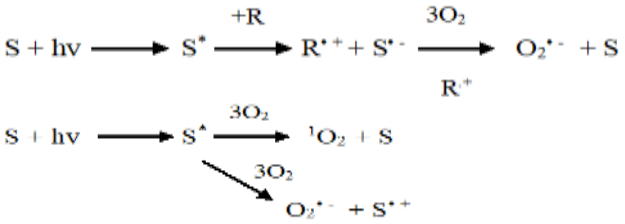

Equation 2.1

Equation 2.2

ROS differ in oxidizing power and toxicity. Primary ROS, with low oxidizing power, can be converted into secondary ROS with high oxidizing power, making them more lethal. Superoxide and hydrogen peroxide have lower oxidizing power as compared to $OH^{\cdot}$ and, therefore, have fewer devastating effects. After formation, they are converted into hydroxyl ($OH^{\cdot}$) radicals which react with molecules within the living cell fast, resulting in cell damage and death (Giannakis *et al*., 2022). $OH^{\cdot}$ formation from O_2^- and H_2O_2 occurs in two ways, as shown in Equation 2.3, Equation 2.4, and Equation 2.5 below.

A. $H_2O_2 + e^- + H^+ \rightarrow H_2O + OH^{\cdot}$ Equation 2.3

B.

I. $M^{3+} + O_2^- \longrightarrow M^{2+} + O_2$ Equation 2.4

II. $M^{2+} + H_2O_2 \rightarrow OH^- + M^{3+} + OH^{\cdot}$ Equation 2.5

Where M is a metal.

UV-induced ROS are only lethal if their presence overpowers the organism. In small amounts, the organism can reduce and neutralize their effects. Microorganisms respond to superoxide using superoxide dismutase enzyme, which reduces its lifetime by 10^9 as shown in Equation 2.6 below (García-Gil *et al*., 2021). Microorganisms respond to hydrogen peroxide by releasing catalase and peroxidase enzymes, which convert hydrogen peroxide to water, as shown in Equation 2.7 and Equation 2.8 (Seo *et al*., 2015; García-Gil *et al*., 2022; Giannakis *et al*., 2022).

$$O_2^- + O_2^- + 2H^+ \rightarrow H_2O_2 + O_2 \qquad \text{Equation 2.6}$$

$$H_2O_2 \rightarrow O_2 + 2H_2O \qquad \text{Equation 2.7}$$

$$H_2O_2 + 2NADPH \rightarrow 2H_2O + 2NADP^+ \qquad \text{Equation 2.8}$$

The pasteurization effects of sunlight depend on the water temperature during treatment. Pasteurization of water during SODIS happens when sunlight heats water to sub-boiling temperatures (usually between 50°C and 70°C) for a prolonged duration (Strauss *et al*., 2016). This inactivation results from the solar heating of infrared radiation, which has a wavelength range of 780 nm-1 mm. Strauss *et al*. (2016) compared the effectiveness of SODIS, which uses UV and the pasteurization effects of sunlight, and solar pasteurization (SOPAS), which uses only the pasteurization effects of sunlight systems, against *E. coli*, *Legionella* spp., and *Pseudomonas* spp. They found that all the bacteria were disinfected by more than 99% when subjected to 52°C or higher for SODIS and 72°C or higher for SOPAS.

Pathogens are equipped with heat-shock proteins that offer microbial heat resistance, allowing them to survive and develop under heat stress. Heat shock proteins protect already formed and forming proteins, which are the building blocks of the cell. Their concentration increases with heat stress until the maximum growth temperature is exceeded. At this temperature, heat shock proteins become ineffective, resulting in cell damage due to the unfolding of proteins and inhibition of proper protein formation (Hong *et al*., 2022).

The treatment bottle and surface on which SODIS is performed directly affect the temperature achieved by the water. The bottle material used should transmit heat, whereas the surface should be a good conductor of heat. Therefore, it has been suggested that the bottle should be clear, directly contacting the heating surface, and the side on which the bottle lies on the surface could be painted black. The treatment surface should be preferably metallic to achieve high water temperature (Luzi *et al*., 2016).

2.1.2 Indicator micro-organisms

Indicator microorganisms are essential to the analysis of water treatment methods. Due to the complexity of waterborne microorganisms, the selection process follows set guidelines (Motlagh and Yang, 2019). For a microorganism to be selected as an indicator microorganism, it should (1) have an easy testing method, (2) be a microflora of warm-blooded animals, (3) be applicable for all types of water, (4) not grow in water, (5) have a reasonably longer survival rate than other pathogens, (6) be present whenever enteric pathogens are present, and (7) have a density alluding faecal pollution. However, since no

single microorganism meets all these requirements, a combination of microorganisms is used (Motlagh and Yang, 2019).

Indicator microorganisms used for SODIS are faecal coliform bacteria. Coliform bacteria are gram-negative bacteria that grow at 37 ºC in bile salts and break down lactose, giving acid and gas. They are categorized into faecal and non-faecal (total) coliform bacteria. Faecal coliform bacteria grow in intestinal environments, while non-faecal coliform bacteria can grow in non-intestinal environments such as soil and water (Motlagh and Yang, 2019). *E. coli* is the indicator microorganism for SODIS due to its higher resistance to the lethal effects of sunlight compared to other bacteria. Its inactivation pattern was also found to be representative of other microorganisms (Nwankwo *et al*., 2022).

Bacteria regrowth is a determinant of the effectiveness of a water treatment method. Effectiveness is achieved when no bacteria regrowth is recorded post-treatment. Research on bacteria regrowth post-SODIS is inconclusive as some researchers have recorded bacteria regrowth while others recorded none (Byrne *et al.*, 2011; Fernández-Ibáñez *et al.*, 2012; Sintubin *et al.*, 2012). Even though the regrowth of bacteria in SODIS is disputed, solutions have been suggested to eliminate it. The incorporation of TiO_2 photocatalyst has been proposed to improve the efficiency of water treatment, with no bacteria regrowth recorded even after long-term water storage (Byrne *et al*., 2011; Castro *et al*., 2012; Sintubin *et al*., 2012; Giannakis *et al*., 2015).

Calculations of the bacteria reduction during treatment give the effectiveness of the treatment method. The Log Reduction Value (LVR) is used to indicate the order of bacteria reduction magnitude during SODIS (Luzi *et al*., 2016). The bacteria removal percentage is calculated from the LVR and is reported as the percentage kill rate achieved using the water treatment method, as shown in Equation 2.9 (Luzi *et al*., 2016). During a 5-hour SODIS water treatment period, a 99.99% kill rate has been observed for *E. coli, Salmonella Typhimurium, Shigella flexneri,* and *Vibrio cholerae* (Luzi *et al*., 2016).

$$\%\ kill\ rate = 1 - ((\frac{C}{C_{\circ}}) \qquad \text{Equation 2.9}$$

Where C is the bacteria (colony-forming unit) CFU before water treatment and Co is the CFU after treatment.

2.1.3 *E. coli* and coliform bacteria enumeration

Enumerating microbe contamination is essential to assessing water quality during water treatment. Various factors, including speed, sensitivity, cost-effectiveness, feasibility, and the specific needs of individual water assessment situations, guide the selection of an appropriate enumeration method (Tambi *et al*., 2023). These methods are generally categorized as immunological, conventional, enzymatic, and nucleic acid-based molecular methods. The most commonly used enumeration methods are conventional methods. They are flexible, easy to use, and support the recovery and growth of damaged organisms. However, these methods can be time-consuming and require proper storage and transportation of samples (Tambi *et al*., 2023). Portable methods have been developed for

onsite analysis, which is especially beneficial in low-income areas where timely results and laboratory costs are significant challenges (Pichel *et al*., 2023).

Several portable methods exist for testing water for *E. coli* and coliform bacteria, including hydrogen sulfide tests, Colilert, and Petrifilm count plates. Petrifilm count plates are popular for their convenience, lightweight design, and pre-prepared nature. With a short incubation time of 18 to 24 hours, they provide quick results and are cost-effective (Mkhwanazi *et al*., 2024). The 3M™ *E. coli*/ Coliform Petrifilm™ are made of a cold-water gelling agent, violet red bile nutrients including lactose, a glucuronidase indicator (BCIG- 5-bromo-4-chloro-indonyl-beta D glucuronide) and a tetrazolium indicator. Figure 2.2 and Figure 2.3 show an unused and used petrifilm showing the *E. coli* colonies, which are blue with air bubbles trapped around them, and coliform colonies, which are red with air bubbles trapped around them (Souza *et al*., 2015).

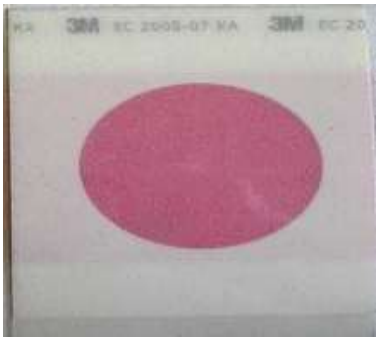

Figure 2.2 An unused petrifilm.

Figure 2.3 A used incubated petrifilm showing the *E. coli* and fecal coliform bacteria colony forming units (CFU).

Each component of the petrifilm serves a specific role in detecting *E. coli* and coliform bacteria. Bile salts and crystal violet inhibit Gram-positive bacteria, allowing only Gram-negative bacteria to be counted. Coliform bacteria ferment lactose, producing gas bubbles that surround their colonies, making them distinguishable. *E. coli* breaks down glucuronide with the enzyme glucuronidase, resulting in a blue precipitate, which helps differentiate it from other coliform bacteria. The tetrazolium indicator enhances the visualization of Gram-negative colonies (Lars, 2010).

Microbial analysis using 3M™ Petrifilm™ plates follows three steps: inoculation, which involves lifting the top film and placing a 1 mL water sample in the circular area; incubation at 35 ˚C for 24 hours, and counting of the *E. coli* and Coliform bacteria colonies.

2.1.4 SODIS variables

Various factors determine the effectiveness of SODIS water treatment. These include climatic conditions, the level of dissolved oxygen in the water under treatment, the type and nature of pathogens, water turbidity, and the bottle material, depth, and position (Luzi *et al*., 2016). These factors are discussed below.

SODIS is highly dependent on sunlight exposure, which is determined by cloud cover. Regions between 15˚ and 35 ˚N latitude, the equator, and 15 ˚N latitude are the most suited for SODIS application due to their low cloud cover. These regions are characterized by below 50% cloud coverage and high solar radiation (Nakada and Urban, 2024). To achieve inactivation within 6 hours of treatment, cloud coverage of less than 50% is required. Increased cloud coverage to 75% doubles the treatment time, whereas, above 75% cloud coverage, alternative water treatment methods should be used (Luzi *et al*., 2016; Nakada and Urban, 2024).

Photo-oxidative disinfection of microbes during SODIS depends on the dissolved oxygen levels in contaminated water undergoing treatment. The influence of dissolved oxygen on SODIS has been evaluated by performing SODIS runs under aerobic and anaerobic conditions. The inactivation of *E. faecalis*, *P. aeruginosa*, and *E. coli* was found to be faster under aerobic conditions as compared to anaerobic conditions, as shown in Figure 2.4 (Martínez-García *et al*., 2023). Additionally, increasing the amount of dissolved oxygen improves treatment efficiency, and this could be achieved by vigorously shaking the PET bottles containing contaminated water before treatment (Luzi *et al*., 2016).

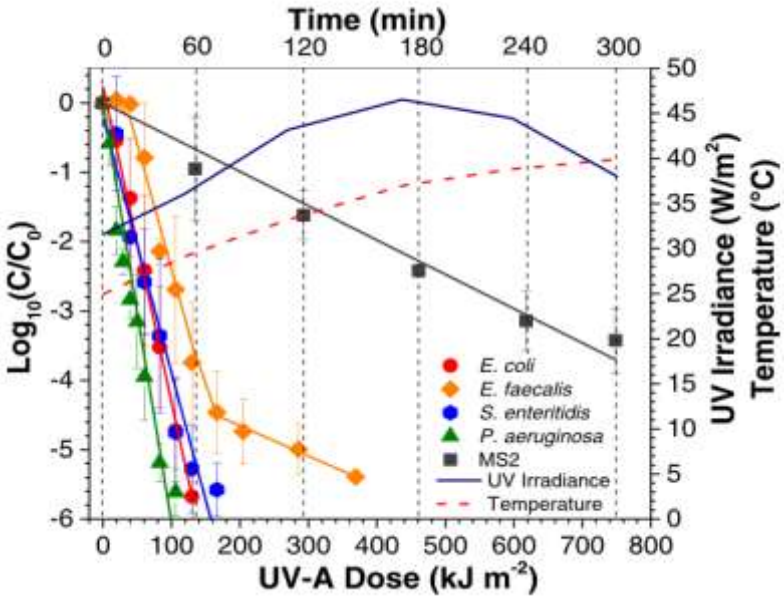

Figure 2.4 The inactivation kinetics of a consortium of pathogens using a combination of solar light and O_2 sparging in synthetic rainwater (SRW) (Martínez-García *et al*., 2023).

The type and nature of pathogenic organisms influence how effectively they can be inactivated during solar water disinfection (SODIS). Waterborne protozoa have a higher resistance to SODIS treatment due to the cyst's dormant stage and oocyst cell structure (Luzi *et al*., 2016). SODIS inactivates most waterborne viruses at almost similar rates as bacteria. The effectiveness of SODIS inactivation in viruses depends on the virus type, temperature, and dissolved organic materials (Calado and Mattle, 2013; Carratalà *et al*., 2016; Luzi *et al*., 2016). SODIS is highly effective against many waterborne bacteria. Bacteria inactivation via SODIS depends on the bacteria type and concentration (Luzi *et al*., 2016; Cardoso-Rurr *et al*., 2019).

The turbidity of treatment water influences the efficiency of SODIS. Suspended particles reduce the effectiveness of SODIS by absorbing and scattering UV radiation. Low pathogen inactivation has been recorded in highly turbid water (Calado and Mattle, 2013). As a result, 30 Nephelometric Turbidity Units (NTU) have been adopted as the upper limit of turbidity for SODIS to be effective. Water with turbidity greater than 30 NTU should be pre-treated using flocculation, sedimentation, and clothe filtration (Luzi *et al*., 2016). Turbidity measurements can be done using the nephelometric method (NTU measurement), turbidimeters, Jackson candle method, and Secchi disk method (visibility-based) (Kitchener *et al*., 2017). Where these methods are inaccessible, the SODIS manual recommends manual observation of the water by placing a cut-out headline from a newspaper and placing it under a bottle filled with contaminated water (Luzi *et al*., 2016).

Bottle material, depth, and position affect the effectiveness of SODIS. The bottle material should transmit UV radiation and heat without emitting harmful chemicals. Therefore, glass and PET bottles are preferred; PET bottles are ideal for household use. This is because their handling and use require little caution as compared to glass, which is prone to breakage (Luzi *et al*., 2016). Bottles used for SODIS water treatment should be 2 L, as UV transmittance drops below 75% beyond a 10 cm width (Luzi *et al*., 2016). To ensure that the bottles are directly exposed to the sun during SODIS, they should be positioned horizontally and fully exposed to the sun during treatment (Luzi *et al*., 2016).

BPA contamination from leaching PET bottles during SODIS compromises water safety post-treatment. Even though BPA is only added to polycarbonates (PC), contamination has

been recorded in PET bottled water, with contamination levels increasing with increased temperature (Ginter-Kramarczyk *et al*., 2022). It is therefore expected that SODIS treatment, which involves temperatures of up to 55℃, would result in chemical contamination. Nitrogen-doped TiO_2 (N-TiO_2) and Ag/TiO_2 have been applied in the degradation of BPA in water, resulting in 90% and 99.7% degradation, respectively (Subagio *et al*., 2010; Sambaza *et al*., 2019).

2.2 Photocatalysis

Photocatalysis is defined as "the acceleration of a photoreaction by a photocatalyst." This acceleration results from the interaction of the photocatalyst with the substrate in the presence of light of a specific wavelength, as shown in Equation 2.10 and Equation 2.11 (Dalrymple and Goswami, 2017). Light and a photocatalyst are, therefore, essential factors during this process.

$$Catalyst + hv \rightarrow Catalyst^{*} \qquad \text{Equation 2.10}$$

$$Catalyst^{*} + A \rightarrow Catalyst + B \qquad \text{Equation 2.11}$$

Where A is the substrate and B is the product.

The applications of TiO_2 as a photocatalyst are due to the advanced oxidation process, which occurs because of the interaction of water and oxygen. This interaction results in ROS, which react with chemical contaminants and microbes (Dalrymple and Goswami, 2017). TiO_2 photocatalysis occurs in three main steps: photo-excitation, charge transfer, and recombination. Photo-excitation occurs when electrons within the valence band (VB)

absorb photon energy, exciting them into the conduction band (CB). Before this step, the valence band is filled with electrons while the conduction band is empty, as shown in Figure 2.5 (Ahmed *et al*., 2010). To excite the electrons, photon energy has to be similar to or more than the energy of the band gap between the valence and conduction band (Dalrymple and Goswami, 2017).

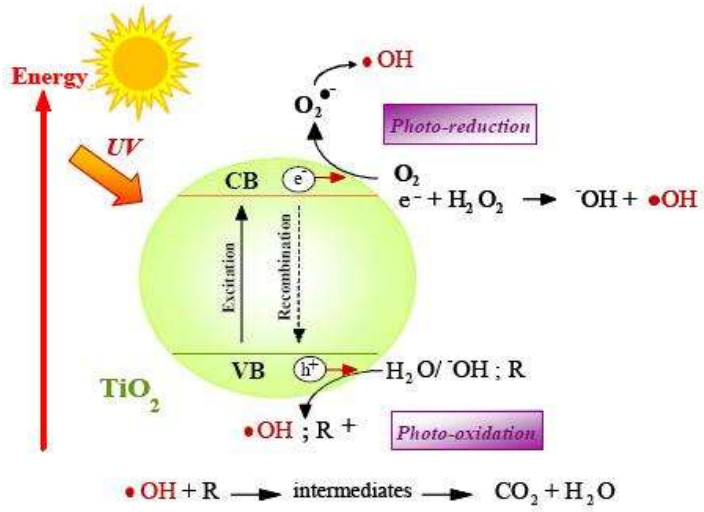

Figure 2.5 Photocatalytic activity of TiO_2

Photocatalytic ROS formation results from the interaction between the electron receptor or scavenger and TiO_2. The photo-generated CB electrons are trapped on the Ti(II) site, forming e^- CB Ti(III) sites where oxygen is adsorbed and acts as an electron scavenger upon contact with the photocatalyst. This adsorption results in the formation of $O_2^{\cdot-}$ as shown in Equation 2.12, which can oxidize cell components, causing death. Water molecules or hydroxide ions (OH^-) interact with the h^+VB, acting as electron receptors to form a highly reactive $OH^\cdot$ as shown in Equation 2.13 and Equation 2.14, respectively,

which has a higher oxidizing power than $O_2^{\cdot -}$ and is therefore majorly accredited for ROS microbial inactivation (Castro-Alférez *et al*., 2017; Dalrymple and Goswami, 2017).

$$e^- CB\ Ti(III) + O_2 \rightarrow Ti(IV) + O_2^{\cdot -} \qquad \text{Equation 2.12}$$

$$H_2O + h^+VB \rightarrow OH^{\cdot} + H^+ \qquad \text{Equation 2.13}$$

or

$$OH^- + h^+VB + \rightarrow OH^{\cdot} \qquad \text{Equation 2.14}$$

Reactive oxygen species (ROS) interact with cellular components, causing cell death through lipid peroxidation, DNA breakage, and protein oxidation. In *E. coli*, lipid peroxidation primar*ily* occurs at the easily oxidizable phospholipid cell membrane. Lipid peroxidation follows three steps: initiation, propagation, and termination. During the initiation step, $OH^{\cdot}$ radical reacts with an H atom in the unsaturated fatty acid, forming a carbon-centred radical and water. During the propagation step, the carbon-centered radical reacts with oxygen to form a peroxyl radical. The peroxyl radical then reacts with an H atom in a secondary unsaturated fatty acid, producing a lipid hydroperoxide and another carbon-centered radical. This radical reacts with oxygen forming a peroxyl radical, and the chain reaction continues. During the termination step, the carbon-centered radical and peroxyl radical react, forming neutral products as shown in Figure 2.6 (Dalrymple and Goswami, 2017).

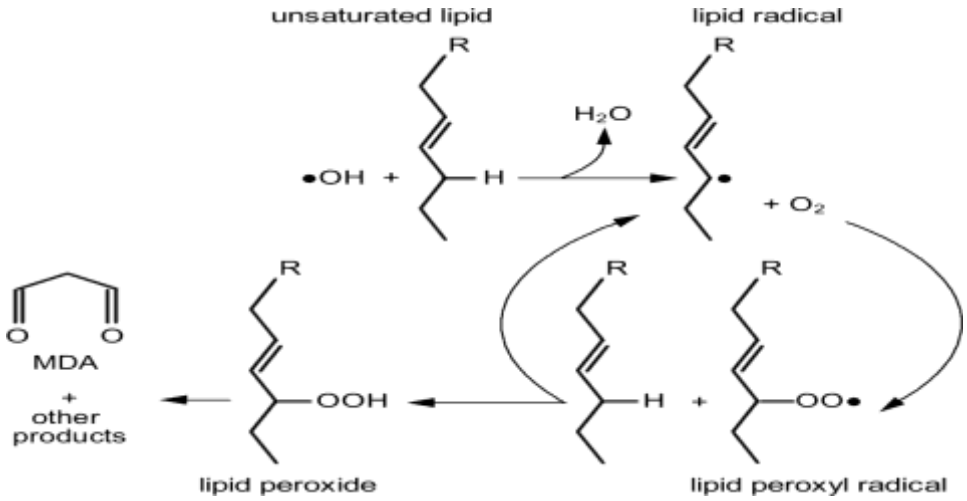

Figure 2.6 The process of photocatalytic lipid peroxidation in the *E. coli* cell membrane.

The application of pure TiO_2 nanoparticles in photocatalysis faces challenges due to their rapid recombination rate, which leads to a low quantum yield. Additionally, their wide band gap restricts their use of UV radiation. As a result, there is a need for various strategies to overcome these challenges and improve the efficiency of TiO_2 nanoparticles (Pelaez *et al*., 2012).

2.2.1 Improving TiO_2 photocatalytic properties

To enhance the photocatalytic activity of TiO_2, chemical impurities can be introduced to reduce electron recombination. This increases quantum yield efficiency and lowers bandgap energy, extending activity into the visible light spectrum. Methods for improvement include semiconductor coupling, dye sensitization, doping, and forming surface aggregates (Sharon *et al*., 2016).

Semiconductor coupling involves coupling TiO_2 nanoparticles with narrow-band semiconductors with a higher CB level. The narrow band gap of the coupled semiconductor results in the absorption of visible light radiation, exciting electrons from the VB into the CB. During relaxation, these electrons are inoculated into the CB of TiO_2, thereby initiating photocatalytic activity (Xu *et al*., 2012). The efficiency of semiconductor coupling depends on the coupled semiconductor concentration. A thin layer of the coupled semiconductor forms on the TiO_2 surface at higher concentrations, shielding it from the substrate. Furthermore, under UV-Vis radiation, an influx of electrons in the VB of TiO_2 could result in photocorrosion of the coupled semiconductor (Guo *et al*., 2019).

Doping involves the introduction of impurities into the TiO_2 crystal. These impurities act as electron traps, slowing down recombination and reducing the band gap energy. Doping occurs either through substitution or interstitial doping. Substitutional doping occurs when oxygen (O) is replaced by a doping atom with a similar atomic size. Interstitial doping occurs when the doping material occupies the interstitial sites within the TiO_2 lattice (Coleman *et al.*, 2015). To retain the integrity of the TiO_2 crystal and observe chemical states created during doping, complex chemical, and energy-intensive synthesis methods are used (Liu *et al*., 2010).

Formation of surface aggregates involves modification of the surface of the photocatalyst with a metal that acts as an e^- trap (Tobaldi *et al.*, 2020). Since chemical reactions take place on the surface of TiO_2, modifying the surface is a more straightforward approach to enhancing photocatalytic activity compared to other methods (Chen *et al*., 2021). Surface

modification forms a Schottky barrier due to the direct contact between the metal aggregate and TiO_2, which ensures greater charge separation. Additionally, the use of noble metals with surface plasmon resonance (SPR) activity results in visible light activity (Ola and Maroto-Valer, 2015). Surface plasmon resonance (SPR) occurs when conducting electrons in metal nanoparticles interact with incident photons, resulting in a resonance effect (Jana *et al*., 2016).

The formed Schottky barrier acts as an electron trap, slowing down electron recombination. This barrier results from the difference in work functions between the metal aggregate and TiO_2. During recombination, the photo-generated electrons are transferred from the CB of TiO_2 nanoparticles to this barrier slowing down electron recombination and increasing the quantum yield, as shown in Figure 2.7 (Hou *et al*., 2015: Di Bartolomeo, 2016). The Schottky barrier height is measured using current-voltage measurements, internal photoemission (IPE), photoemission spectroscopy (PES), and capacitance-voltage (C-V) measurements (Wang *et al*., 2013; Bhattacharya *et al*., 2015; Geisz *et al*., 2015; Khokhra and Kumar, 2015; Roy *et al*., 2016).

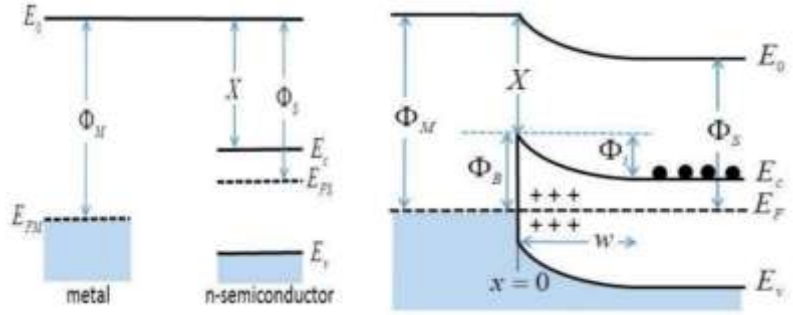

Figure 2.7 Schottky barrier between a metal and semiconductor (Di Bartolomeo, 2016).

Surface modification of TiO_2 with Ag nanoparticles improves photocatalytic properties and increases photo-disinfection. This is due to the anti-microbial activity of Ag nanoparticles. The activity of Ag nanoparticles against bacteria follows two approaches: binding with the cell membrane and penetrating it, attacking internal cell processes. Those bound to the cell membrane interact with the sulphur and phosphorous found in cell components, interrupting replication and eventually causing death. Those that enter the cell membrane interfere with cell division and the respiratory chain, consequently causing death (Omar *et al*., 2017; Haghighat *et al*., 2020).

Bacteria inactivation using Ag/TiO_2 nanocomposite has been found to give better outcomes than pure TiO_2 nanoparticles and UV-A. Ma *et al*. (2011) found that complete *E. coli* inactivation was only achieved using Ag/TiO_2 nanocomposite. Ibrahim *et al.* (2022) compared the antibacterial activity of Ag/TiO_2 nanocomposite with a standard antibiotic, streptomycin, against *Staphylococcus aureus, Shigella flexneri,* and *Bacillus sp.* They found that the Ag/TiO_2 nanocomposite had a higher zone of inhibition than the test antibiotic. This improved photo-disinfection was attributed to the improved photocatalytic activity of TiO_2 and the antibacterial activity of Ag nanoparticles.

2.2.2 Photocatalyst support

When incorporating a photocatalyst into water treatment, it is necessary to use a support. This support must strongly adhere to the catalyst, the attachment process should not degrade the photocatalyst's reactivity, and it should offer a high specific surface area (Chong *et al.*, 2010; Shan *et al*, 2010). Commonly used materials include glass, activated

charcoal, polymeric, and silica gel. The support systems are either mobile or immobile, with the supporting medium suspended in the water or acting as the reaction vessel. Gadgil and Shetty (2021) found that the suspended Ag@TiO_2/polyaniline nanocomposites were more efficient in photo-disinfection than the immobile system.

For SODIS water treatment applications, glass support is the most used. Specifically, borosilicate glass is due to its capacity to resist high calcination temperatures and its transparent nature. Glass application is made in various forms: tubes, rings, beads, plates, and walls of the reactor. Glass beads are preferred over the other forms because they increase the surface area to volume ratio and reduce the mean distance between the target microorganisms and the photocatalyst surface. Their only challenge is that separation mechanisms are required after water treatment (Keane *et al*., 2014). The glass beads in this work could be separated using a plastic sieve and stored in PET bottles until further use.

2.3 Green Synthesis of Ag/TiO_2 Nanocomposite

Green synthesis involves using natural agents such as plant extracts, microorganisms, or biopolymers to produce nanoparticles in an eco-friendly manner. These natural agents act as reducing and stabilizing agents, with water or ethanol as solvents instead of toxic organic chemicals. Reactions occur under mild conditions to conserve energy (Rajoriya *et al*., 2017). The applications of green synthesis are extensive, encompassing medicine (e.g., drug delivery and antimicrobial agents), environmental remediation (such as pollutant removal), and catalysis (Vijayaram *et al*., 2024). However, there still is a need to address scalability and reproducibility for broader industrial use (Javed *et al*., 2023).

Green synthesis has continued to gain attention in research and application. This is because it ensures waste prevention, use of benign water solvents, use of energy-effective designs, real-time reduction of pollution, design of safer chemicals, use of renewable feedstock, improved catalysis, chemical synthesis that is non-hazardous and better degradation designs (López-Lorente *et al*., 2022). Plants are composed of nucleic acids, carbohydrates, proteins, fats, and secondary metabolites. These secondary metabolites contain polyphenols, which make various plants attractive due to their antioxidant properties (Bankar *et al*., 2010; Tahir *et al*., 2013; Siddiqi *et al*., 2018).

The scope of green synthesis is unlimited since different plants and plant parts can be used. *Sarac Indica, Aloe Vera, Mangifera Indica, Pinus Eldarica, Citrullus lanatus, Hyacinthus Orientalis,* and *Dianthus Caryophyllus* are just but a few of the many plants that have been utilized in the synthesis of various nanoparticles (Ndikau *et al*., 2017; Sorescu *et al*., 2016; Tippayawat *et al*., 2016; Siddiqi *et al*., 2018). Synthesis methods can, therefore, be adjusted in multiple ways to utilize different plants and plant parts.

Green waste is the result of discarded plant parts that are considered unpleasant or proven to be inedible. Green waste still contains polyphenols that make the plants attractive due to their antioxidant activity and potential uses (Bankar *et al*., 2010; Tahir *et al*., 2013; Siddiqi *et al*., 2018). For instance, the rind of the *Citrullus lanatus* (watermelon) is discarded due to its unpleasantness, yet it contains saponins, tannins, alkanoids, polyphenols, flavonoids, and phenolic acids, which have hydroxyl and carboxylic functional groups and can

therefore be applied as a reducing agent and stabilizer during green synthesis of nanoparticles (Oko, 2016).

The surface modification of TiO_2 with Ag using plant extracts has been done using goji berry (*Lycium barbarum* L.) fruit extract (Ahmed and Badri, 2021), Rambutan (*Nephelium lappaceum* L.) peel extract (Kumar *et al*., 2016), and *Mirabilis jalapa* plant extract (Purnomo *et al*., 2021). They found that under optimal operating conditions, the activity of the synthesized Ag/TiO_2 nanocomposites in various applications was superior to that of pure TiO_2 and similar to that of chemically synthesized Ag/TiO_2 nanocomposite.

2.3.1 Green synthesis of Ag/TiO_2 nanocomposite using *Citrullus lanatus* rind extract

The modification of TiO_2 nanoparticles with Ag nanoparticles is characterized by the reduction and stabilization of Ag^+ , as shown in Equation 2.15, and their attachment to the TiO_2 surface, as shown in Equation 2.16 (Chakhtouna *et al*., 2021). When Ag synthesis is done using plant extracts, it happens under controlled conditions. Optimization of reaction parameters is, therefore, necessary to achieve optimal synthesis (Ndikau *et al*., 2017).

$$TiO_2 + Ag^+ \rightarrow \quad (Ag^+)/TiO_2 \qquad \text{Equation 2.15}$$

$$(Ag^+)/TiO_2 + WMRE \rightarrow Ag/TiO_2 \qquad \text{Equation 2.16}$$

Citrullus lanatus plant, commonly called watermelon, is a tropical fruit composed of red pulp, seeds, and rind. The red pulp is the most consumed part of the fruit, with the rind and seeds being discarded. Though edible, the rind and seeds are disposed of due to their bitter

taste (Bhattacharjee *et al*., 2020). The global production of watermelon fruit was 103 tonnes in 2018. The rind, which contributes 30% of the fruit's total mass poses a challenge for green waste management (Méndez *et al*., 2021). The rind, like the red pulp and seeds, contains antioxidant polyphenols and can be used as a reducing and stabilizing agent (Ndikau *et al*., 2017; Lakshmanan *et al*., 2018). These polyphenols range in structure from simple phenolic molecules to complex, high-molecular-weight polymers. They contain aromatic rings with one or more hydroxyl (OH) and carboxylic (COOH) groups (Šamec *et al*., 2021). During synthesis, the hydroxyl and carboxylic groups inactivate ions through chelation, acting as the reducing agent and stabilizer (Vidhu *et al*., 2011; Liu *et al*., 2018).

During green synthesis, the synthesized nanoparticles have been analysed to observe the activity of the OH and functional groups. In accordance with Liu *et al*. (2018) suggestion that the green synthesis of Ag nanoparticles follow two major steps, a synthesis mechanism using chlorogenic acid has been recommended, as seen in Figure 2.8. The first step is the reduction of Ag^{+}, which results from releasing one H^{+} and an electron from the OH in chlorogenic acid, forming an unstable radical. This radical interacts with another chlorogenic acid, releasing one H^{+} and electron from the OH in this chlorogenic acid. The two radicals form stable ortho-quinone compounds or react via oxidative polymerization, forming quinones. These quinones then stabilize the formed nanoparticles through the C=O group. Additionally, Liu *et al*. (2018) performed absence tests on the phenolic acids contained in rice husks while synthesizing Ag nanoparticles. They found that nanoparticle formation occurred even when the individual phenolic acids were absent. Therefore, the green synthesis of nanoparticles occurs in the presence of any of the phenolic acids.

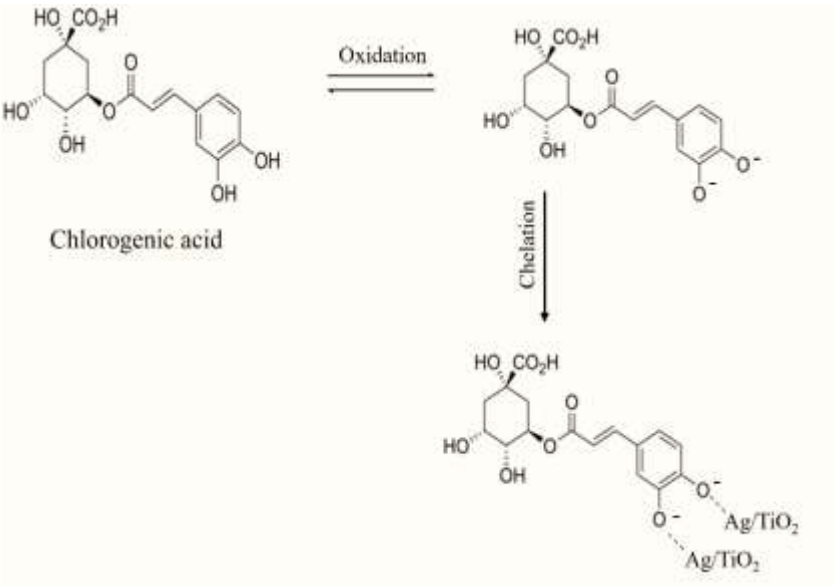

Figure 2.8 Possible mechanism of Ag nanoparticles synthesis using chlorogenic acid in WMRE.

In their findings, Bankar *et al*. (2010) and Khan et al. (2014) suggested that the reduction of the Ag^{+} resulted from their binding to oxygen originating from hydroxyl groups found in banana peel and *P. glutinosa* extracts, respectively. This resulted in the formation of a new C=O group, either a ketone, an aldehyde, or a carboxylic acid, which binds to the Ag nanoparticles, stabilizing them. Both findings proposed that Ag^{+} in the Ag nanoparticles precursor was reduced by OH groups and stabilized by the C=O groups. Mallikarjuna *et al*. (2011) synthesized Ag nanoparticles using *Ocimum sanctum* leaf extract and found a thin protein layer composed of carboxylic acid functional groups, which they suggested stabilized the nanoparticles. Their findings supported previous findings that indicated that C=O groups capped the nanoparticles.

The green synthesis of Ag/TiO_2 using WMRE is expected to utilise the OH and CO components of the WMRE, yielding monodisperse Ag nanoparticles modified on the

surface of the TiO_2. This modification would then improve photocatalytic activity and also contribute to improved SODIS efficiency.

2.4 Characterisation methods

2.4.1 Ultraviolet-Visible Spectroscopy

UV-Vis spectroscopy is an analytical method measuring the transmittance or absorbance of ultraviolet and visible radiation irradiated on a sample. Upon irradiation, photon energy is absorbed by electrons in the ground state, resulting in excitation to higher energy levels (Skoog *et al*., 2018). TiO_2 nanoparticles absorb UV radiation with an absorption peak in the region of 310-380 nm. Purnomo et al. (2021) found that modifying TiO_2 nanoparticles with Ag nanoparticles resulted in a peak at 460 nm attributed to the SPR effects of Ag nanoparticles.

UV-Vis spectroscopy can also be applied to assess nanoparticle size, shape, agglomeration, and refractive index. Changes in these characteristics result in variations of the absorbance and/ or wavelength and allow the analysis of these variations and their causes (Horikoshi and Serpone, 2013). Ndikau *et al*. (2017) used UV-Vis spectroscopy to optimize the green synthesis of Ag nanoparticles using WMRE. They found that changes in operating conditions resulted in bathochromic and hypsochromic shifts in the wavelength and, hyperchromic and hypochromic shifts in the absorbance. Assessment of these shifts then directed the selection of the optimal operation conditions.

2.4.2 X-Ray Fluorescence Spectroscopy (XRF)

Elemental XRF is a non-destructive analytical method measuring the characteristic x-rays emitted by a sample upon irradiation with incident x-rays. This analysis allows for the qualitative and qualitative analysis of identified elements since the intensity of their characteristic X-rays can also be measured (Skoog *et al*., 2018). Portable XRF instruments are limited by their low detection limit for light elements, typically with an atomic number <16.

Elemental analysis permits the identification of elements and assessment of the level of modification achieved during the synthesis of Ag/TiO_2. Mezbour and Ghorab (2019) performed elemental XRF on synthesized Ag/TiO_2 nanocomposite to assess the effectiveness of the modification method used. They found that the synthesized nanocomposite contained 0.762 % Ag, which agreed with the loading of ≤ 1% during synthesis. They concluded that the modification method used was effective based on these findings.

2.4.3 Fourier-Transform Infra-Red Spectroscopy (FTIR)

FTIR is an analytical method that assesses the interaction of matter with infrared (IR) radiation. Due to the low energy of IR radiation, its interaction with matter does not result in electronic transitions as with Ultraviolet and visible light radiation but in changes in the vibrational and rotational states of molecules. Qualitative analysis of molecular species and their vibrational and rotational states can, therefore, be done (Skoog *et al*., 2018).

FTIR spectroscopy would, therefore, help identify the molecular species present in green synthesized nanoparticles. Sahaya *et al*. (2014) synthesized TiO_2 nanoparticles with and without *Hibiscus-rosa-sinensis L* flower extract and used FTIR spectroscopy to analyse the nanoparticles. They found that green-synthesized nanoparticles contained OH and CO functional groups, which were absent in the chemically synthesized ones. This difference was attributed to the plant extract's reducing and stabilizing properties.

2.4.4 X-ray Diffraction (XRD) Analysis

X-ray diffraction is a non-destructive analytical method used to study crystallite materials. This analysis involves the interaction of a sample with constructive monochromatic X-rays (Bunaciu *et al*., 2015). These X-rays are generated by a cathode beam tube, separated by a monochromator, and directed to the sample. In accordance with Bragg's law, as seen in Equation 2.17, the bombardment of the sample with this X-ray beam results in diffraction; the diffracted rays are then detected. This analysis gives the structure of the crystals, detailing the crystal sizes and atom spacing.

$$n\lambda = 2dsin\theta \qquad \text{Equation 2.17}$$

Where n is an integer, **λ** is the wavelength of the x-rays, d is the plane spacing resulting in diffraction, and θ is the diffraction angle.

Characterization of Ag/TiO_2 nanocomposite using XRD has been used to identify the TiO_2 phase and the effect of modification on the crystallite structure. Petica *et al*. (2019) identified the peaks characteristic of anatase and reported it as the dominant phase. They

also observed low-intensity peaks that they attributed to Ag; however, since their intensity was low, they suggested that Ag did not change the anatase crystal structure. These findings were supported by those of Bhardwaj and Singh (2021) who synthesized Ag/TiO_2 using *Origanum majorana* leaf extract. They also observed peaks that were attributed to the anatase phase and low-intensity peaks attributed to Ag.

2.4.5 Energy Dispersive- Scanning Electron Microscopy (EDS-SEM)

Scanning electron microscopy is an analytical imaging technique used for surface analysis. During analysis, a beam of electrons strikes the sample's surface, resulting in secondary electrons, back-scattered electrons, and characteristic X-rays. SEM images are obtained from the detection of secondary and back-scattered electrons while EDS images are obtained from the detection of characteristic X-rays (Skoog *et al.*, 2018).

Images obtained from SEM give the surface characteristics, while EDS allows the qualitative and quantitative analysis of the elements present. Avciata *et al*. (2016) observed changes in the surface of Ag/TiO_2 nanocomposite based on the reducing agent and emphasized the importance of selecting an appropriate reducing agent. Balachandran *et al*. (2021) used EDS to identify and quantify Ag and TiO_2 nanoparticles during the characterization of $Ag\text{-}TiO_2$ nanocomposite. They also observed the interstitial doping of Ag nanoparticles in the TiO_2 lattice.

2.4.6 Transmission Electron Microscopy (TEM)

Transmission Electron Microscopy is a high-level imaging analytical method. This analysis method is similar to SEM; however, in TEM, the primary beam of electrons used is parallel, whereas in SEM, the primary beam of electrons used is broad. As a result, TEM allows for analysis beyond the surface, giving images that show the size and shape of material components (Skoog *et al*., 2018).

Ghasemi et al. (2020) used TEM for the morphological study of the green-fabricated Ag/AgCl@TiO_2 nanocomposite, synthesized using the aqueous leaf extract (ALE) from the mangrove plant *Avicennia marina*. They found that the optimal ratio for ALE/$AgNO_3$ and $AgNO_3$/TiO_2 was 1.61 and 0.31 and yielded improved photocatalysis.

CHAPTER THREE: METHODOLOGY

3.1 Introduction

3.1.1 Materials

TiO_2 nanoparticles were purchased from ChromAfrica LLC (Nairobi, Kenya), silver nitrate ($AgNO_3$) (99.9%) was purchased from Advent Chembio PVT.LTD (Rabale, Mumbai, India), 69% nitric acid (HNO_3), and sodium borohydride ($NaBH_4$) (97%) were purchased from Loba Chemie PVT.LTD (Colaba, Mumbai, India) and 25% Ammonia (NH_3) were purchased from Kobian Kenya Limited (Nairobi, Kenya). TiO_2, $AgNO_3$, and $NaBH_4$ were of analytical grade and were therefore used without further purification. Deionised (DI) water was used.

3.1.2 Instrumentation

Ultrasonication was done using the WUC-A03H Ultrasonic Cleaner Set. Mixing was done using DLAB MX-S50Hz Vortex Mixer 50Hz. The UV-Vis spectroscopy analysis was performed using the SHIMADZU UV-Vis Spectrophotometer UV-1900, manufactured in 2018. Fourier Transform IR (FTIR) Spectroscopy was done using SHIMADZU IR –Spirit with QATR-S Fourier transform IR spectrophotometer, manufactured in 2018. X-ray Fluorescence (XRF) spectroscopy elemental analysis was done using BRUKER XRF S1 TITAN /TRACER 5/CTX, manufactured in 2019. Surface micrographs of TiO_2 nanoparticles and WMRE and $NaBH_4$ synthesized Ag/TiO_2 nanocomposites were obtained using a FEI XL40 ESEM, which is equipped with two EDAX Sapphire Si (Li) EDS detectors and updated MLA software. Nanoparticle size for TiO_2 nanoparticles and WMRE

and $NaBH_4$ synthesized Ag/TiO_2 nanocomposites was obtained using Oxford SDD Detector for TEM: X-MaxN 80T.

3.1.3 Study site

This study was conducted in Obunga slum (GPS coordinates of 0°04'41.6"S 34°46'20.1"E), which has a total of 18,421 residents with 9,398 males and 9,022 females; an area of 8.6 km and a population density is 2,133 people per km². Administratively, Obunga slum is located in the Kanyakwar sub-location, Kisumu East location, Winam division, Kisumu Central Constituency, Kisumu West sub-county in Kisumu County. As shown in Figure 3.1 The slum has four smaller administrative units: Kasarani, Sega, Obunga Central, and Kamakowa, which were labelled as zones I, II, III, and IV, respectively.

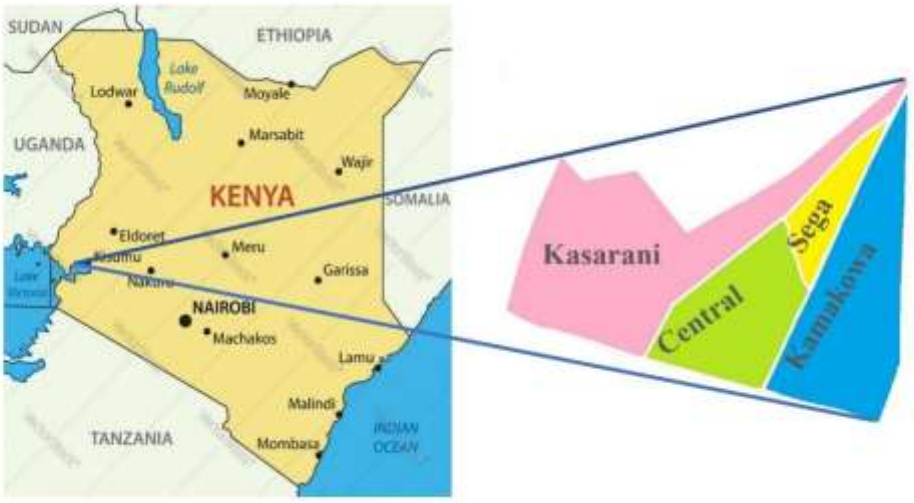

Figure 3.1 Map of Obunga slum.

3.2 Evaluation of the water and sanitation practices of Obunga slum residents

Organized questionnaires were randomly administered through individual interviews with the household heads. These interviews focused on the participants' demographic information, water sources, collection and treatment methods, incidences of disease

resulting from poor water and sanitation practices, and the cost of accessing and treating drinking water. The interviews were carried out according to the zoning. The survey questions were developed following the (WHO, 2018) guidelines on the questions to ask during a water and sanitation assessment.

Sample size (n) determination was done using the Snedecor and Cochran equation shown in Equation 3.1 (Al-Kassab and Majeed, 2022).

$$n = \frac{4pq}{(L)^2} \qquad \text{Equation 3.1}$$

Where p is the proportion of the target population, $q = 1 - p$ and L is the accepted error (0.05). The target population is the number of households in each of the zones and was obtained from the Kenya National Bureau of Statistics 2019 survey (KNBS, 2019). Parameters were calculated as; $p = \frac{5796}{18421}$ = 0.3145, $q = 1 - 0.3145$ = 0.6855 and

$(L)^2 = (0.05)^2$

= 0.0025.

The sample size n as;

$n = \frac{4 \times 0.3145 \times 0.6855}{0.0025}$ = 345

3.3 Investigating the effectiveness of SODIS in water purification

Four unprotected wells were randomly selected from zones I, II, III, and IV. Source one was obtained from Zone I, source two from Zone II, source three from Zone III, and source four from Zone IV. Replicates of three 2 L water samples were taken from each source and placed in clear 2 L PET bottles; this was repeated for all water sources.

The turbidity of the sources was manually observed by placing a cut-out headline from the newspaper under the bottle filled with contaminated water (Luzi *et al*., 2016). The headline was legible for all water samples, so the contaminated water could be treated without pre-treatment.

3.3.1 The SODIS setup for water purification

Field experiments were carried out on the 20th of September 2018. The SODIS experiment was run on the roof of the Kanyakwar sub-chief's office. The twelve 2 L bottles obtained from the work done in section 3.3 Investigating the effectiveness of SODIS were placed on a metallic roof for six hours, as shown in Figure 3.2. Temperature, UV intensity, and humidity readings were taken during this time. Water samples, 1 mL, were taken from each bottle pre-SODIS, hourly during SODIS, and post-SODIS and analysed using labelled 3M™ *E. coli*/ Coliform Petrifilm™. This was done following the Luzi *et al*. (2016) manual, which gives guidelines on SODIS household utilization and assessment of effectiveness.

Figure 3.2 SODIS treatment set-up.

3.4 Watermelon rind extract (WMRE) preparation

During this step, 70% ethanol was used to decontaminate and sterilize surfaces and apparatus. This was to ensure the integrity of the prepared extract by avoiding contamination from external microbes or chemicals. One ripe watermelon was carefully cleaned using DI water. Then, on a surface, a knife was used to cut it into four-quarter portions. The pulp and seeds were removed entirely from each quarter, leaving the rind.

The rind was cut into 10mm x 10mm pieces. These pieces were then weighed (150g) and placed in a 1000-mL beaker, and 500 mL DI water was added to the beaker. The mixture was placed in a blender, and blending was done for 10 minutes. The blended solution was transferred into a beaker, heated to 100 ˚C, and magnetically stirred for ten minutes.

Cooling at room temperature followed. The resulting solution was then filtered with Whatman No. 1 filter paper, collected into a flask, and stored at 4 ˚C.

3.5 Optimization of operating conditions for WMRE-mediated synthesis of Ag/TiO_2

The WMRE-mediated Ag/TiO_2 nanocomposite synthesis was done via an aqueous reduction method. Temperature, pH, and time were chosen as the operating parameters to vary to obtain the optimal operating conditions for the WMRE-mediated synthesis of Ag/TiO_2 nanocomposite.

3.5.1 Effect of time

At first, 0.2 g of TiO_2 nanoparticle powder was dispersed in 100 mL DI water using an ultrasonic treatment for ten minutes. This was followed by the immediate addition of 0.02 g $AgNO_3$ powder, subsequent pH adjustment to 7 by the dropwise addition of 1% HNO_3, and the solution magnetically stirred for 30 minutes. After this, 30 mL of previously prepared 300 g/L WMRE was added, followed by pH adjustment to 12 and subsequent heating at 100 ℃. The pH and temperature were constant under magnetic stirring for 15, 25, 35, and 45 minutes. The obtained solution was then centrifuged at 7000 rpm for 20 minutes, and the supernatant was carefully drained. The resulting pellet was diluted in 100 mL DI water. A 1 mL sample was then collected and characterized using UV-Vis spectroscopy.

3.5.2 Effect of temperature

Initially, 0.2 g TiO_2 nanoparticle powder was dispersed in 100 mL DI water via ultrasonic treatment for 10 minutes. Subsequently, 0.02 g $AgNO_3$ powder was added, pH adjusted to 7 by the dropwise addition of 1% HNO_3 and stirred magnetically for 30 minutes. After this, 30 mL 300 g/L WMRE was added, and the pH was adjusted to 12 by the dropwise addition of 33% NH_4OH and done at room temperature, 40, 80, and 100 ℃ under magnetic stirring for 45 minutes. The solution was centrifuged at 7000 rpm for 20 minutes, and the supernatant was carefully drained. The resulting pellet was diluted in 100 mL DI water, and a 1 mL sample was obtained and characterized using UV-Vis spectroscopy.

3.5.3 Effect of pH

$AgNO_3$ powder (0.02 g) was added to TiO_2 nanoparticles powder (0.2 g), previously dispersed in 100 mL DI water using ultrasonic treatment for 10 minutes; the pH was adjusted to 7 via dropwise addition of 1% HNO_3 and stirred magnetically for 30 minutes. Afterward, 30 mL 300 g/L WMRE was added, and the pH was adjusted to 8, 10, and 12 via the dropwise addition of 33% NH_4OH and heating done at 100 ℃ under magnetic stirring for 45 minutes. The solution was centrifuged at 7000 rpm for 20 minutes, and the supernatant was carefully drained.

The resulting pellet was then diluted in 100 mL DI water. A 1 mL sample was obtained, and characterization was done using UV-Vis spectroscopy.

3.6 Synthesis of Ag/TiO_2 nanocomposite

3.6.1 Synthesis of Ag/TiO_2 nanocomposite using WMRE

The synthesis method developed after optimization was as follows; first 1g TiO_2 nanoparticles powder was dispersed in 500 mL deionized water using ultrasonic treatment for ten minutes. This was followed by the immediate addition of 0.1 g $AgNO_3$ powder, the pH adjustment to 7 by the dropwise addition of 1% HNO_3, and the solution magnetically stirred for 30 minutes. After this, 150 mL 300 g/L WMRE was added, the pH was adjusted to 12 by the dropwise addition of 33% NH_4OH, and heating was done at 100 ℃ under magnetic stirring for 45 minutes. The solution was centrifuged at 7000 rpm for 20 minutes, and the supernatant was carefully drained. The pellet obtained was diluted in 100 mL DI water and centrifuged at 7000 rpm for 20 minutes; this last step was done thrice. The final pellet was diluted in 50 mL DI water and freeze-dried at -55 ˚C for 3 hours. This involved bringing the temperature back to room temperature under a vacuum and then decreasing the pressure to 0.20 bar for 24 hours. Freeze-drying was conducted for WMAT to retain the active capping agents in the WMRE biomass for FTIR characterization. The resulting Ag/TiO_2 powder was labelled WMAT and stored in sealed PET petri dishes at room temperature until further use.

3.6.2 Synthesis of Ag/TiO_2 nanocomposite using sodium borohydride

Using ultrasonic treatment, 0.2 g TiO_2 particles were initially dispersed in 100 mL deionized water. This was followed by the immediate addition of 0.02 g $AgNO_3$, the pH adjustment to 7, and the solution magnetically stirred for 30 minutes. Sodium borohydride ($NaBH_4$) (0.1 mmol), previously diluted in 10 mL of deionized water, was added. Then,

the pH was adjusted to 10 by the dropwise addition of 33% NH_4OH and stirred magnetically for 35 minutes. The resulting solution was centrifuged at 7000 rpm for 20 minutes, and the supernatant was carefully drained. This was followed by adding 100 mL DI water into the pellet and the solution centrifuged at 7000 rpm for 20 minutes; this last step was done thrice. The final pellet was dissolved in 50 mL DI water and calcined at 400 ℃ for 2 hours. The resulting Ag/TiO_2 powder was labelled NBAT and stored in sealed PET petri-dishes at room temperature until further use.

3.7 Characterization

3.7.1 Visible light activity of synthesized nanocomposites using UV-Vis Spectroscopy

Precisely 4 mL DI water was put in a quartz cuvette with a 1 cm path length. The cuvette was inserted in a UV-Vis Spectrophotometer, and the spectrum was recorded in the wavelength range of 220-700 nm. This acted as the blank.

After this, 1 mg of WMAT and NBAT nanocomposite powders were individually dispersed in 4 mL DI water. The solutions were mixed using a vortex for 2 minutes and placed in a cuvette, and the spectrum was recorded using a UV-Vis spectrophotometer in the wavelength range of 220-700 nm.

3.7.2 Elemental composition of synthesized nanocomposites using XRF Spectroscopy

Individually, 0.1 g of TiO_2 WMAT and NBAT nanocomposite powders were placed in plastic bottles, which were then illuminated with X-rays. The output from this analysis

indicated the type of elements present in the sample and their amounts relevant to the TiO_2 and Ag elemental composition.

3.7.3 Identification of functional groups in the synthesized nanocomposites using FTIR Spectroscopy

Individual FTIR analysis was conducted on TiO_2 nanoparticles, WMAT, and NBAT nanocomposite powders using 80 scans in the wavenumber range of 4000 - 400 cm^{-1}.

3.7.4 Crystallite characterization using XRD

The starting material and synthesized nanocomposites were characterized by X-ray powder crystallization using the Thermo Scientific™ ARL™ EQUINOX 100 X-ray Diffractometer with Cu Kα1 (λ = 1.5406 Å). This was done at room temperature, where the individual homogenous powder samples of TiO_2, WMAT, and NBAT were analysed at a two-theta (2θ) scan. This was done at the Analytical and Imaging Laboratory at Murang'a University.

3.7.5 Elemental composition and surface imaging using EDS-SEM

The individual surface morphologies of the TiO_2 nanoparticles, WMAT, and NBAT nanocomposites were analysed using an FEI XL40 ESEM, which is equipped with two EDAX Sapphire Si(Li) EDS detectors and updated MLA software. Suspensions of TiO_2, WMAT, and NBAT were coated via spin coating and analysed under 20 kV voltage. This was done at the Faculty of Science at the University of Johannesburg.

3.7.6 Nanoparticle size determination using TEM

The nanoparticle size of the TiO_2 and Ag nanoparticles in the starting material (TiO_2 nanoparticles) and the WMAT and NBAT nanocomposites was analysed using Oxford SDD Detector for TEM: X-MaxN 80T. Individual aqueous TiO_2, WMAT, and NBAT suspensions were coated on copper grids with a thin carbon film, and the grids dried. TEM analysis was then performed at a voltage of 120 kV. This was done at the Faculty of Science at the University of Johannesburg.

3.8 Incorporation of Ag/TiO_2 nanocomposite into SODIS

The first step of incorporating the nanocomposite into SODIS was coating it on glass beads. The glass beads needed to be cleaned before coating. Initially, they were cleaned using DI water and then with acetone; they were then rinsed in sequence with DI water, ethanol, then isopropyl alcohol; the final rinse was done using DI and they were then stored in DI water overnight at 80 ˚C (Vrooman, 2016). The glass beads were then submerged into a nanofluid of WMAT and NBAT nanocomposite, allowed to sit in a drying oven overnight, and calcined at 400 ℃ for three hours. They were then rinsed with DI water and stored in PET bottles. This coating process was done using 80g glass beads for each nanocomposite. The second step was placing the coated glass beads in 500 mL clear PET bottles and section 3.3 Investigating the effectiveness of SODIS repeated.

3.9 Data analyses

Descriptive analysis of the qualitative and quantitative data generated from the survey was done using Statistical Package for Social Sciences (SPSS) 22 computer software. The

Spearman's rank correlation was used to establish possible relationships between the: age and frequency of occurrence of waterborne diseases, level of education and choice of drinking water sources, drinking water sources and water treatment methods, drinking water sources and frequency of occurrence of waterborne diseases, level of education and water treatment methods, level of education and level of sanitation, level of sanitation and frequency of occurrence of waterborne diseases, and water treatment methods and frequency of occurrence of waterborne diseases.

SAS version 21 was used to carry out the Analysis of Variance (ANOVA) of the bacteria counts obtained during SODIS treatment, while Tukey's HSD test was used for means separation at $p \leq 0.05$. XRD data was analyzed using Origin software while ImageJ software was used to analyse the nanoparticle size distribution of Ag and TiO_2 nanoparticles.

CHAPTER FOUR: RESULTS AND DISCUSSION

4.1 Water and Sanitation Assessment

4.1.1 Sources of drinking water

Most Obunga slum residents were found to use unimproved drinking water sources. Their major source of drinking water was unprotected wells, which originated from the ground. Other sources included piped water, public tap water, protected wells, and water vendors selling water in jerrycans on carts. 92% of the residents of Obunga slum preferred to use a single source, while 8% used a combination of two water sources.

In the survey, and as shown in Figure 4.1, 58.42% of the residents were using unprotected well water, 12.87% were using protected well (W) water, 7.92% were using public tap water, 6.93% were using public tap water to yard (WTY)/ plot, 5.94% were using cart with jerrycan water (WJ), 3.96% were using rain/cart with jerrycan water, 1.98% were using surface water, 0.99% were using protected well or cart with jerrycan water, while 0.99% used piped water to yard/plot or unprotected well.

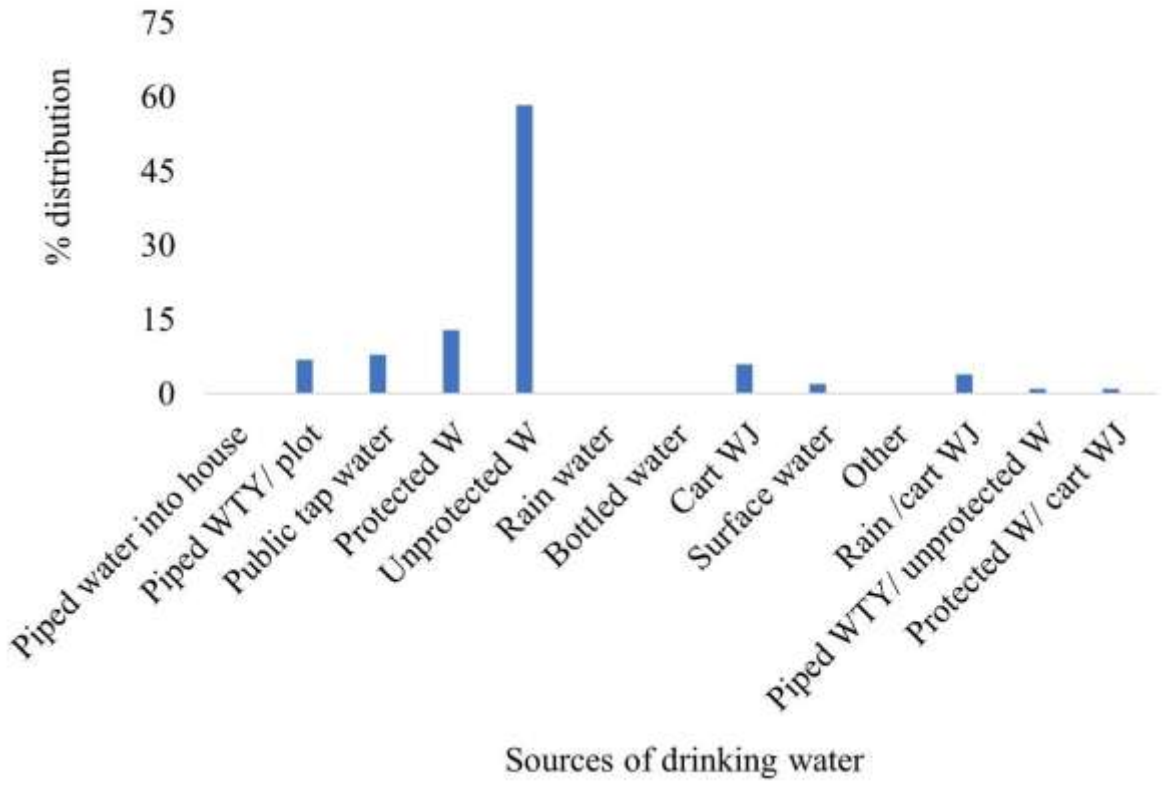

Figure 4.1 Percentage distribution of the drinking water sources used by Obunga slum residents.

The water practices assessment conducted on 8th August 2018 in Obunga slum revealed inadequate water standards. Only 34.65% of the residents had access to improved water sources. According to JMP for Water Supply Sanitation and Hygiene, (2018) unprotected wells, surface water, and uncontrolled rainwater collection are considered unimproved drinking water sources. In contrast, public tap water, piped water to the yard, protected wells, and carts with jerrycan are improved drinking water sources. As seen in Figure 4.2, this translated to 65.35% of Obunga slum residents having access to unimproved drinking water sources. This indicated a need for WASH interventions for the residents.

These findings varied from those of Maoulidi, (2012) and Herman, (2017), who found that 84% and 79.5% of the residents used public taps or standing pipes, respectively. This decrease in the use of safe water sources could be attributed to the drought being experienced in Kenya, which has lowered the water supply and increased water rationing (Robinson *et al*., 2022). The financial strain occasioned by the global recession has also resulted in a very high rise in the cost of living, causing most Kenyans, especially slum dwellers, to struggle with keeping up with water bills (Papyrakis, 2022). These factors combined have resulted in what could be seen as a pattern of decreased access to safe water sources, supporting Kenya's projected failure to achieve SDG 7 of having all citizens access safe water sources.

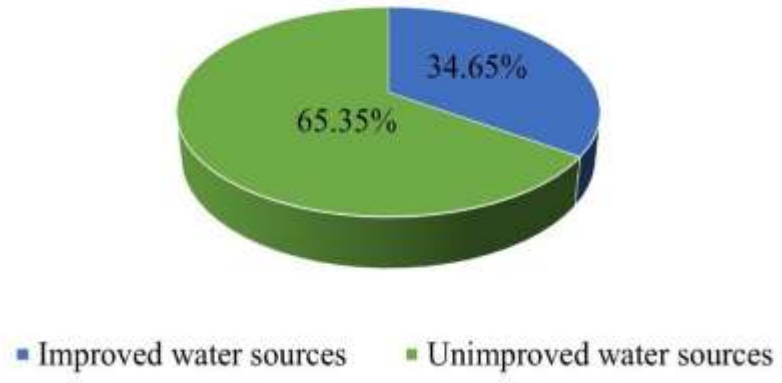

Figure 4.2 The percentage distribution of Obunga slum residents' access to improved and unimproved water sources.

4.1.2 Treatment of drinking water

This study revealed that most residents knew the need to treat their drinking water. As shown in Figure 4.3, 59.0% of the residents reported that they treated their water, 10.0% reported that they did not, and 31% reported that they treated their water sometimes; none of them reported a lack of awareness of whether their water was treated.

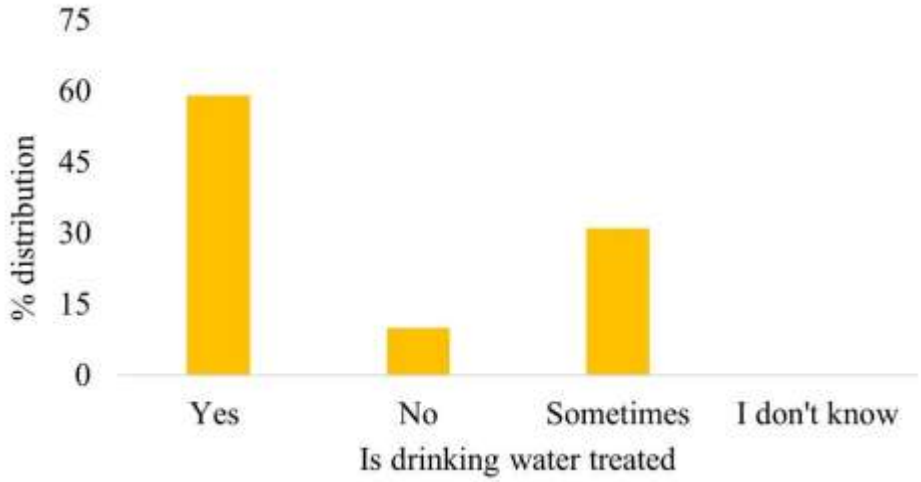

Figure 4.3 The percentage distribution of Obunga slum residents' choice to treat their drinking water.

4.1.3 Water treatment methods

The residents were found to prefer traditional methods of water treatment. As shown in Figure 4.4, 57.43% of the residents boiled their water, 16.83% used a cloth filter, 9.90% used chlorination, 7.92% used other treatment methods, 0.99% did not treat their water, 0.99% used a combination of chlorination and boiling, 0.99% used sedimentation, 0.99% used boiling and SODIS, whereas 0.99% used sedimentation, boiling, and chlorination.

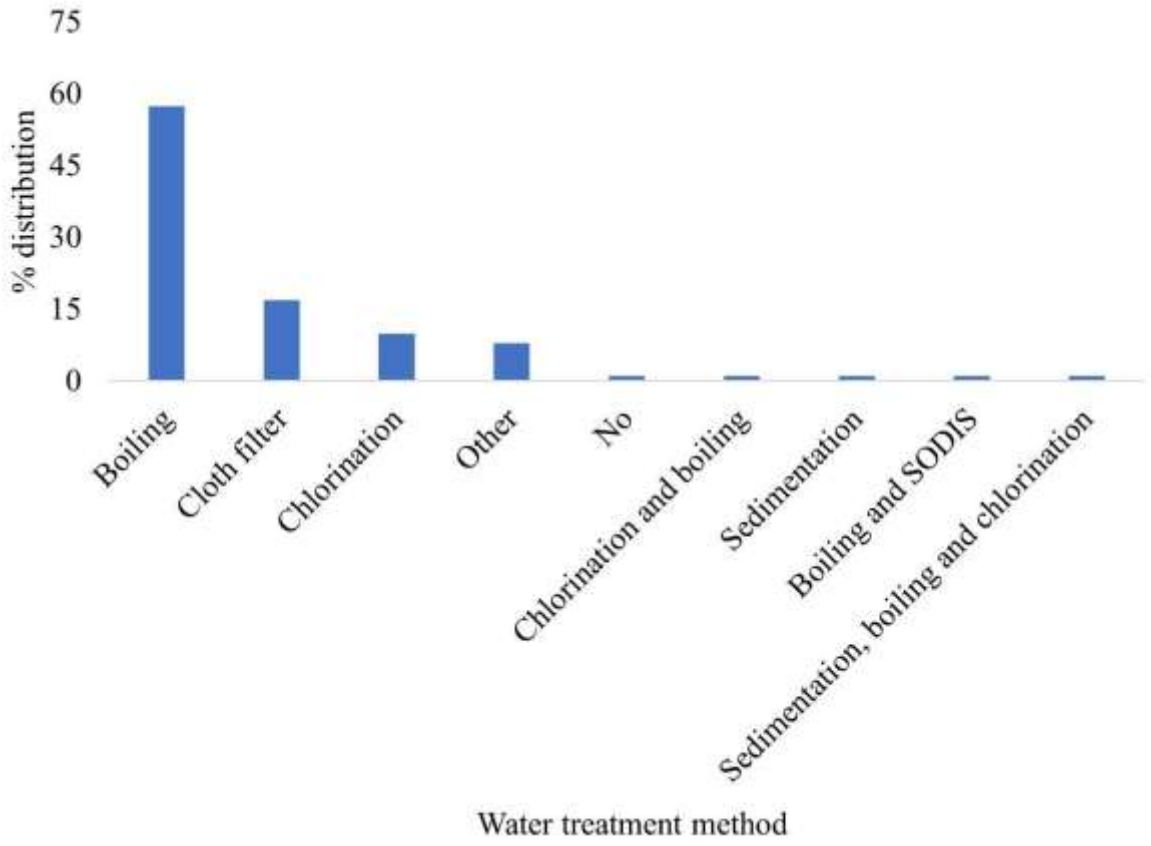

Figure 4.4 The percentage distribution of water treatment methods used by Obunga slum residents.

4.1.4 Presumed effectiveness of water treatment methods

Most residents knew that their preferred water treatment method was ineffective and they would have preferred other alternatives. As shown in Figure 4.5, 80.19% of the residents believed that chlorination was efficient, 9.90% believed that SODIS was efficient, 5.94% believed that sedimentation was efficient, 2.97% believed that filtration was efficient, and 0.99% believed that boiling was efficient.

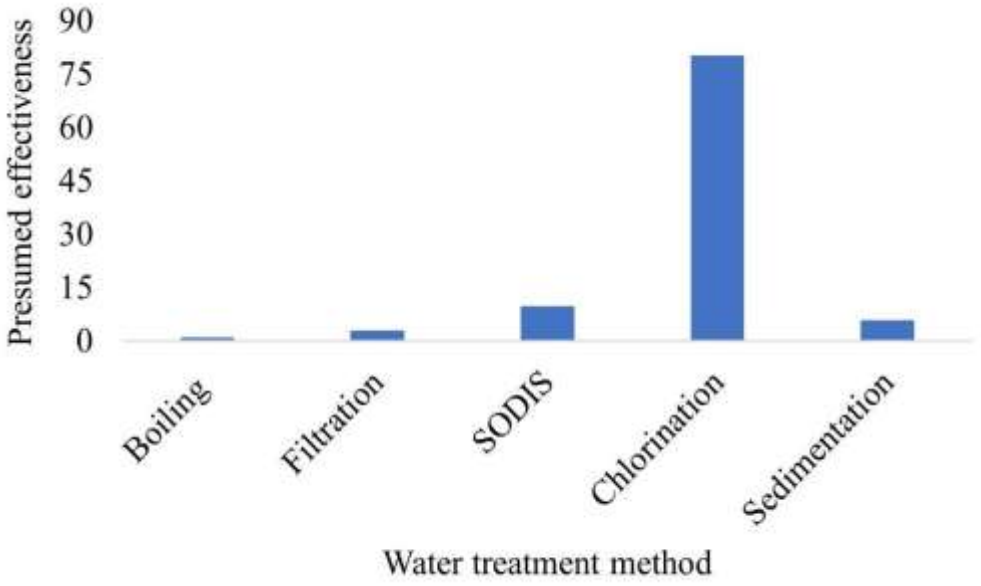

Figure 4.5 The percentage distribution of the presumed efficiency of water treatment methods by Obunga slum residents

A comparison was made between their methods of water treatment and their presumed effectiveness and is shown in Figure 4.6. Boiling, the most commonly used water treatment method had only 1% confidence in its effectiveness. The residents' assumption was incorrect, as boiling effectively eliminates many bacteria, viruses, and protozoa. The water must be brought to a rolling boil for effectiveness, as different microorganisms have varying inactivation temperatures and boiling times (Cohen and Colford, 2017). The limitations of boiling that might impact residents' willingness to use it include the demand for fuel to boil, which means an additional demand for finances.

Additionally, 81% of the residents considered chlorination the most effective water treatment method. The residents' assumption is accurate, as chlorination effectively treats water by killing most bacteria and viruses (Braun *et al*., 2018). However, due to its cost

implications, only 10% of residents used it. Clothe filtration, utilized by 16.83% of the residents, had no presumed effectiveness. This water treatment method only removes some organic matter from the water and does not impact the microbial quality of drinking water (Siwila and Brink, 2019). Additionally, sedimentation, which was utilized by 0.99% of the residents, also received no vote of confidence. Like cloth filtration, sedimentation only removes suspended solids, which settle at the bottom of the treatment medium, and does not affect the microbial quality of water. Therefore, the residents' lack of trust in these water treatment methods was justified. This work highlights the residents' lack of trust in their most commonly used water treatment method. Additionally, the added expense of obtaining fuel, mainly firewood, to boil water emphasizes the need for interventions tailored to the residents.

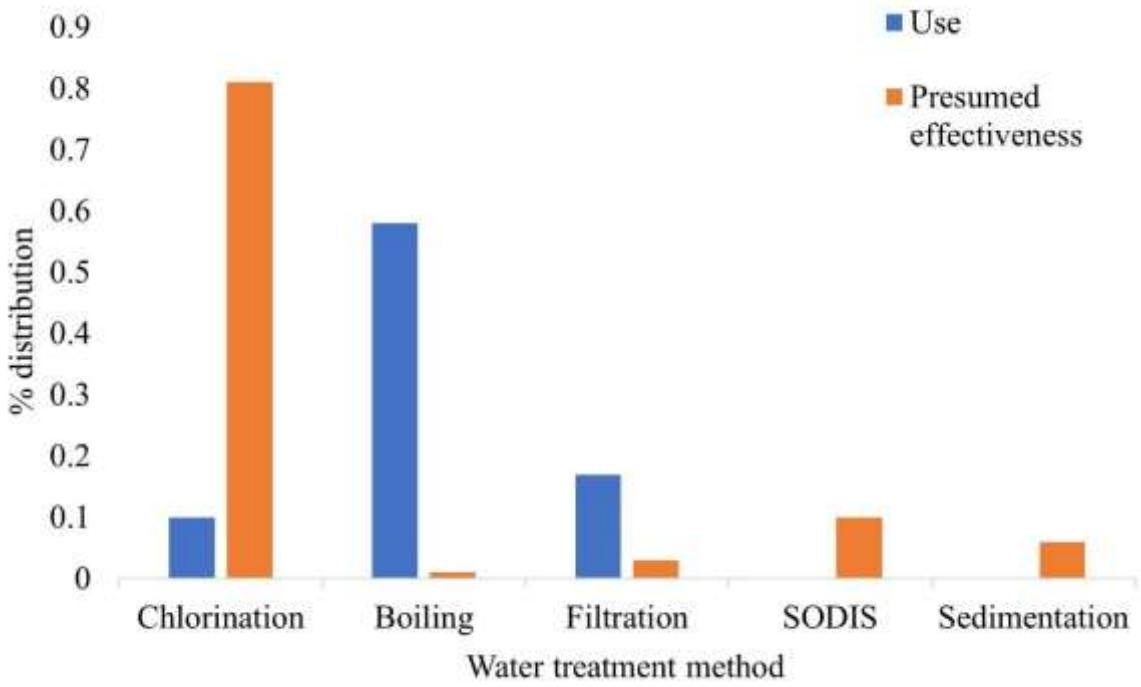

Figure 4.6 The percentage distribution of Obunga slum residents' utilized water treatment methods and their presumed effectiveness.

4.1.5 Type of toilet

It was found that most Obunga slum residents lived under unimproved sanitary conditions. As shown in Figure 4.7, 86% of the residents used pit latrines without a cover, 6% used pit latrines with a cover, 5% defecated in the open, 3% used a bucket and water for flushing, and none had a piped sewer system toilet.

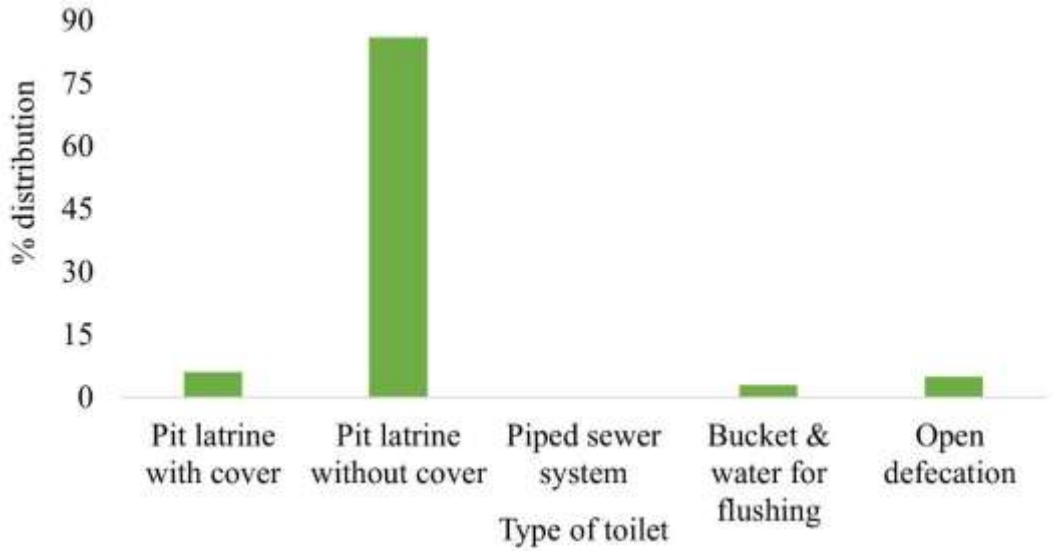

Figure 4.7 The percentage distribution of the type of toilet used by Obunga slum residents.

The sanitation practices assessment on 8th August 2018 revealed poor sanitation in Obunga slum. According to JMP for Water Supply Sanitation and Hygiene (2018), pit latrines with and without covers, buckets, and water for flushing and open defecation are all considered unimproved sanitation facilities. These were the only sanitation facilities used by the residents and indicated that Obunga slum residents sorely accessed unimproved sanitation facilities, as shown in Figure 4.8. This was also indicative of Kenya's expected failure to meet SDG 7 of having all citizens access to improved sanitation, emphasizing the need for

solutions to increase the number of residents with improved sanitation.

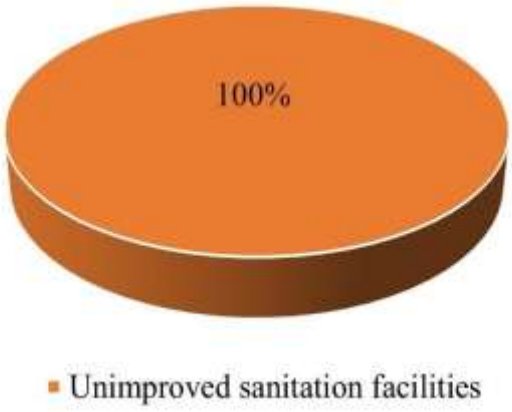

Figure 4.8 The distribution of access to improved and unimproved sanitation facilities by the residents of Obunga slum.

4.1.6 Level of cleanness of the toilets

None of the respondents found their toilets to be clean or very clean. As shown in Figure 4.9, 49.50% of the toilets were reported to be very dirty, 24.75% were dirty, 22.72% were fairly clean, and 2.97% of the respondents did not know the level of cleanliness of their toilets.

Figure 4.9 The cleanliness levels of toilets in Obunga slum.

4.1.7 Spearman's correlation of variables

Table 4.1 Correlation coefficients between water and sanitation factors

	Age	Level of education	Main source of drinking water	Choice to treat drinking water	Water treatment method	Cleanliness of toilet	Frequency of waterborne diseases
Age	1						
Level of education	-0.50	1					
Main source of drinking water	-0.011	0.084	1				
Choice to treat drinking water	0.134	0.149	0.306**	1			
Water treatment method	0.103	0.254 **	0.149	0.491**	1		
Cleanliness of toilet and sanitation	0.323**	0.016	-0.164	-0.122	-0.112	1	
Frequency of occurrence of waterborne diseases	-0.393**	0.068	-0.198*	-0.07	-0.063	-0.123	1

** Correlation is significant at the 0.01 level (2-tailed)

* Correlation is significant at the 0.05 level (2-tailed)

A moderate, significant, and negative correlation was observed between the age of the respondents and the frequency of occurrence of waterborne diseases, as seen in Table 4.1 (R^2 = -0.393, n = 345, $p \leq 0.05$). This indicated that children had the highest occurrence of infections. The UN categorizes children as the most vulnerable in the general population to infection with waterborne diseases and consequent death (ONU, 2022). The findings of this survey agreed with this statement and further emphasized the need for POU water treatment interventions to reduce the occurrence of waterborne diseases in children and generally improve their life outcomes.

There was a weak, significant, and positive correlation observed between the main source of drinking water and the choice to treat water, as seen in Table 4.1 (R^2 = 0.306, n = 345, p= 0.001). This meant that the safety of the water sources did not strongly influence the choice to treat the water. As can be seen in Figure 4.1 and Figure 4.3 65.35% of the residents used unsafe water sources, with only 59% of the population choosing to treat their water. Due to the various issues raised by the residents regarding the safety of all sources, the choice to treat drinking water probably depended more on the availability and cost of the treatment method than the source.

As seen in Table 4.1, a significant, weak, and negative correlation was observed between the main source of drinking water and the frequency of occurrence of waterborne diseases (R^2 = -0.198, n = 345, p = 0.039). This indicated that the safety of the source of drinking water did not strongly influence the occurrence of waterborne diseases. Most residents expressed a lack of capacity to access the improved water sources, which were costlier

than the unimproved sources. They also didn't trust the water availed by KIWASCO through the pipes shared within households, which they reported to be foggy due to vandalism exposing them to the open sewers. These factors, amongst others, resulted in their consumption of unsafe drinking water, exposing them to waterborne related diarrheal diseases. Therefore, water from all sources, regardless of safety, could result in infection of these diseases.

A weak, positive, and significant correlation was observed between the residents' level of education and the water treatment methods they used, as seen in Table 4.1 (R^2 =0.254, n = 345, $p \leq 0.05$). This meant that their level of education did not significantly influence the water treatment method chosen. With higher levels of education, it would be expected that the chosen water treatment method would be effective. However, cost also plays a significant role for the

in Table 4.1, a strong, positive, and significant correlation was observed between the residents' choice to residents. Therefore, the residents chose methods that were well-suited to their financial situation.

As is seen treat their drinking water and the methods of treatment used (R^2 = = 0.491, n = 345, $p \leq 0.05$). This means that the more likely residents were to treat their water, the more likely they were to use effective water treatment methods. As a result, most residents used boiling (57.43%), while very few used sedimentation (0.99%), which has no impact on the microbial safety of the water.

4.2 Testing the effectiveness of SODIS

Water samples obtained from the sources in zones I, II, III, and IV were fairly clear with below 26 NTU turbidity, as shown in Figure 4.10. The weather was hot and very sunny, with very few scattered clouds, making the conditions well suited for treatment. By noon, the temperature was an average of 29.4 ˚C, with the highest temperature being 32.6 ˚C. The SODIS experiments were set up between 10-11 am and 5-6 pm, with the sun intensity, temperature, and *E. coli* enumeration recorded during water treatment as shown in Table 4.2.

Figure 4.10 Water samples in 2-L PET bottles before SODIS.

Table 4.2: Field test results for 21st September.

Time (hrs)	**UV-A intensity mW/cm²**	**Temper-ature °F**	**Humid-ity %**	**Time in seconds**	**UV-A intensity in J/s.m²**	**Dose in J/m²**	**Dose in Kj/m²**	**Cum. Dose in Kj/m²**
1040-1140	2.49	79.9	47	3600	24.9	89640	89.64	89.64
1140-1240	2.755	83.5	42	3600	27.55	99180	99.18	188.82
1240-1340	2.818	86.7	40	3600	28.18	101448	101.448	290.268
1340-1440	2.655	90.7	37	3600	26.55	95580	95.58	385.848
1440-1540	1.667	89.5	40	3600	16.67	60012	60.012	445.86
1540-1640	1.952	89.1	37	3600	19.52	70272	70.272	516.132
1640-1740	1.153	88.7	41	3600	11.53	41508	41.508	557.64
1740-1805	0.269	87.3	40	1500	2.69	4035	4.035	561.675

Key: UV intensity, temperature and humidity readings were taken hourly. The UV-A dose was calculated using the formula: Dose= UV intensity in J/s.m² × time in seconds.

4.2.1 Results for water collected from Zone I

Water replicates obtained from Kasarani were collected from an open well, as shown in Figure 4.11 and labelled source 1a, source 1b and source 1c. Microbial analysis was done using labelled 3M™ Petrifilm™ *E. coli*/ Coliform count plates, as shown in Figure 4.12.

Figure 4.11 Ground source for water samples collected from zone I.

Figure 4.12 Incubated Petrifilms for water samples obtained from zone I during treatment: pre to post-SODIS.

Bacteria kill rates during water treatment depended on the type of bacteria and level of contamination. For *E. coli* bacteria, a > 99.99% kill rate was achieved. However, incomplete inactivation was achieved for coliform bacteria, with a 99.18% kill rate, as shown in Figure 4.13.

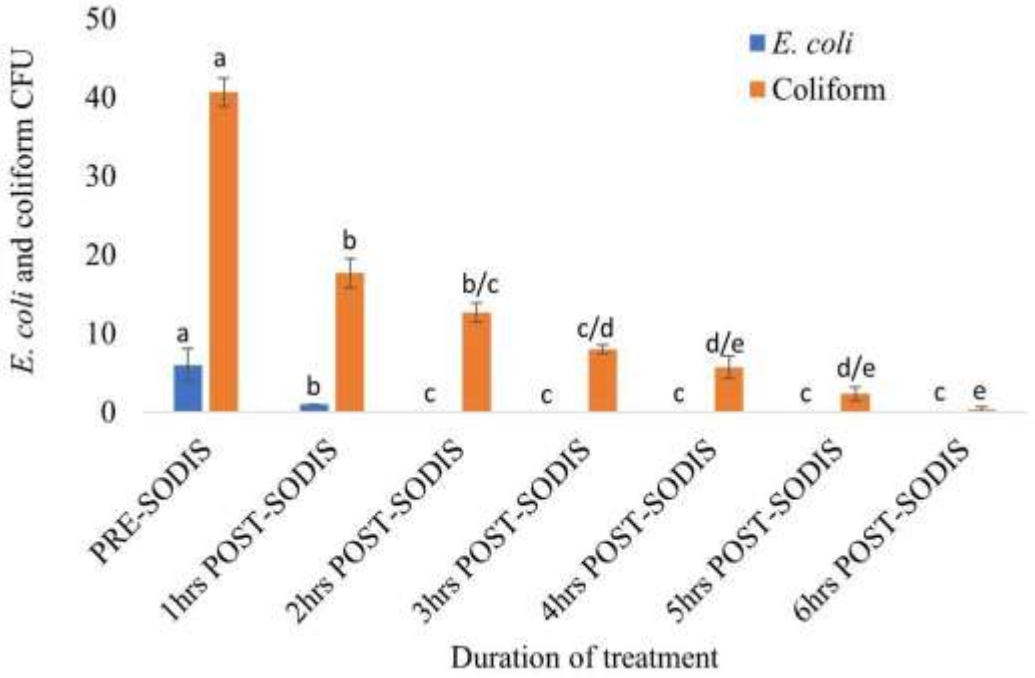

Figure 4.13 Inactivation of *E. coli* and coliform bacteria in water samples obtained from zone I during 6 hours of SODIS water treatment. Values within the same chart followed by the same letter did not differ significantly at $p \leq 0.05$.

4.2.2 Results for water collected from Zone II

Water replicates obtained from Sega were collected from an open well, as shown in Figure 4.14 and labelled source 2a, source 2b and source 2c. Microbial analysis was done using labelled 3M™ Petrifilm™ *E. coli*/ Coliform count plates, as shown in Figure 4.15.

Figure 4.14 Ground source for water samples collected from zone II.

Figure 4.15 Incubated Petrifilms for water samples obtained from zone II during treatment: pre to post-SODIS.

Complete bacteria inactivation was achieved when water samples from zone II were treated. The inactivation rate differed, however, with > 99.99% *E. coli* kill rate being achieved an hour before > 99.99 % coliform kill rate was achieved, as is shown in Figure 4.16.

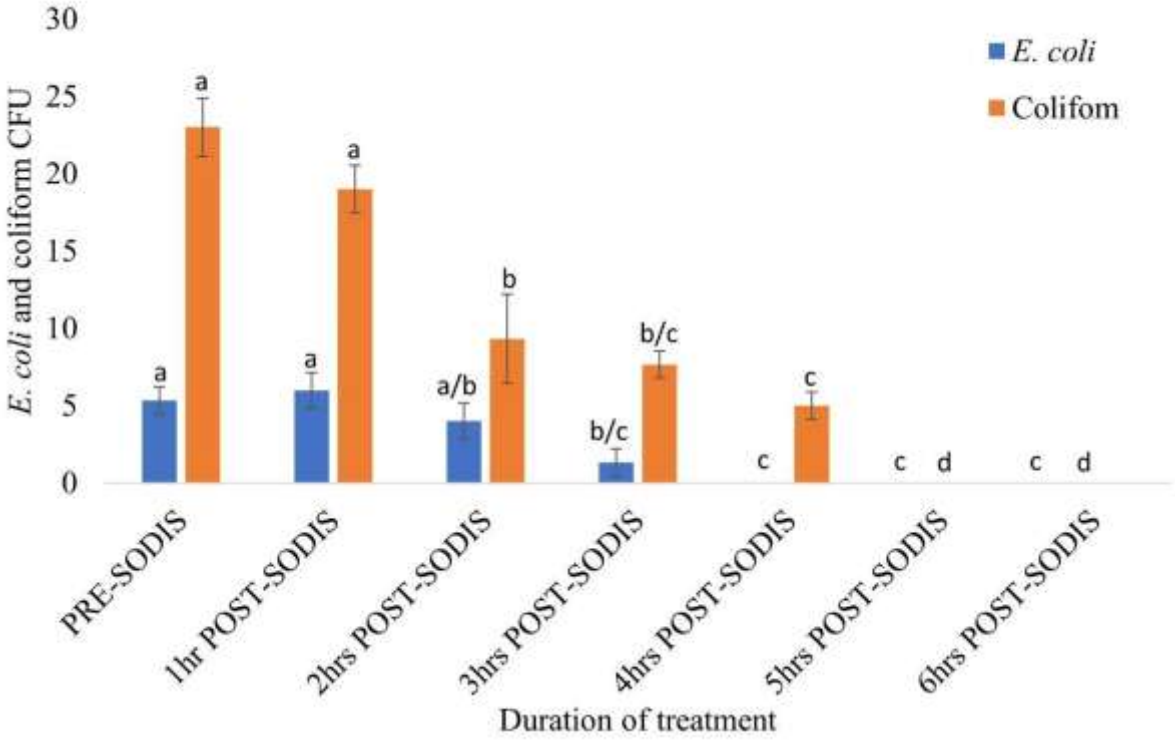

Figure 4.16 Inactivation of *E. coli* and coliform bacteria in water samples obtained from zone II during 6 hours of SODIS water treatment. Values within the same chart followed by the same letter did not differ significantly at $p \leq 0.05$.

4.2.3 Results for water collected from Zone III

Water replicates obtained from Central were collected from an open well, as shown in Figure 4.17 and labelled source 3a, source 3b and source 3c. Microbial analysis was done using labelled 3M™ Petrifilm™ *E. coli*/ Coliform count plates, as shown in Figure 4.18.

Figure 4.17 Ground source for water samples collected from zone III.

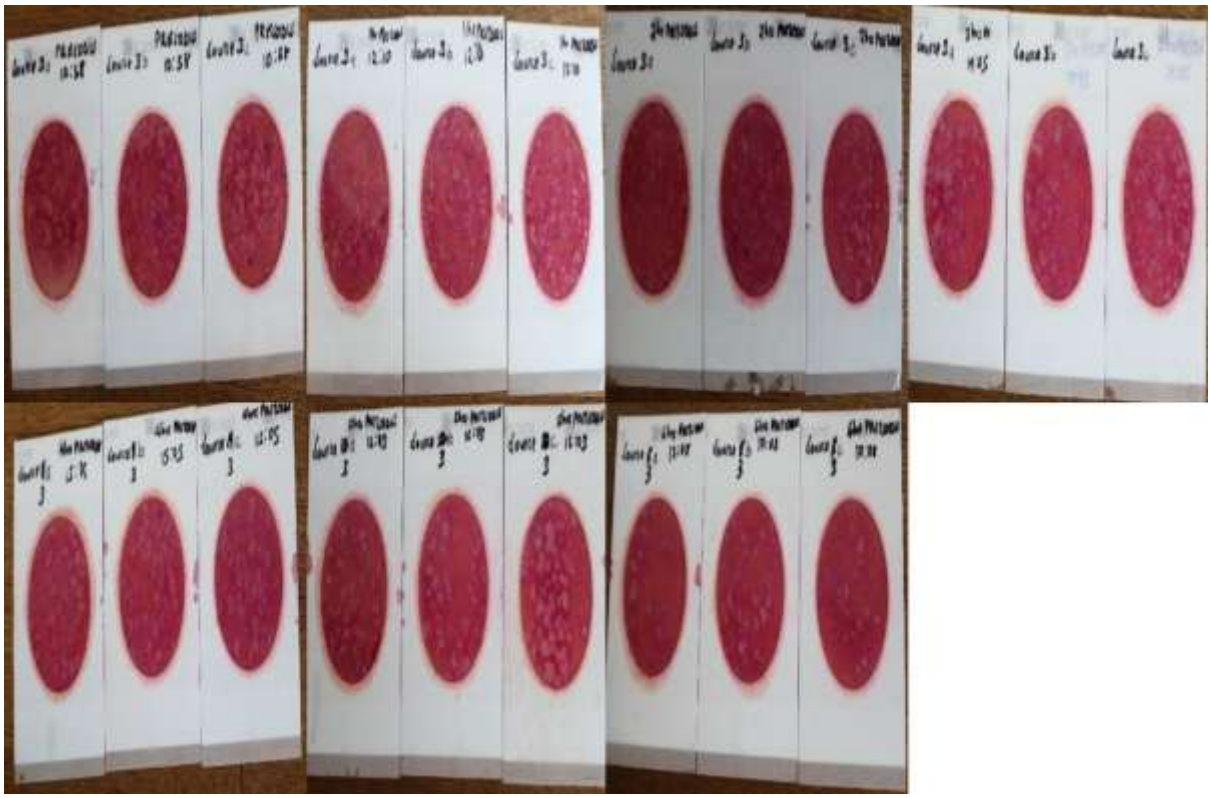

Figure 4.18 Incubated Petrifilms for water samples obtained from zone III during treatment: pre to post-SODIS.

Water obtained from zone III had the highest level of contamination of *E. coli* and coliform bacteria, which was attributed to cattle grazing around this source, as seen in Figure 4.17. Bacteria kill rates during water treatment were also found to depend on the type of bacteria and level of contamination. For *E. coli* bacteria, a > 99.99% kill rate was achieved. However, due to the high coliform contamination, only a 69.32% kill rate was achieved, as shown in Figure 4.19.

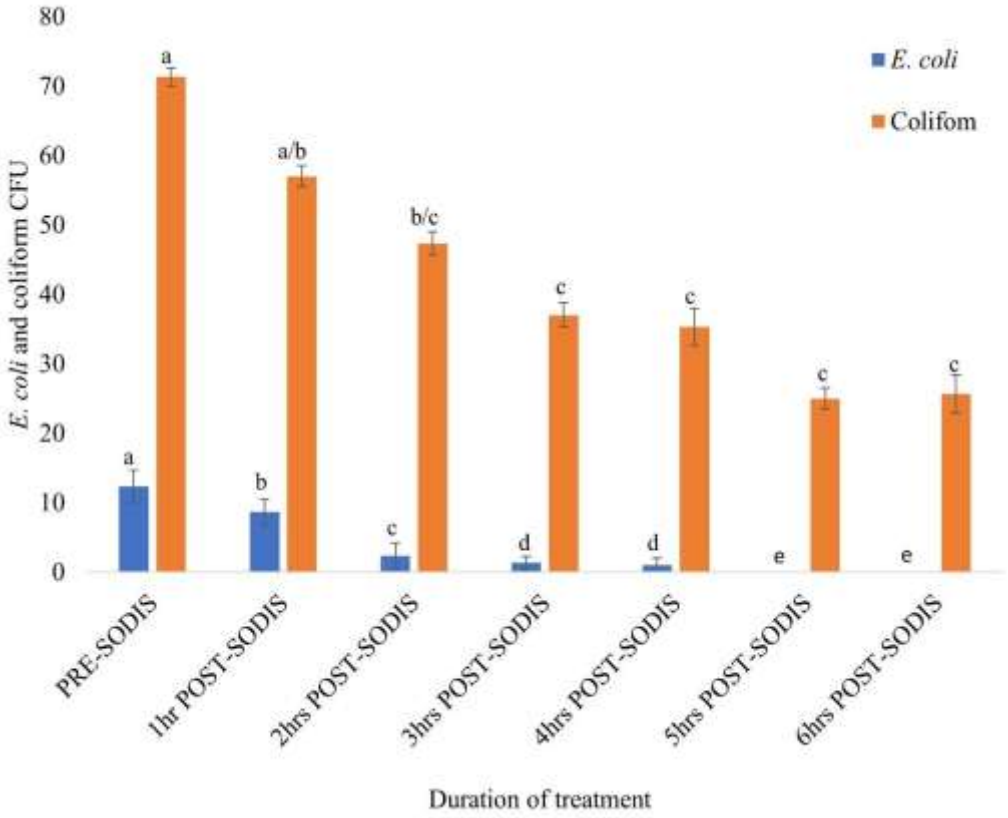

Figure 4.19 Inactivation of *E. coli* and coliform bacteria in water samples obtained from zone III during 6 hours of SODIS water treatment. Values within the same chart followed by the same letter did not differ significantly at $p \leq 0.05$.

4.2.4 Results for water collected from Zone IV

Water replicates obtained from Kamakowa were collected from an open well, as shown in Figure 4.20 and labelled source 4a, source 4b and source 4c. Microbial analysis was done using labelled 3M™ Petrifilm™ *E. coli*/ Coliform count plates, as shown in Figure 4.21.

Figure 4.20 Ground source for water samples collected from zone IV.

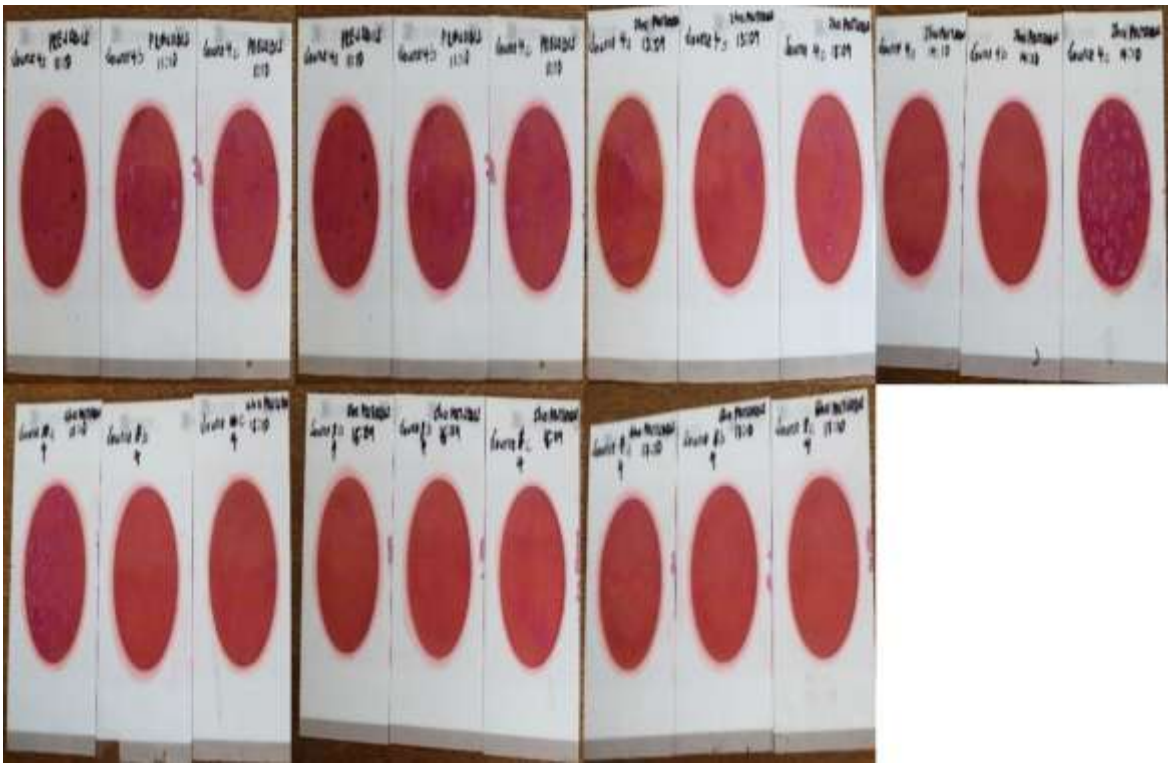

Figure 4.21 Incubated Petrifilms for water samples obtained from zone IV during treatment: pre to post-SODIS.

Water samples obtained from zone IV had the lowest level of contamination as compared to water samples from the other zones. Complete inactivation was achieved for *E. coli* bacteria, with a > 99.99% kill rate. Even though coliform contamination was low, incomplete inactivation was achieved, with a 97.67% kill rate, as shown in Figure 4.22.

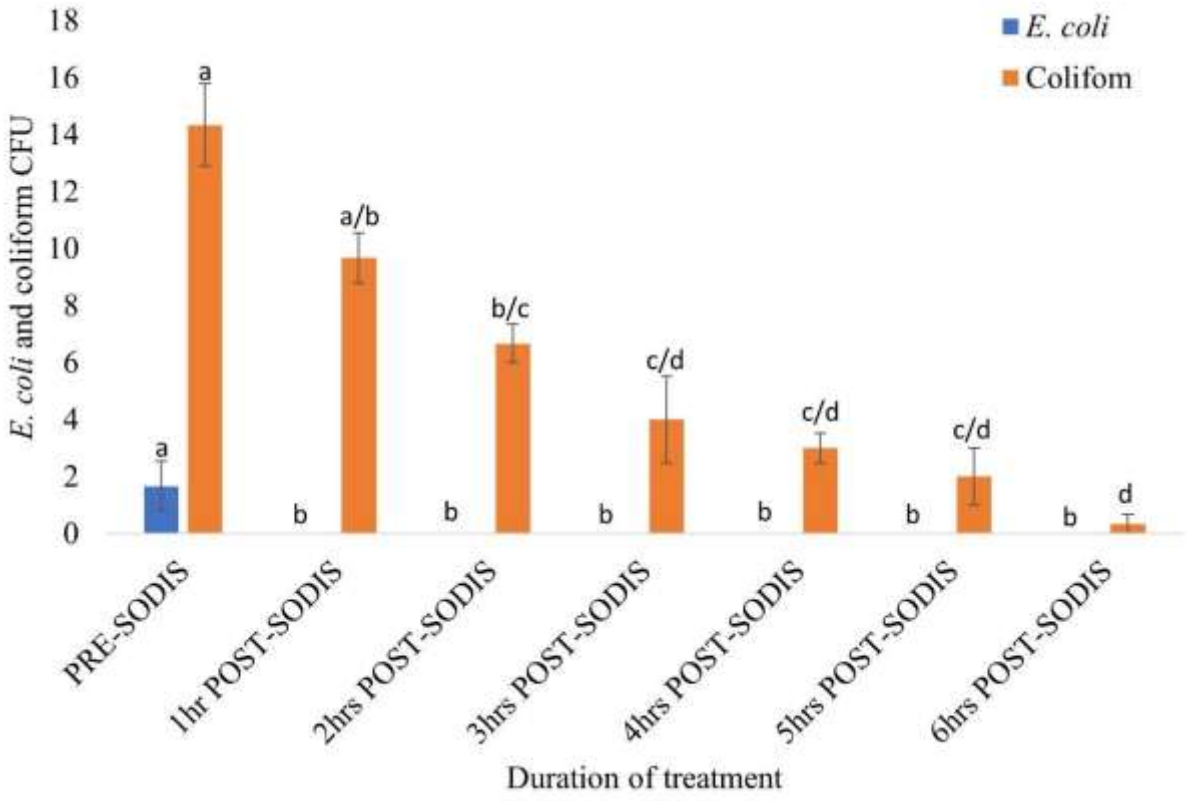

Figure 4.22 Inactivation of *E. coli* and coliform bacteria in water samples obtained from zone IV during 6 hours of SODIS water treatment. Values within the same chart followed by the same letter did not differ significantly at $p \leq 0.05$.

All the sources were found to be contaminated, which was expected as none met the requirements for delivery of safe water: they were left open and close to pit latrines, as shown in Table 4.3. The sources were also found to have different levels of contamination;

this affected the effectiveness of SODIS, as can be seen in the progression of disinfection in Figure 4.13, Figure 4.16, Figure 4.19 and Figure 4.22.

Table 4.3 Means of the bacteria counts for the sources obtained from zones I, II, III, and IV throughout SODIS water treatment.

Sources	**Bacteria mean (CFU)**
Zone I	6.738 ± 1.701^{b}
Zone II	5.762 ± 1.113^{b}
Zone III	23.167 ± 3.562^{a}
Zone IV	2.976 ± 0.683^{c}
p-value	0.001

Key: Values within the same column followed by the same letter did not differ significantly at $p < 0.005$.

As seen in Table 4.4, the level of *E. coli* and coliform bacteria contamination differed, with coliform bacteria contamination being significantly higher. As is also seen in Figure 4.13, Figure 4.16, Figure 4.19, Figure 4.22, and Figure 4.23 the inactivation rates differed, with complete inactivation only being achieved for *E. coli* bacteria. Even though higher non-*E. coli* coliform CFU were observed, a faster inactivation rate was achieved as compared to the inactivation of the lower *E. coli* CFU. Higher non-*E. coli* coliform bacteria contamination, compared to *E. coli* bacteria contamination, has been recorded by various researchers in contaminated water treated using SODIS compared to that observed during

research. They also found that the non-*E. coli* coliform bacteria inactivation was slower than *E. coli* bacteria inactivation (Al-Gheethi *et al*., 2013; Atikul Islam *et al*., 2015).

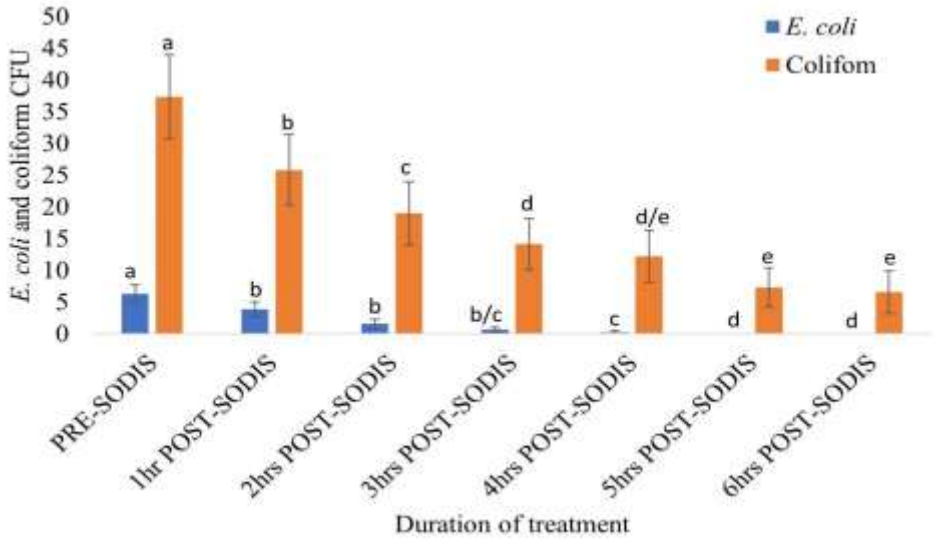

Figure 4.23 Inactivation of *E. coli* and coliform bacteria for water samples obtained from zones I, II, III, and IV during SODIS. Values within the same chart followed by the same letter did not differ significantly at $p \leq 0.05$.

Atikul *et al*. (2015) found that higher non-*E. coli* coliform inactivation rates were achieved compared to *E. coli* inactivation rates, with the initial non-*E. coli* coliform count being much higher than the initial *E. coli* count. This was attributed to *E. coli* having higher resistance to SODIS. However, as shown in Figure 4.23, complete inactivation was only achieved for *E. coli* bacteria. The non-*E. coli* coliform contamination observed during this work was lower than that observed by Atikul *et al*. (2015). Therefore, complete inactivation was expected. This study's findings suggest a possible higher resistance of non-*E. coli* fecal coliform bacteria to SODIS. However, further research is needed.

The selection of *E. coli* bacteria as the indicator micro-organism for SODIS was based on its higher resistance to SODIS and representative pattern of disinfection (Luzi *et al*., 2016).

However, research continues to prove that other microorganisms have a higher resistance to SODIS, and their deactivation patterns differ from those of *E. coli*. Wang *et al*. (2016) suggested the use of *Salmonella* sp. as the indicator micro-organism instead of *E. coli* due to its higher resistance to SODIS. The findings of this research support the need for research and the possible selection of a new indicator microorganism with a higher resistance to SODIS.

Table 4.4 Means of the *E. coli* and Coliform bacteria count for all water sources throughout SODIS water treatment.

Bacteria	**Bacteria mean (CFU)**
E. coli	1.821 ± 0.366^{b}
Coliform	17.500 ± 2.041^{a}
p-value	0.001

Key: Values within the same column followed by the same letter did not differ significantly at $p < 0.005$.

As seen in Table 4.5, a significant reduction in bacteria count was observed when water from all the sources was treated using SODIS. A 4 LVR equivalent to a 99.99% kill rate was only achieved for *E. coli* bacteria when the water from all the sources was exposed to the sun for 5 hours and a UV-A lethal dose of 516.13 Kj/m², as shown in Figure 4.24. It is generally assumed that a lethal dose of 2000 Kj/m² for a wavelength range of 350-450nm is required to achieve a 3 LRV for *E. coli* bacteria (Luzi *et al*., 2016). However, research findings have found that the lethal dose varies based on the bottle size, weather, and the

level of contamination (Lawrie *et al*., 2015; Samoili *et al*., 2022). The bottles under treatment were exposed to similar conditions, so the lethal dose reported in this work is expected to be true for Obunga slum. Additionally, treatment was only done for 6 hours, which is recommended as the ideal treatment period by the SODIS manual (Luzi *et al*., 2016).

Table 4.5 Means of the *E. coli* and Coliform bacteria count throughout SODIS water treatment.

Duration	Bacteria mean (CFU)
PRE-SODIS	21.833 ± 4.618^{a}
Ihr POST-SODIS	14.875 ± 3.609^{b}
2hrs POST-SODIS	10.292 ± 3.064^{c}
3hrs POST-SODIS	7.417 ± 2.431^{d}
4hrs POST-SODIS	6.250 ± 2.359^{d}
5hrs POST-SODIS	3.667 ± 1.705^{e}
6hrs POST-SODIS	3.292 ± 1.787^{e}
p-value	0.001

Key: Values within the same column followed by the same letter did not differ significantly at $p < 0.005$.

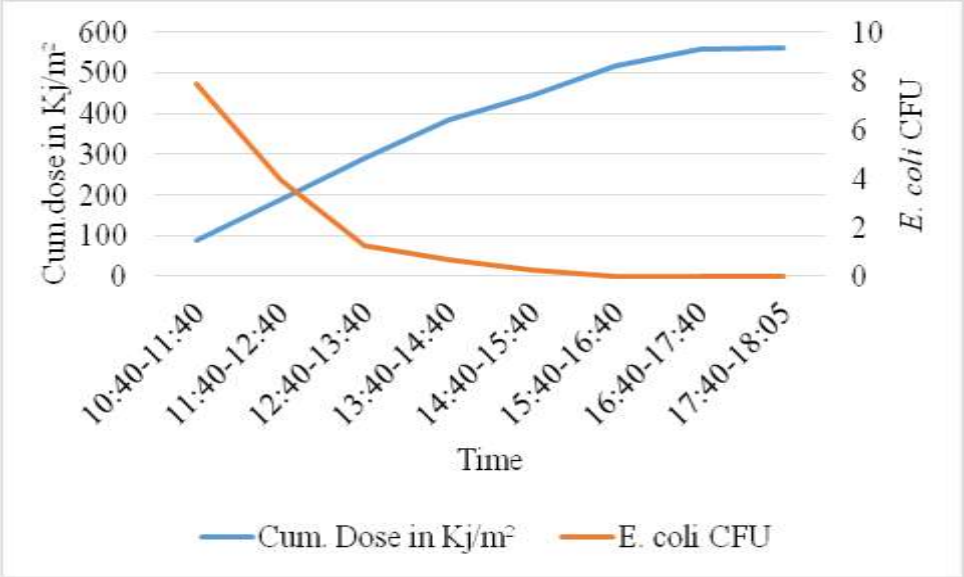

Figure 4.24 *E. coli* bacteria inactivation profile showing the lethal UV-A dose.

The tap water availed through standing pipes shared within households is supplied by KIWASCO. Therefore, comparing the water treatment methods used by KIWASCO and SODIS would be viable. However, it is impossible to compare the disinfection methods of KIWASCO Dunga and Kajulu water treatment plants with SODIS because there is no documented evidence of the specific disinfection method used. However, it is assumed that KIWASCO follows conventional water treatment processes, which align with best practices. The main steps involved in their water treatment processes are coagulation, sedimentation, filtration, and disinfection (Colorado, n.d.). Disinfection can be done using chlorination, ozonation, and UV radiation, which are highly effective methods of decontamination.

4.3 Optimization of Green Synthesis of Ag/TiO_2 Nanocomposite

This work did not involve the profiling of phenolic compounds for WMRE. However, previous research has covered this profile. Mushtaq *et al.* (2015) performed the

watermelon rind phenolic compound profile following the Response Surface Methodology (RMS). They found that the major phenolic compounds were sinapic, chlorogenic, vanillic, *p*-coumaric, and *p*-hydroxybenzoic acid, with chlorogenic acid having the highest concentration. The identification of the peaks around 270nm as C=O chromophore in the WMRE is based on the findings of Navarra et al. (2017), who attributed the peak at 275nm to the C=O chromophore in the caffeine molecule.

4.3.1 Effect of Time on the synthesis of WMAT nanocomposite

The effect of reaction time on the synthesis of WMAT nanocomposite was investigated at 15, 25, 35, and 45 minutes, while the other operating conditions were held constant at 100 ℃ and pH 12. The resulting solutions, before centrifugation, are shown in Figure 4.25. The UV-Vis spectra recorded are shown in Figure 4.26. The reaction time influences the size of nanoparticles during synthesis (Darroudi *et al*., 2011). This is because it affects the time available for the reagents to interact. At optimal reaction time, the reagents react completely, resulting in desirable particle size. However, when the reaction is carried out below the optimal time, the reactants do not react entirely and would, therefore, result in a lower concentration of formed nanoparticles. Whereas beyond the optimal reaction time, agglomeration occurs (Kobese, 2018).

Figure 4.25 The WMAT solutions resulting from optimization at 15, 25, 35, and 45 minutes prior to centrifugation.

When performed for 15 minutes, a brown solution was observed, with two peaks at 267 and 370 nm. These peaks related to the C=O chromophore in the WMRE and TiO_2 nanoparticles, respectively (Navarra *et al*., 2017; Zhao *et al*., 2017). When the synthesis was done for 25 minutes, a brown solution was observed with two peaks at 267 and 370 nm, which were related to the C=O chromophore in the WMRE and TiO_2 nanoparticles, respectively, with no peak in the visible light region. The absence of a peak in the UV region when the reaction was done for 15 and 25 minutes, as seen in Figure 4.26, was attributed to the lack of formation of Ag nanoparticles since the reaction time did not permit their complete formation and modification on the surface of TiO_2.

When the synthesis was done for 35 minutes, visible light activity was observed, with a brownish-grey solution with two peaks at 270 and 412 nm, which were related to the C=O chromophore in the WMRE and Ag/TiO_2 nanocomposite, respectively. When it was done for 45 minutes, a hyperchromic shift in the visible light absorbance was observed, with a brownish-grey solution with peaks at 274 and 425 nm, which were related to the C=O chromophore in the WMRE and Ag/TiO_2 nanocomposite, respectively. The peaks

observed in the visible light region when the reactions were done for 35 and 45 minutes were due to the SPR of Ag nanoparticles, which caused a shift to the visible region upon modification (Sharma, 2021). A peak at 425 nm with a higher absorbance of 0.37 au was observed for 45 minutes, compared to the peak at 412 nm with an absorbance of 0.14 au when the synthesis was done for 35 minutes. Therefore, 45 minutes was chosen as the optimal WMRE mediated-Ag/TiO_2 synthesis time.

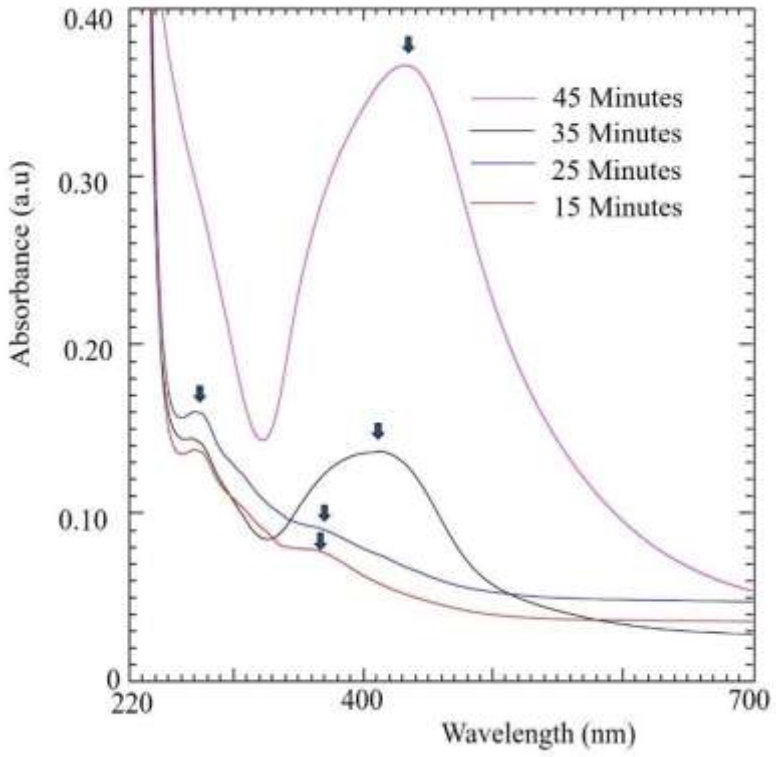

Figure 4.26 UV-Vis spectra showing the influence of time on the synthesis of WMAT nanocomposite.

4.3.2 Effect of temperature on synthesis of WMAT nanocomposite

The effect of temperature on the synthesis of WMAT was investigated at room temperature (25 ℃), 40 ℃, 80 ℃, and 100 ℃ while the pH and time were kept constant at 12 and 45

minutes. The resulting solutions, before centrifugation, are shown in Figure 4.27. The UV-Vis spectra for the optimizations were recorded, as shown in Figure 4.28. Temperature is an important parameter during the green synthesis of nanoparticles. This is due to its influence on the nucleation and growth of nanoparticles and the solubility of phenolic components of the plant extract. A steady increase in temperature has been found to promote nucleation overgrowth, resulting in the formation of small nanoparticles. This increase also results in higher solubility of the phenolic components of the plant extract (Che *et al*., 2017; Stavinskaya *et al*., 2019).

Figure 4.27 The WMAT solutions resulting from optimization at 25, 40, 80, and 100 ℃ before centrifugation.

At room temperature, a brown solution with two peaks was observed at 270 and 370 nm, related to the C=O chromophore in the WMRE and TiO_2 nanoparticles, respectively. An increase in temperature to 40 ˚C resulted in a brown solution with two peaks at 270 and 370 nm, which were related to the C=O chromophore in the WMRE and TiO_2 nanoparticles, respectively. The absence of an absorption peak in the visible light region indicated no modification of Ag nanoparticles on TiO_2 nanoparticles.

At 80 ℃, a brownish-grey solution with two peaks which were observed at 270 and 420 nm, relating to the C=O chromophore in the WMRE and Ag/TiO_2 nanocomposite, respectively. At 100 ˚C, a hyperchromic shift in the visible light activity was observed with a brownish-grey solution with two peaks at 270 and 425 nm, which were related to the C=O chromophore in the WMRE and Ag/TiO_2 nanocomposite, respectively. Visible light activity attributed to Ag/TiO_2 was only observed when synthesis was done at 80 and 100 ℃. Kredy *et al*. (2018) and Ndikau *et al*. (2017) found that higher temperatures favoured the green synthesis of silver nanoparticles, which they attributed to the promotion of nucleation overgrowth owing to an increase in the kinetic energy (k.e) of the nanoparticles and increased solubility of the phenolic components of the plant extract. Therefore, a temperature of 100 ℃ was chosen as the optimal operating temperature, resulting in a peak with higher absorbance.

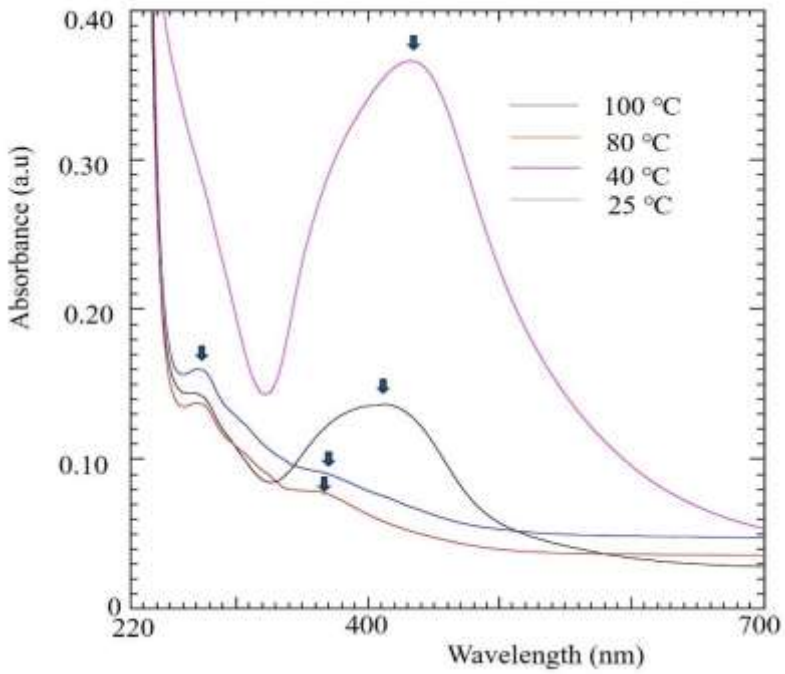

Figure 4.28 UV-Vis spectra showing the influence of temperature on the synthesis of WMAT nanocomposite.

4.3.3 Effect of pH on the synthesis of WMAT nanocomposite

The effect of pH on the synthesis of WMAT nanocomposite was investigated at pH 8, 10, and 12 while the temperature and time were held constant at 100 ℃ and 45 minutes. The resulting solutions, before centrifugation, are shown in Figure 4.29. The UV-Vis spectra were recorded for each optimization, as seen in Figure 4.30. Basic conditions favour the green synthesis of Ag nanoparticles. This is because, under acidic pH, a high concentration of H^+ ions is created and repels the Ag^+ ions, forming large nanoparticles (Khan *et al*., 2022). Under basic pH, the high concentration of OH^- ions creates a large number of available active functional groups, which interact with Ag^+ , thereby reducing them.

Figure 4.29 The WMAT solutions resulting from optimization at pH 8, 10, and 12 prior to centrifugation.

At pH 8, a brown solution with two peaks which were observed at 260 and 361 nm relating to the C=O chromophore in the WMRE and TiO_2 nanoparticles, respectively. At pH 10, a brownish-grey solution with visible light activity was observed with three peaks at 270, 361, and 412 nm, which were related to the C=O chromophore in the WMRE, TiO_2 nanoparticles, and Ag/TiO_2 nanocomposite, respectively. At pH 12, a brownish-grey solution with a hyperchromic shift in visible light activity was observed with two peaks at 270 and 425 nm. Handayani et al. (2020) found that the synthesis of Ag nanoparticles using *Pometia pinata* was favoured by basic conditions; an increase in pH from 4 to 11 resulted in the formation of smaller nanoparticles. Figure 4.30 shows that visible light activity was only observed at pH 10 and 12. The peak observed at pH 12 had a higher absorbance and was chosen as the optimal pH.

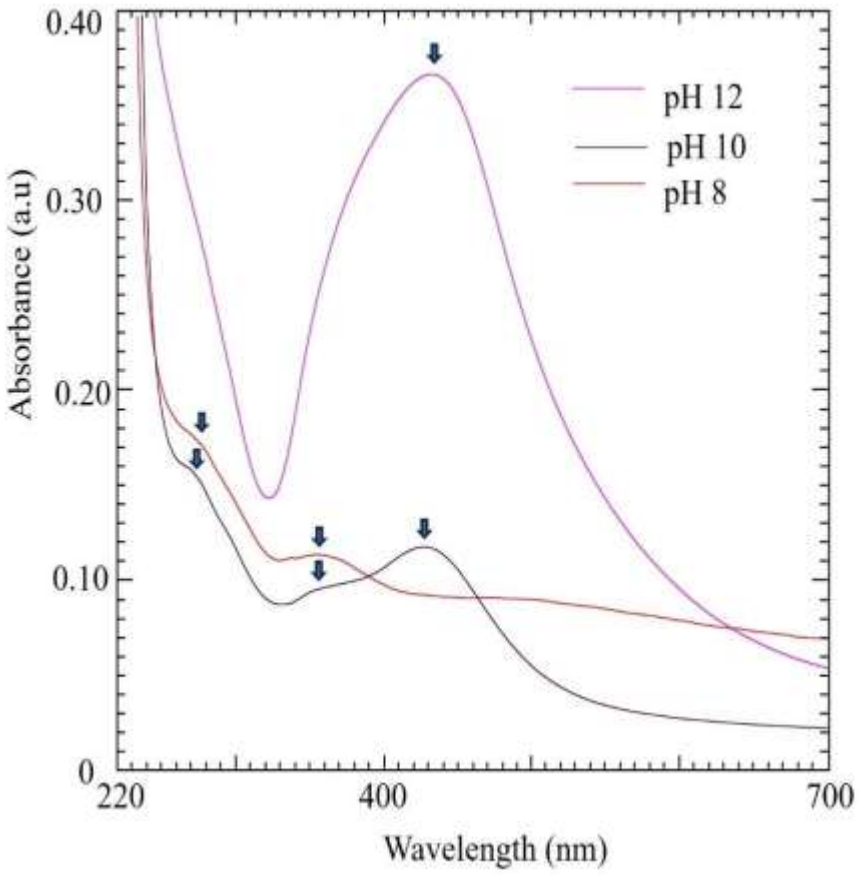

Figure 4.30 UV-Vis spectra showing the effect of pH on the synthesis of WMAT nanocomposite.

4.4 Synthesis of Ag/TiO_2 nanocomposite using WMRE and $NaBH_4$ as the reducing agents

Comparisons were made between the visible light absorption peaks of the WMAT and NBAT nanocomposites, as shown in Figure 4.31. The solutions resulting from their synthesis before centrifugation are shown in Figure 4.32. Absorbance peaks were observed at 425 nm, with an absorbance of 0.37 au for WMAT nanocomposite, and a small peak was observed at 519 nm, with an absorbance of 0.017 au for NBAT nanocomposite. Even though both synthesis methods resulted in the extension of the activity into the visible light region, a hyperchromic shift was observed for the WMAT nanocomposite.

This was indicative of better synthesis efficiency of the WMRE compared to $NaBH_4$. These results were in agreement with those of Ndikau et al. (2017), who found that green synthesis of Ag nanoparticles using WMRE resulted in smaller nanoparticles than when synthesis was done using trisodium citrate dihydrate ($C_6H_5O_7Na_3.2H_2O$).

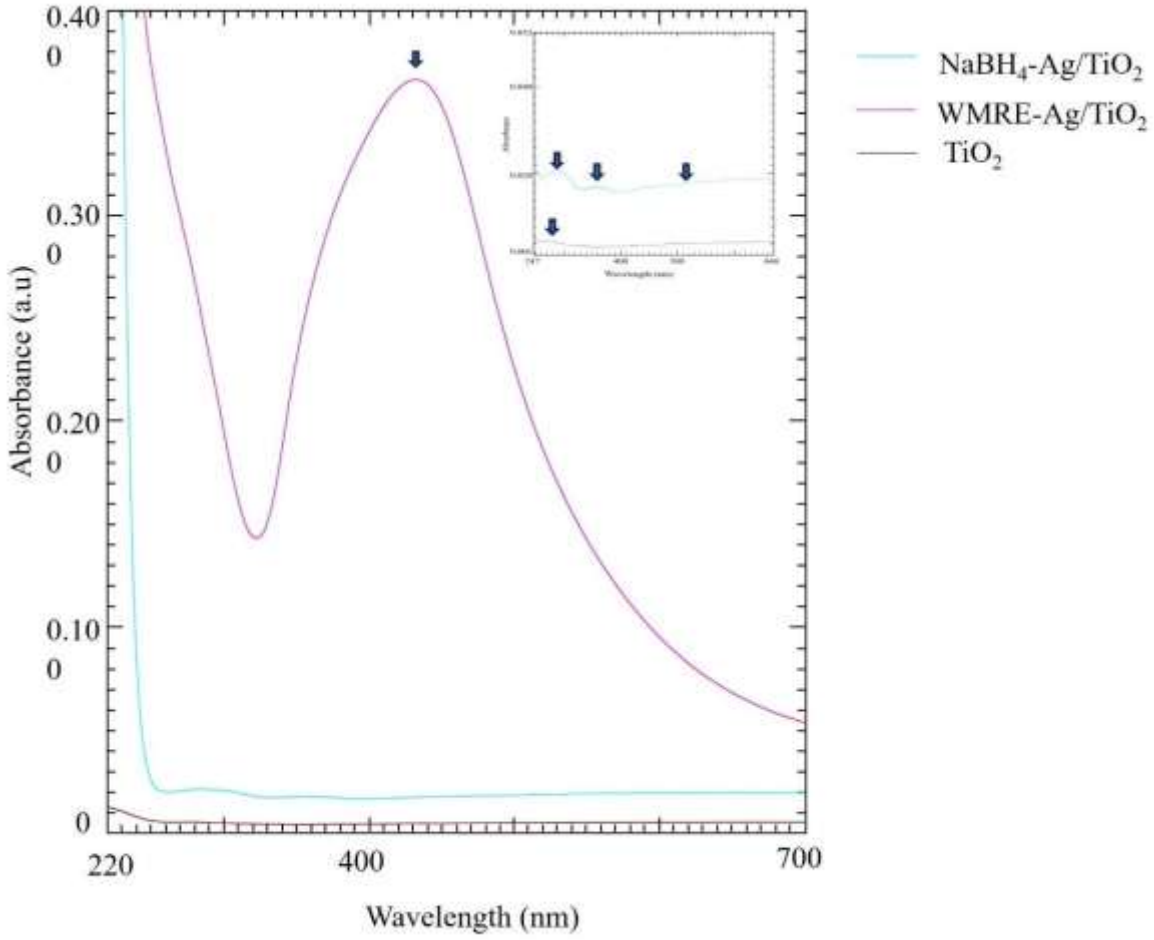

Figure 4.31 UV-Vis spectra for TiO_2, WMAT, and NBAT nanocomposites.

Figure 4.32 The WMAT solutions resulting from WMAT and NBAT synthesis prior to centrifugation.

4.5 Characterization

4.5.1 FTIR Spectra

Figure 4.33 shows the FTIR spectra for pure TiO_2, WMAT, and NBAT nanocomposites. Absorption peaks were observed at 3398, 2974, 1465, 1068, 875, and 470 cm^{-1} for the starting material, pure TiO_2. The band observed at 3398 cm^{-1} was attributed to the vibration of the O-H, indicating the presence of chemically adsorbed water in the starting material. Absorption bands at 2974 cm^{-1} and 1068 cm^{-1} could be attributed to C-H and C-O stretching vibrational frequencies (Renuga Devi and Gayathri, 2010). The peaks are attributed to the presence of residual carbon in the TiO_2, WMAT, and NBAT, with C-H and C-O functional groups (Henegar and Gougousi, 2015). The bands at 1465 cm^{-1} and the symmetric bands between 500-900 cm^{-1} found in the starting material and synthesized materials were attributed to the vibration of the Ti-ligand bond (Rao *et al*., 2019).

Additional bands were observed for the Ag/TiO_2 nanocomposites at 1649, 1383, 1387, and 1062 cm^{-1}. The band at 1649 cm^{-1} in the WMAT nanocomposite was attributed to the

stretching vibration of the C=O bond (Wei *et al*., 2017). The symmetric bands observed at 1383 and 1387 cm^{-1} in WMAT and NBAT were attributed to the Ag-O-Ti vibration (Rao *et al*., 2019). The band at 1062 cm^{-1} and 1075 cm^{-1} in the WMAT and NBAT nanocomposites were attributed to C-O stretching vibrational frequencies (Renuga and Gayathri, 2010).

The absorption bands and intensities observed in WMAT nanocomposite supported previous findings on the activity of OH and CO functional sites in reducing and stabilizing nanoparticles during green synthesis (Liu *et al*., 2018). As seen in Figure 4.33, the unique peak observed at 1649 cm^{-1} in WMAT, and attributed to the stretching vibration of the C=O, supported the findings that stabilization of Ag nanoparticles occurred at the C=O bond. This process is shown in Figure 2.8 and is described in 2.3.1 Green synthesis of Ag/TiO2 nanocomposite using *Citrullus lanatus* rind extract.

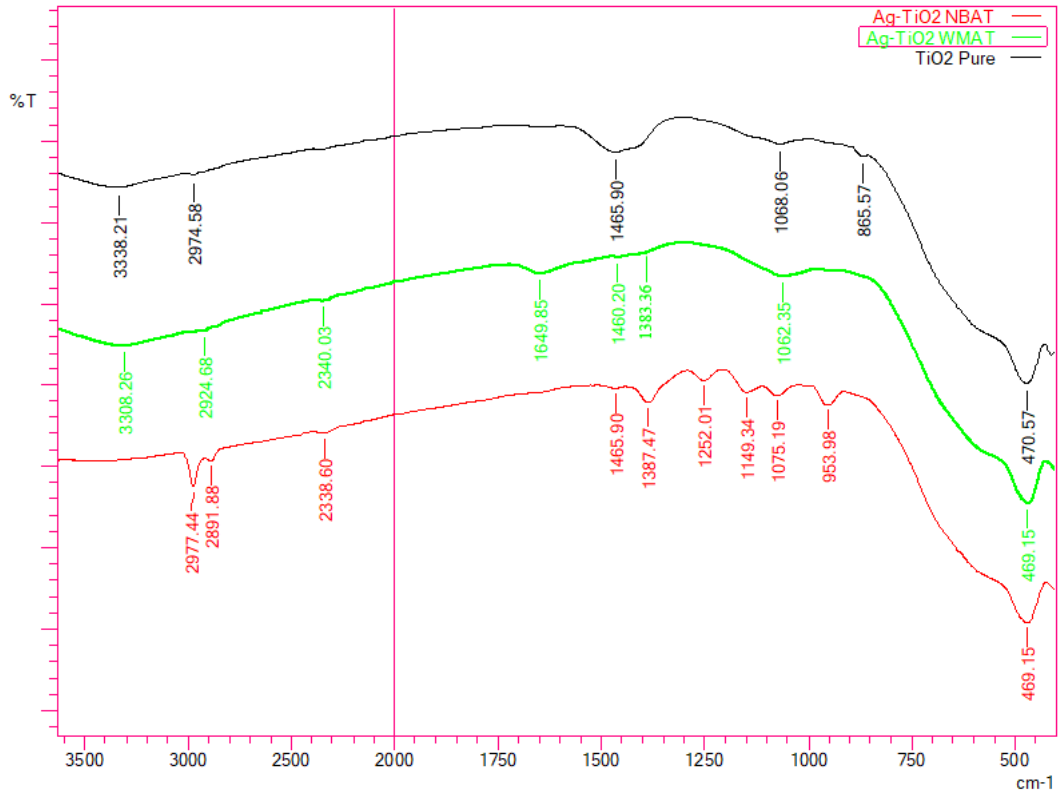

Figure 4.33 FTIR spectra of the TiO_2 nanoparticles, WMAT, and NBAT nanocomposites.

4.5.2 Elemental Analysis

Table 4.6 shows the elemental composition of TiO_2 nanoparticles and WMAT and NBAT nanocomposites. These results show that the modification of TiO_2 nanoparticles with Ag nanoparticles using WMRE as the reducing agent resulted in 10.3966% modification, while using a chemical method using $NaBH_4$ as the reducing agent resulted in 17.8652% modification.

Table 4.6 XRF Elemental composition by percentage weight of the starting material and synthesized nanocomposites.

Element wt%	Ti	Zn	Si	Mg	Ag
TiO_2	95.5610	1.5967	0.4793	0.4046	-
WMAT	85.4629	1.7825	0.2783	-	10.3966
NBAT	77.9384	1.8788	0.3080	-	17.8652

Elemental EDS identified elements below the detection limit of XRF. Figure 4.34 shows the elemental composition of TiO_2 nanoparticles, WMAT, and NBAT nanocomposites. The main elements in the WMAT were 83.3 and 3.5% TiO_2 and Ag, respectively, while the main elements in NBAT were 85.4 and 6.0% TiO_2 and Ag, respectively. The strong peak observed at 4.5 keV for TiO_2 in TiO_2 nanoparticles, WMAT, and NBAT nanocomposites confirmed that it was the major component. Additionally, 10.4, 11.3, and 7.2% elemental carbon (C) was observed in TiO_2 nanoparticles, WMAT, and NBAT nanocomposites. This elemental carbon was attributed to residual carbon in the TiO_2 and probable electron-beam-induced carbon contamination (Henegar and Gougousi, 2015; Hettler *et al*., 2017; Hugenschmidt *et al*., 2023). Aluminium (Al) was observed in TiO_2 nanoparticles, WMAT, and NBAT nanocomposites with a composition of 1, 1.3, and 1.4%, respectively. Chlorine (Cl) was observed only in WMAT at a composition of 0.6%.

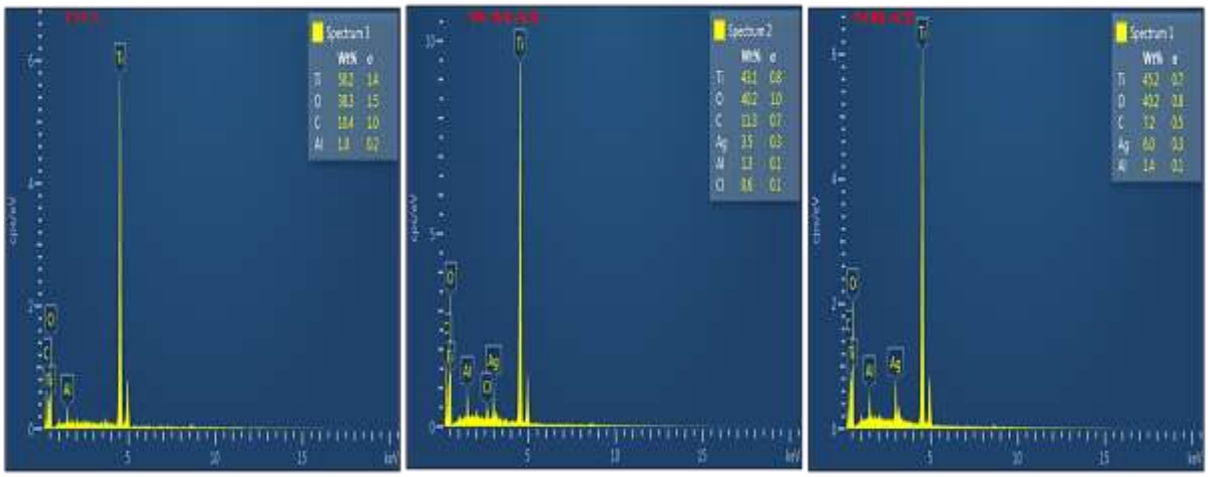

Figure 4.34 EDS elemental composition of the starting material and synthesized nanocomposites.

4.5.3 X-ray Diffraction (XRD)

The crystallite size and phase composition of the starting material and synthesized nanocomposites were determined using XRD analysis. Figure 4.35 shows the X-ray diffraction spectra for pure TiO_2 nanoparticles, WMAT, and NBAT nanocomposites.

The major diffraction peaks observed, for TiO_2, at two-theta (2θ) = 28.00°, 34.67°, 46.81°, 54.77° and 65.85° corresponding to the tetragonal rutile phase crystal planes of (110), (101), (210), (211) and (221) [ICSD No. 00-021-1276]. The peak splitting observed in the (110) and (101) crystal planes was attributed to various stresses (Ali, 2024). On the other hand, the tetragonal anatase phase was observed with major peaks at two-theta (2θ) = 37.78°, 45.93° and 66.93° corresponding to the crystal planes of (004), (200) and (116) [ICSD No. 00-021-1272]. Diffraction peaks were observed at two-theta (2θ) = 26.09° and 34.53°corresponding to the anatase crystal planes of (110) and (101); 52.49° corresponding to the rutile crystal plane of (105) for both WMAT and NBAT. As can be seen, no new peaks were observed after modification of the surface of TiO_2 with Ag nanoparticles. Singh

and Kumar (2021) suggested that the absence of new peaks upon modification of TiO_2 with Ag was due to the uniform distribution of the Ag nanoparticles, which resulted in no new peaks.

The crystallite sizes of the starting material and synthesized nanocomposites were calculated using Equation 2.17. The crystallite sizes were 26.87nm for TiO_2 nanoparticles, 25.49nm for WMAT, and 21.85nm for NBAT. This finding indicates that modification with Ag generally inhibits grain growth.

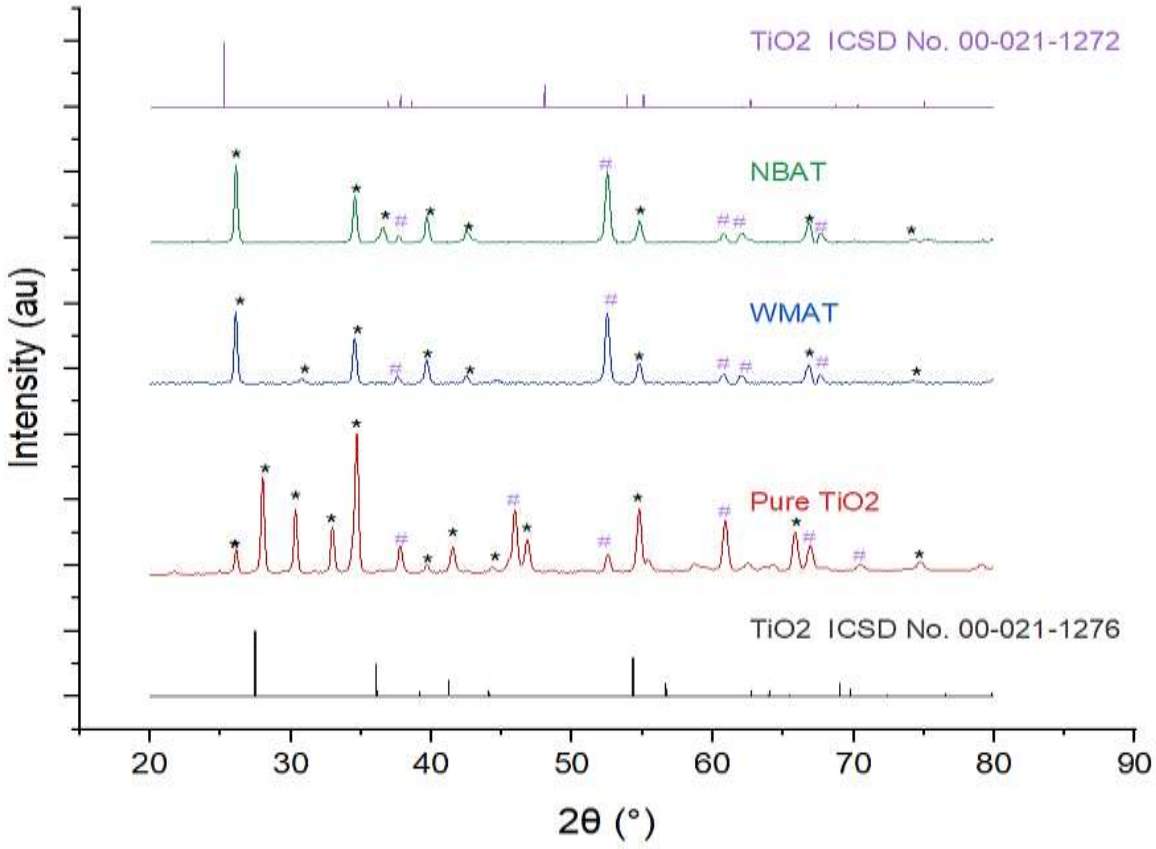

Figure 4.35 X-ray diffraction spectra of the starting material and synthesized nanocomposite where * and # are the rutile and anatase phases, respectively.

4.5.4 Scanning Electron Microscopy (SEM)

Figure 4.36 shows the SEM micrographs of the pure TiO_2 nanoparticles, WMAT, and NBAT nanocomposites. The surface properties of the Ag/TiO_2 nanocomposites were found to differ depending on the synthesis method. The $NaBH_4$ synthesized Ag/TiO_2 nanocomposite was found to have a higher dominance of darker grey shading than the WMRE-synthesized Ag/TiO_2 nanocomposite. However, the TiO_2 and Ag nanoparticles could not be distinguished, necessitating TEM imaging.

Even though the Ag and TiO_2 nanoparticles could not be distinguished, variations in grey shading were observed upon modification. The intensity of the grey shading depends on the atomic weight, increasing with increasing atomic weight (Saladra and Kopernik, 2016). This variation was attributed to modifying Ag nanoparticles on the TiO_2 surface. Ag atoms were the heaviest observed, weighing 107.87 amu compared to 47.9 amu for TiO_2. When modification was done using $NaBH_4$ as the reducing agent, the patches of very dark grey were higher than when WMRE was used as the reducing agent. This was attributed to a higher modification when $NaBH_4$ was used as the reducing agent, as shown in Table 4.6.

Some agglomeration was observed in WMAT, as seen in Figure 4.36. This was attributed to the electrostatic attraction of the WMRE capping agents coating the surface of Ag nanoparticles. Aminuzzaman *et al*. (2018) synthesized zinc oxide (ZnO) nanoparticles using *Garcinia mangostana* fruit pericarp aqueous extract and observed some agglomeration in the nanoparticles. They attributed this to the attraction of the biomass layer of the extract formed on the surface of the nanoparticles. These findings have also

been supported by those of Shanavas *et al*. (2019) and Abdullah *et al*. (2020) who observed agglomeration in TiO_2 nanoparticles synthesized using *Phyllanthus niruri* leaf extract and iron oxide (Fe_2O_3) nanoparticles synthesized using *Pheonix dactylifera* leaf extract.

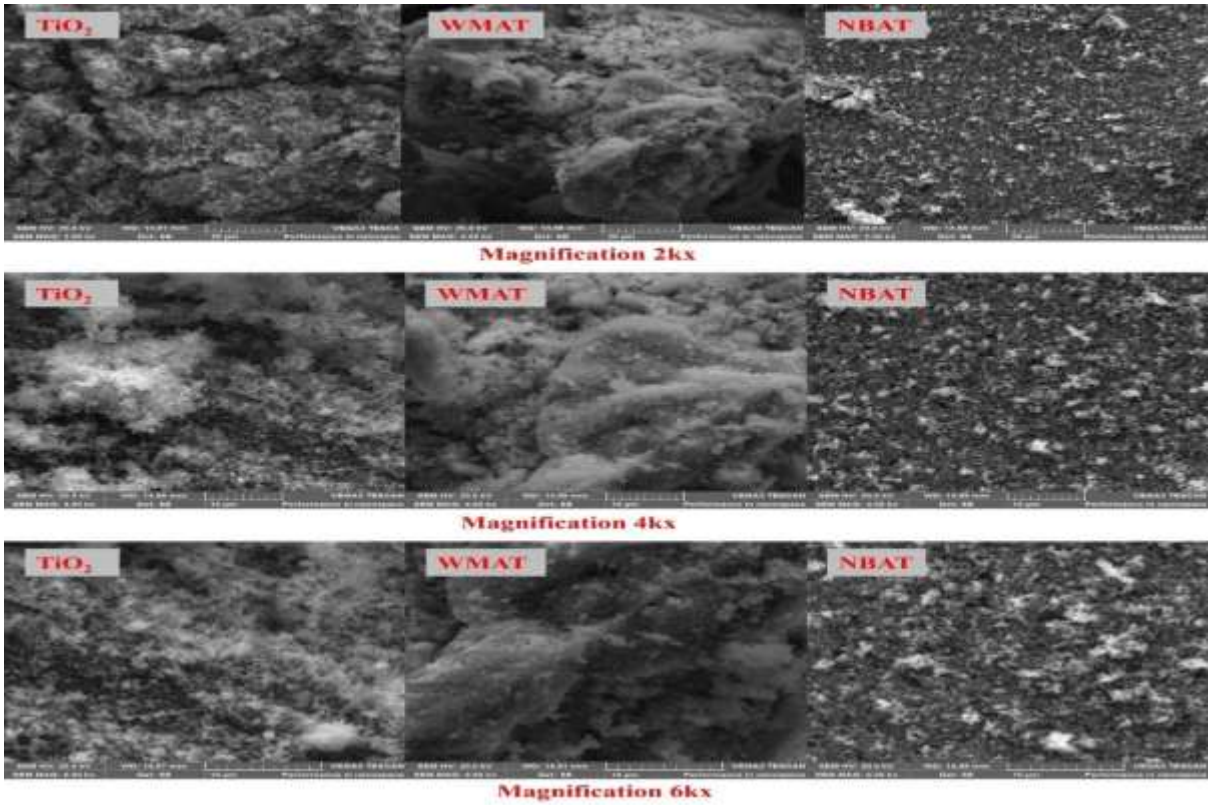

Figure 4.36 SEM images of the starting material and synthesized nanocomposites.

4.5.5 Transmission Electron Microscopy

Figure 4.37 shows the TEM micrographs of TiO_2 nanoparticles, WMAT, and NBAT nanocomposites. The TiO_2 nanoparticles had a spherical shape with an average diameter of 152.62 ± 64.11 nm. They were also observed to have an irregular thin layer, which was due to the presence of a layer of aluminium oxide (Al_2O_3) (Niño-Martínez *et al*., 2008). The shape of synthesized Ag nanoparticles was spherical for both synthesis methods, with their

size varying. When synthesis was done using $NaBH_4$ as the reducing agent, Ag nanoparticles with an average diameter of 14.87 ± 14.61 nm were formed. When synthesis was done using WMRE as the reducing agent, Ag nanoparticles with an average diameter of 7.48 nm ± 4.06 nm were formed.

As seen in Figure 4.37, the TiO_2 nanoparticles were observed to have a thin layer due to a layer of Al_2O_3 nanoparticles. The presence of elemental Al in the starting material and synthesized nanocomposites was confirmed by EDS elemental analysis, as seen in Figure 4.34. This layer is intentionally coated on the surface of TiO_2 to improve stability and photocatalytic properties (Veronovski, 2018). The effect of this layer during modification is that Ag nanoparticles are only modified in areas without it (Niño-Martínez *et al*., 2008). Consequently, elemental Al was also observed in both nanocomposites in almost similar amounts, with a 1.3 and 1.4 % composition for WMAT and NBAT, respectively.

The synthesis of Ag/TiO_2 using WMRE resulted in homogeneous Ag nanoparticles as compared to synthesis using $NaBH_4$. This finding was indicative of the efficiency of WMRE as a reducing and stabilizing agent, as it resulted in small Ag nanoparticles with uniform size and supported the findings of M. Ndikau et al. (2017) who found that Ag nanoparticles synthesized using WMRE were smaller and more stable than those produced using trisodium citrate.

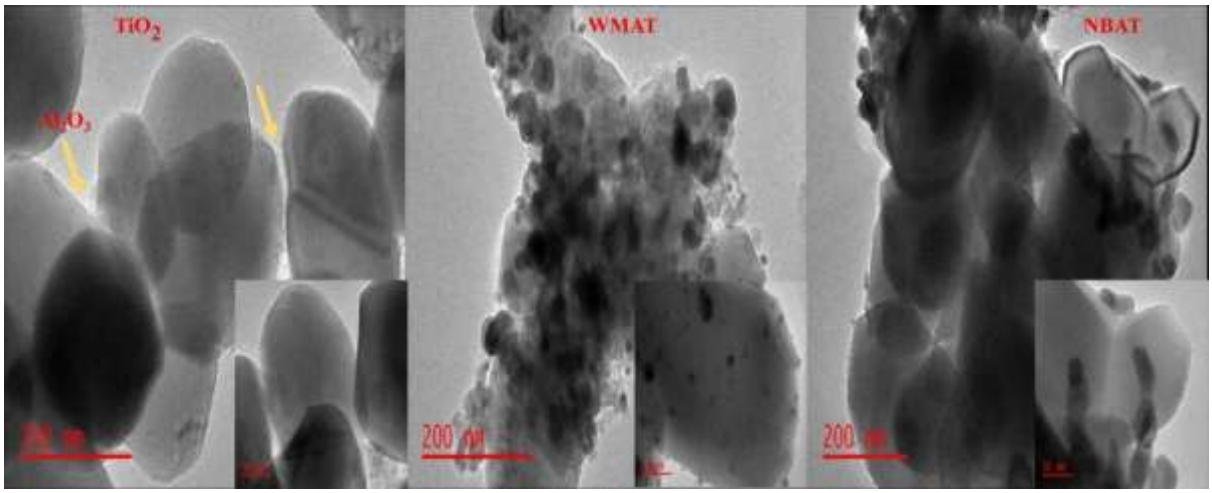

Figure 4.37 TEM images of the starting material and the synthesized nanocomposites.

4.6 Ag/TiO_2 nanocomposite incorporated SODIS

SODIS was performed without modification (control) and with 3-4mm glass beads coated with WMAT and NBAT; a significant decrease in *E. coli* and coliform bacteria contamination was observed, as shown in Figure 4.38. However, the deactivation pattern was statistically similar, with a kill rate of > 99.98% achieved during the 6 hours of treatment for the control and modified SODIS. Ag/TiO_2 has been extensively studied and recorded to have antibacterial effects on gram-negative and gram-positive bacteria. Jafar et al. (2022) found that chemically synthesized Ag/TiO_2 had a higher zone of inhibition for *Staphylococcus aureus*, *Shigella flexneri*, and *Bacillus sp* bacteria compared to the standard antibiotic streptomycin. Additionally, Ahmed et al. (2021) synthesized Ag/TiO_2 nanocomposite using goji berry (*Lycium barbarum L.*) fruit extract and found that it had broad antibacterial activity against *E. coli* and *S. aureus* bacteria. These findings suggest that green synthesized Ag/TiO_2 nanocomposite has a similar antimicrobial effect to chemically synthesized Ag/TiO_2 nanocomposite.

The ineffectiveness of SODIS improvement was not due to the bacteria inactivation potential of the synthesized Ag/TiO_2 nanocomposite, but rather to the interaction of the photocatalyst support with water during treatment. Though the glass beads were small, 3-4mm, they settled at the base of the bottle during treatment, minimizing interaction with microbes in the water. To keep the glass beads suspended required constant shaking, the challenge being that it cooled the water under treatment, interfering with microbial inactivation attributed to the pasteurization effects of sunlight. Additionally, the weight of the nanoparticles coated on the glass beads was carefully chosen at 1.2g. Increasing the weight resulted in excess powder that visibly dissolved in the water during treatment, staining the water. One benefit of using glass beads is that both the glass beads and PET bottles can be reused.

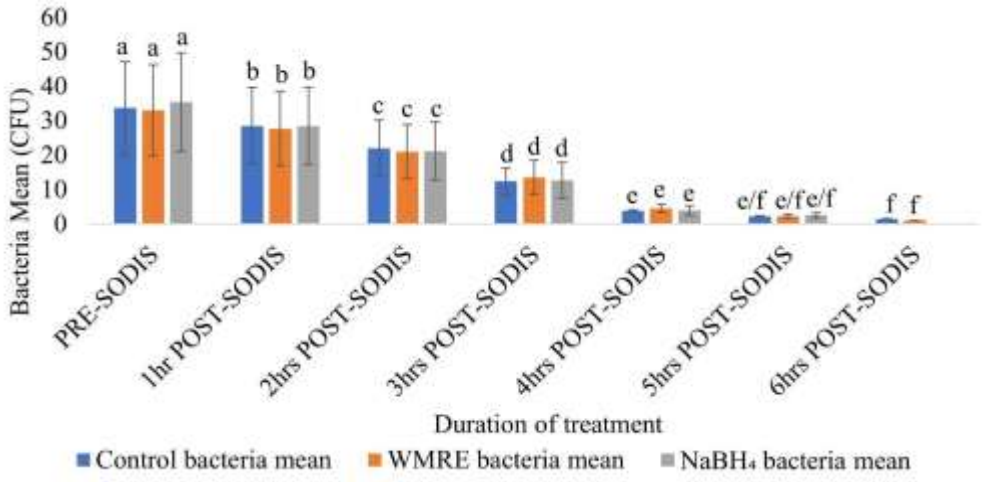

Figure 4.38 Inactivation of bacteria during control SODIS, WMAT, and NBAT-modified SODIS.

The contaminated water treated using control SODIS, WMAT, and NBAT-modified SODIS was collected from the same source. The *E. coli* and coliform bacteria contamination was therefore found to be statistically similar, as seen in Table 4.7.

Table 4.7 Bacteria mean for control SODIS, WMAT, and NBAT SODIS.

Modification	**Bacteria mean (CFU)**
Control	14.857 ± 3.230^{a}
WMRE-mediated Ag/TiO_2	14.877 ± 3.164^{a}
$NaBH_4$-mediated Ag/TiO_2	14.714 ± 3.396^{a}
p-value	0.915

Key: Values within the same column followed by the same letter did not differ significantly at $p < 0.005$.

CHAPTER FIVE: CONCLUSIONS AND RECOMMENDATIONS

5.1 Conclusions

The water and sanitation survey revealed that 65.35% and 100% of Obunga slum residents lack access to improved water sources and improved sanitation, respectively. Even though 59% of the residents treated their water by boiling, only 1% believed that this treatment method was effective, with a majority of the residents, 81%, believing that chlorination was highly effective. However, only 10% used this water treatment method. Whereas none of the residents used SODIS, 10% thought it was an effective water treatment method.

Water treatment using SODIS was highly effective, achieving over a > 99.99% kill rate against *E. coli* bacteria, which is an indicator of treatment efficacy. However, only an 84.64% kill rate was achieved for faecal coliform bacteria. The aim for treating microbial-contaminated water is complete inactivation. The incomplete inactivation of faecal coliform bacteria indicates the need to modify SODIS to achieve a 100% kill rate.

The synthesis of Ag/TiO_2 nanocomposite using WMRE resulted in the formation of small, stable Ag nanoparticles with an average diameter of 7.48 ± 4.06 nm, which were modified on the surface of the TiO_2 nanoparticles. The visible light activity of the NBAT was comparable to that of the WMAT. However, some agglomeration was observed in the WMAT due to the presence of capping agents in WMRE. These agents effectively stabilized the Ag nanoparticles but also caused some agglomeration due to electrostatic attraction. This situation highlights the need for further study to compare the advantages of capping with the disadvantages of agglomeration during green synthesis. The goal of

achieving improved nanoparticle monodispersity was accomplished, as confirmed by TEM analysis.

When modified with WMAT and NBAT, the SODIS method resulted in kill rates of > 99.98% and > 99.99% for *E. coli* and coliform bacteria, respectively. These rates were statistically similar to the > 99.98% kill rate achieved for control SODIS during a 6-hour water treatment. This indicates that the modified SODIS method did not improve efficiency.

5.2 Recommendations

i. Interventions for improving the water and sanitation standards to improve the quality of life of Obunga slum residents.
ii. Adoption of the developed method for the synthesis of Ag/TiO_2 nanocomposite using *Citrullus lanatus* rind extract.
iii. SODIS modification is recommended by incorporating alternative, cheap photocatalyst support materials such as glass rods, glass rings, and porcelain beads coated with WMRE synthesized Ag/TiO_2 nanocomposite.
iv. Monitoring BPA contamination levels during SODIS with and without modification using Ag/TiO_2.
v. Monitoring any chemical contamination from incorporating Ag/TiO_2 nanocomposite into SODIS.

REFERENCES

Abdullah, J. A. A., Salah Eddine, L., Abderrhmane, B., Alonso-González, M., Guerrero, A., and Romero, A. (2020). Green synthesis and characterization of iron oxide nanoparticles by pheonix dactylifera leaf extract and evaluation of their antioxidant activity. *Sustainable Chemistry and Pharmacy*, *17*(May). https://doi.org/10.1016/j.scp.2020.100280

Ahmed, S., Rasul, M. G., Martens, W. N., Brown, R., and Hashib, M. A. (2010). Heterogeneous photocatalytic degradation of phenols in wastewater: A review on current status and developments. *Desalination*, *261*(1–2), 3–18. https://doi.org/10.1016/j.desal.2010.04.062

Ahmed Sharwani, A., Badri Narayanan, K., Ehtisham Khan, M., and Soo Han, S. (2021). Sustainable fabrication of silver-titania nanocomposites using goji berry (*Lycium barbarum* L.) fruit extract and their photocatalytic and antibacterial applications. *Arabian Journal of Chemistry*, *14*(12), 103456. https://doi.org/10.1016/j.arabjc.2021.103456

Al-Gheethi, A. A. S., Norli, I., and Kadir, M. O. A. (2013). Elimination of enteric indicators and pathogenic bacteria in secondary effluents and lake water by solar disinfection (SODIS). *Journal of Water Reuse and Desalination*, *3*(1), 39–46. https://doi.org/10.2166/wrd.2013.060

Al-Kassab, M. M., and Majeed, A. H. (2022). THE USE OF TWO-SAMPLE t-TEST IN THE REAL DATA. *Advances and Applications in Statistics*, *81*, 13–22. https://doi.org/10.17654/0972361722071

Ali, M. (2024). Determining and quantifying chemically produced stresses in (atoms of) electronic and crystalline materials. March. https://doi.org/10.13140/RG.2.2.23849.40808

Aminuzzaman, M., Ying, L. P., Goh, W. S., and Watanabe, A. (2018). Green synthesis of zinc oxide nanoparticles using aqueous extract of *Garcinia mangostana* fruit pericarp and their photocatalytic activity. *Bulletin of Materials Science*, *41*(2). https://doi.org/10.1007/s12034-018-1568-4

Ananga, E. O. (2015). The Role of Community Participation in Water Production and Management: Lessons From Sustainable Aid in Africa International Sponsored Water Schemes in Kisumu, Kenya. *3733847*(October), 214. http://0-search.proquest.com.wam.leeds.ac.uk/docview/1737850915?accountid=14664%0A http://openurl.ac.uk/?genre=dissertations+%26+theses&issn=&title=The+Role+of+Community+Participation+in+Water+Production+and+Management%3A+Lessons+From+Sustainable+Aid+in+Af

Anderson, Mark Mwelu, K. (2004). Kenya Slum Upgrading Programs: KISIP & KENSUP. *Journal of Chemical Information and Modeling*, 12. https://www.google.com/url?sa=t&rct=j&q=&esrc=s&source=web&cd=&cad=rja&uact=8&ved=2ahUKEwipx-TuzcaCAxWOVaQEHSe2CKcQFnoECAoQAQ&url=http%3A%2F%2Fhealthycities.berkeley.edu%2Fuploads%2F1%2F2%2F6%2F1%2F12619988%2Fkenya.pdf&usg=AOvVaw2zEu8Hv35b03AKnfNaHwrp&opi

Arun Kumar and Ashok Ghosh, N. S. (2016). The Human Right to Water: From Concept to Reality. In *The Human Right to Water: From Concept to Reality*. https://link-springer-com.libproxy1.nus.edu.sg/book/10.1007%2F978-3-319-40286-4#editorsandaffiliations

Atikul Islam, M., Azad, A. K., Ali Akber, M., Rahman, M., and Sadhu, I. (2015). Effectiveness of solar disinfection (SODIS) in rural coastal Bangladesh. *Journal of Water and Health*, *13*(4), 1113–1122. https://doi.org/10.2166/wh.2015.186

Avciata, O., Benli, Y., Gorduk, S., and Koyun, O. (2016). Ag doped TiO_2 nanoparticles prepared by hydrothermal method and coating of the nanoparticles on the ceramic pellets for photocatalytic study: Surface properties and photoactivity. *Journal of Engineering Technology and Applied Sciences*, *1*(1), 34–50. https://doi.org/10.30931/jetas.281381

Bankar, A., Joshi, B., Kumar, A. R., and Zinjarde, S. (2010). Banana peel extract mediated novel route for the synthesis of silver nanoparticles. *Colloids and Surfaces A: Physicochemical and Engineering Aspects*, *368*(1–3), 58–63. https://doi.org/10.1016/j.colsurfa.2010.07.024

Bar, H., Bhui, D. K., Sahoo, G. P., Sarkar, P., Pyne, S., and Misra, A. (2009). Green synthesis of silver nanoparticles using seed extract *of Jatropha curcas*. *Colloids and Surfaces A: Physicochemical and Engineering Aspects*, *348*(1–3), 212–216. https://doi.org/10.1016/j.colsurfa.2009.07.021

Bartolomeo, A. Di. (2016). Graphene Schottky diodes: an experimental review of the rectifying graphene/semiconductor. *Journal of Chemical Information and Modeling*, *53*(9), 1689–1699. https://doi.org/https://doi.org/10.1016/j.physrep.2015.10.003

Bhardwaj, D., and Singh, R. (2021). Green biomimetic synthesis of Ag–TiO_2 nanocomposite using Origanum majorana leaf extract under sonication and their biological activities. *Bioresources and Bioprocessing*, *8*(1), 1–12. https://doi.org/10.1186/s40643-020-00357-z

Bhattacharjee, C., Dutta, S., and Saxena, V. K. (2020). A review on biosorptive removal of dyes and heavy metals from wastewater using watermelon rind as biosorbent. *Environmental Advances*, *2*(September), 100007. https://doi.org/10.1016/j.envadv.2020.100007

Bhattacharya, P., Dhibar, S., Kundu, M. K., Hatui, G., and Das, C. K. (2015). Graphene and MWCNT based bi-functional polymer nanocomposites with enhanced microwave absorption and supercapacitor property. *Materials Research Bulletin*, *66*, 200–212. https://doi.org/10.1016/j.materresbull.2015.02.040

Braun, L., Grimes, J. E. T., and Templeton, M. R. (2018). The effectiveness of water treatment processes against schistosome cercariae: A systematic review. *PLoS Neglected Tropical Diseases*, *12*(4), 1–22. https://doi.org/10.1371/journal.pntd.0006364

Brown, J., & Sobsey, M. D. (2012). Boiling as household water treatment in Cambodia: A longitudinal study of boiling practice and microbiological effectiveness. *American Journal of Tropical Medicine and Hygiene*, *87*(3), 394–398. https://doi.org/10.4269/ajtmh.2012.11-0715

Buckner, C. A., Lafrenie, R. M., Dénommée, J. A., Caswell, J. M., Want, D. A., Gan, G. G., Leong, Y. C., Bee, P. C., Chin, E., Teh, A. K. H., Picco, S., Villegas, L., Tonelli, F., Merlo, M., Rigau, J., Diaz, D., Masuelli, M., Korrapati, S., Kurra, P., and Mathijssen, R. H. J. (2016). Drinking Water Treatment and Challenges in Developing Countries. In *Intech* (Vol. 11, Issue tourism). https://www.intechopen.com/books/advanced-biometric-technologies/liveness-detection-in-biometrics

Bunaciu, A. A., Udriştioiu, E. gabriela, and Aboul-Enein, H. Y. (2015). X-Ray Diffraction: Instrumentation and Applications. *Critical Reviews in Analytical Chemistry*, *45*(4), 289–299. https://doi.org/10.1080/10408347.2014.949616

Byrne, J. A., Fernandez-Ibañez, P. A., Dunlop, P. S. M., Alrousan, D. M. A., and Hamilton, J. W. J. (2011). Photocatalytic Enhancement for Solar Disinfection of Water: A Review. *International Journal of Photoenergy*. https://doi.org/10.1155/2011/798051

Calado, A. D., and Mattle, M. J. (2013). Solar disinfection of viruses (SODIS): inactivation of coliphages MS2 and phiX174 , human adenovirus and echovirus in water from Switzerland and India. https://www.google.com/url?sa=t&rct=j&q=&esrc=s&source=web&cd=&cad=rja&uact=8&ved=2ahUKEwjsvtTgzsaCAxWrVKQEHSpwA44QFnoECAgQAQ&url=https%3A%2F%2Finfoscience.epfl.ch%2Frecord%2F187538%3Fln%3Den&usg=AOvVaw0_fmPT3QU6pxJks7nOnBzv&opi=89978449

Cardoso-Rurr, J. S., de Paiva, J. P., Paulino-Lima, I. G., de Alencar, T. A. M., Lage, C. A. S., and Leitão, A. C. (2019). Microbiological Decontamination of Water: Improving the Solar Disinfection Technique (SODIS) with the Use of Nontoxic Vital Dye Methylene Blue. *Photochemistry and Photobiology*, *95*(2), 618–626. https://doi.org/10.1111/php.12999

Carratalà, A., Calado, A. D., Mattle, M. J., Meierhofer, R., Luzi, S., and Kohn, T. (2016). Solar disinfection of viruses in polyethylene terephthalate bottles. *Applied and Environmental Microbiology*, *82*(1), 279–288. https://doi.org/10.1128/AEM.02897-15

Castro-Alférez, M., Polo-López, M. I., Marugán, J., and Fernández-Ibáñez, P. (2017). Mechanistic model of the Escherichia coli inactivation by solar disinfection based on the photo-generation of internal ROS and the photo-inactivation of enzymes: CAT and SOD. *Chemical Engineering Journal*, *318*, 214–223. https://doi.org/10.1016/j.cej.2016.06.093

Castro, C. A., Jurado, A., Sissa, D., and Giraldo, S. A. (2012). Performance of Ag-TiO 2 photocatalysts towards the photocatalytic disinfection of water under interior-lighting and solar-simulated light irradiations. *International Journal of Photoenergy*, *2012*. https://doi.org/10.1155/2012/261045

Chakhtouna, H., Benzeid, H., Zari, N., Qaiss, A. el kacem, and Bouhfid, R. (2021). Recent progress on Ag/TiO2 photocatalysts: photocatalytic and bactericidal behaviors. *Environmental Science and Pollution Research*, *28*(33), 44638–44666. https://doi.org/10.1007/s11356-021-14996-y

Che Sulaiman, I. S., Basri, M., Fard Masoumi, H. R., Chee, W. J., Ashari, S. E., and Ismail, M. (2017). Effects of temperature, time, and solvent ratio on the extraction of phenolic compounds and the anti-radical activity of Clinacanthus nutans Lindau leaves by response surface methodology. *Chemistry Central Journal*, *11*(1), 1–11. https://doi.org/10.1186/s13065-017-0285-1

Chen, T., Foo, C., and Tsang, S. C. E. (2021). Interstitial and substitutional light elements in transition metals for heterogeneous catalysis. *Chemical Science*, *12*(2), 517–532. https://doi.org/10.1039/d0sc06496c

Chong, M. N., Jin, B., Chow, C. W. K., and Saint, C. (2010). Recent developments in photocatalytic water treatment technology: A review. *Water Research*, *44*(10), 2997–3027. https://doi.org/10.1016/j.watres.2010.02.039

Cohen, A., and Colford, J. M. (2017). Effects of boiling drinking water on diarrhea and pathogen-specific infections in low- and middle-income countries: A systematic review and meta-analysis. *American Journal of Tropical Medicine and Hygiene*, *97*(5), 1362–1377. https://doi.org/10.4269/ajtmh.17-0190

Coleman, N., Perera, S., and Gillan, E. G. (2015). Rapid solid-state metathesis route to transition-metal doped titanias. *Journal of Solid State Chemistry*, *232*, 241–248. https://doi.org/10.1016/j.jssc.2015.09.028

Colorado, C. C. of. (n.d.). Water Treatment Plant Process | Canon City, CO. In *www.canoncity.org*. Retrieved October 14, 2024, from https://www.canoncity.org/180/Water-Treatment-Plant-Process

Dalrymple, O. K., and Goswami, D. Y. (2017). Mechanistic Modeling of Photocatalytic Water Disinfection (pp. 273–315). https://doi.org/10.1007/978-3-662-53496-0_13

Danwittayakul, S., Songngam, S., and Sukkasi, S. (2020). Enhanced solar water disinfection using ZnO supported photocatalysts. *Environmental Technology (United Kingdom)*, *41*(3), 349–356. https://doi.org/10.1080/09593330.2018.1498921

Darroudi, M., Ahmad, M. Bin, Zamiri, R., Zak, A. K., Abdullah, A. H., and Ibrahim, N. A. (2011). Time-dependent effect in green synthesis of silver nanoparticles. *International Journal of Nanomedicine*, *6*(1), 677–681. https://doi.org/10.2147/IJN.S17669

de Oliveira, C. M. (2017). Acesso sustentável à água potável: Direito humano fundamental no cenário internacional e nacional. *Revista Ambiente e Agua*, *12*(6), 985–1000. https://doi.org/10.4136/ambi-agua.2037

de Souza, L. M. J., Costa, A. C., Nero, L. A., Couto, E. P., and Ferreira, M. de A. (2015). Evaluation of Petrifilm™ system compared with traditional methodology in count of indicators of sanitary-hygienic quality and pathogenic microorganisms in sheep milk. *Food Science and Technology (Brazil)*, *35*(2), 375–379. https://doi.org/10.1590/1678-457X.6430

Di Bartolomeo, A. (2016). Graphene Schottky diodes: An experimental review of the rectifying graphene/semiconductor heterojunction. *Physics Reports*, *606*(June 2015), 1–58. https://doi.org/10.1016/j.physrep.2015.10.003

Du Preez, M., Conroy, R. M., Ligondo, S., Hennessy, J., Elmore-Meegan, M., Soita, A., and McGuigan, K. G. (2011). Randomized intervention study of solar disinfection of drinking water in the prevention of dysentery in Kenyan children aged under 5 years. *Environmental Science and Technology*, *45*(21), 9315–9323. https://doi.org/10.1021/es2018835

Faried, M., Shameli, K., Miyake, M., Hajalilou, A., Zamanian, A., Zakaria, Z., Abouzari-Lotf, E., Hara, H., Ahmad Khairudin, N. B. B., and Binti Mad Nordin, M. F. (2016). A Green Approach for the Synthesis of Silver Nanoparticles Using Ultrasonic Radiation's Times in Sodium Alginate Media: Characterization and Antibacterial Evaluation. *Journal of Nanomaterials*, *2016*. https://doi.org/10.1155/2016/4941231

Fernández-Ibáñez, P., Gómez-Couso, H., Ares-Mazás, E., and Fontán-Sainz, M. (2012). Evaluation of the Solar Water Disinfection Process (SODIS) Against Cryptosporidium parvum Using a 25-L Static Solar Reactor Fitted with a Compound Parabolic Collector (CPC). *The American Journal of Tropical Medicine and Hygiene*, *86*(2), 223–228. https://doi.org/10.4269/ajtmh.2012.11-0325

Gadgil, D. J., and Shetty Kodialbail, V. (2021). Suspended and polycaprolactone immobilized Ag @TiO_2/polyaniline nanocomposites for water disinfection and endotoxin degradation by visible and solar light-mediated photocatalysis. *Environmental Science and Pollution Research*, *28*(10), 12780–12791. https://doi.org/10.1007/s11356-020-11206-z

Gandhi, J., and Prakash, H. (2023). Photo-disinfection processes for bacterial inactivation and underlying principles for water constituents' impact: A review. In *Chemical Engineering Journal Advances* (Vol. 14, p. 100482). Elsevier. https://doi.org/10.1016/j.ceja.2023.100482

García-Gil, Á., Feng, L., Moreno-SanSegundo, J., Giannakis, S., Pulgarín, C., and Marugán, J. (2022). Mechanistic modelling of solar disinfection (SODIS) kinetics of *Escherichia coli*, enhanced with H_2O_2 – Part 2: Shine on you, crazy peroxide. *Chemical Engineering Journal*, *439*(February). https://doi.org/10.1016/j.cej.2022.135783

García-Gil, Á., García-Muñoz, R. A., McGuigan, K. G., and Marugán, J. (2021). Solar water disinfection to produce safe drinking water. A review of parameters, enhancements, and modelling approaches to make SODIS faster and safer. *Molecules*, *26*(11). https://doi.org/10.3390/molecules26113431

Geisz, J. F., Garciá, I., McMahon, W. E., Steiner, M. A., Ochoa, M., France, R. M., Habte, A., and Friedman, D. J. (2015). Energy yield determination of concentrator solar cells using laboratory measurements. *AIP Conference Proceedings*, *1679*(2015). https://doi.org/10.1063/1.4931516

Gerryshom, M. (2015). Socio-cultural influences that Determines Sanitation Facilities Use in the Informal Settlements. Routray, P, 1–11. https://doi.org/10.1017/CBO9781107415324.004

Ghasemi, Z., Abdi, V., and Sourinejad, I. (2020). Green fabrication of Ag/AgCl@TiO_2 superior plasmonic nanocomposite: Biosynthesis, characterization and photocatalytic activity under sunlight. *Journal of Alloys and Compounds*, *841*, 155593. https://doi.org/10.1016/j.jallcom.2020.155593

Giannakis, S., Darakas, E., Escalas-Cañellas, A., and Pulgarin, C. (2015). Solar disinfection modeling and post-irradiation response of *Escherichia coli* in wastewater. *Chemical Engineering Journal*, *281*, 588–598. https://doi.org/10.1016/j.cej.2015.06.077

Giannakis, S., Gupta, A., Pulgarin, C., & Imlay, J. (2022). Identifying the mediators of intracellular *E. coli* inactivation under UVA light: The (photo) Fenton process and singlet oxygen. *Water Research*, *221*(May). https://doi.org/10.1016/j.watres.2022.118740

Ginter-Kramarczyk, D., Zembrzuska, J., Kruszelnicka, I., Zając-Woźnialis, A., and Ciślak, M. (2022). Influence of Temperature on the Quantity of Bisphenol A in Bottled Drinking Water. *International Journal of Environmental Research and Public Health*, *19*(9). https://doi.org/10.3390/ijerph19095710

GoK. (2019). The National Treasury and Planning State Department for Planning Projects and Programmes Department SDGs PROGRESS REPORT. https://www.google.com/url?sa=t&rct=j&q=&esrc=s&source=web&cd=&cad=rja&uact=8&ved=2ahUKEwjCoKCQz8aCAxV8T6QEHZYICnIQFnoECBYQAQ&url=https%3A%2F%2Fwww.planning.go.ke%2Fwp-content%2Fuploads%2F2020%2F11%2FSDGs-Progress-Report-2019.pdf&usg=AOvVaw3xzjLH_SH32Wujw

Guo, Q., Zhou, C., Ma, Z., and Yang, X. (2019). Fundamentals of TiO_2 Photocatalysis: Concepts, Mechanisms, and Challenges. *Advanced Materials*, *31*(50), 1–26. https://doi.org/10.1002/adma.201901997

Haghighat, N., Vatanpour, V., Sheydaei, M., and Nikjavan, Z. (2020). Preparation of a novel polyvinyl chloride (PVC) ultrafiltration membrane modified with Ag/TiO_2 nanoparticle with enhanced hydrophilicity and antibacterial activities. *Separation and Purification Technology*, *237*, 116374. https://doi.org/10.1016/j.seppur.2019.116374

Hamilton, J. W. J., Byrne, J. A., McCullagh, C., and Dunlop, P. S. M. (2008). Electrochemical investigation of doped titanium dioxide. *International Journal of Photoenergy*. https://doi.org/10.1155/2008/631597

Handayani, W., Ningrum, A. S., and Imawan, C. (2020). The Role of pH in Synthesis Silver Nanoparticles Using *Pometia pinnata* (Matoa) Leaves Extract as Bioreductor. *Journal of Physics: Conference Series*, *1428*(1). https://doi.org/10.1088/1742-6596/1428/1/012021

Henegar, A. J., and Gougousi, T. (2015). Stability and Surface Reactivity of Anatase TiO_2 Films . *ECS Journal of Solid State Science and Technology*, *4*(8), P298–P304. https://doi.org/10.1149/2.0041508jss

Herman, T. (2017). Quality of Water in Relation to Diarrheal Disease Incidence in Obunga.

Hettler, S., Dries, M., Hermann, P., Obermair, M., Gerthsen, D., and Malac, M. (2017). Carbon contamination in scanning transmission electron microscopy and its impact on phase-plate applications. *Micron*, *96*, 38–47. https://doi.org/10.1016/j.micron.2017.02.002

Hong, Y., Shi, W., Wang, H., Ma, D., Ren, Y., Wang, Y., Li, Q., and Gao, B. (2022). Mechanisms of *Escherichia coli* inactivation during solar-driven photothermal disinfection. *Environmental Science: Nano*, *9*(3), 1000–1010. https://doi.org/10.1039/d1en00999k

Horikoshi, S., & Serpone, N. (2013). Introduction to Nanoparticles. In *Microwaves in Nanoparticle Synthesis: Fundamentals and Applications* (pp. 1–24). https://doi.org/10.1002/9783527648122.ch1

Hou, X., Ma, H., Liu, F., Deng, J., Ai, Y., Zhao, X., Mao, D., Li, D., and Liao, B. (2015). Synthesis of Ag ion-implanted TiO<inf>2</inf> thin films for antibacterial application and photocatalytic performance. *Journal of Hazardous Materials*, *299*, 59–66. https://doi.org/10.1016/j.jhazmat.2015.05.014

Hugenschmidt, M., Adrion, K., Marx, A., Müller, E., and Gerthsen, D. (2023). Electron-Beam-Induced Carbon Contamination in STEM-in-SEM: Quantification and Mitigation. *Microscopy and Microanalysis*, *29*(1), 219–234. https://doi.org/10.1093/micmic/ozac003

Ivanković, A. (2017). Review of 12 Principles of Green Chemistry in Practice. *International Journal of Sustainable and Green Energy*, *6*(3), 39. https://doi.org/10.11648/j.ijrse.20170603.12

Jafar Ali Ibrahim, S., Rajasekar, S., Kalyan Chakravarthy, N. S., Varsha, Singh, M. S., Kumar, V., and Saruchi. (2022). Synthesis, characterization of Ag/TiO_2 nanocomposite: Its anticancer and anti-bacterial activities. *Global Nest Journal*, *24*(2), 262–266. https://doi.org/10.30955/gnj.004255

Jana, J., Ganguly, M., and Pal, T. (2016). Enlightening surface plasmon resonance effect of metal nanoparticles for practical spectroscopic application. *RSC Advances*, *6*(89), 86174–86211. https://doi.org/10.1039/c6ra14173k

Javed, M., Sajid, A., Bangash, K., Abbas, M., Ahmed, S., Kaplan, A., Iqbal, S., Khan, N., Adnan, M., Ali, A., Zaman, F., and Wahab, S. (2023). Potential and Challenges in Green Synthesis of Nanoparticles: A Review. *Xi'an Shiyou Daxue Xuebao (Ziran Kexue Ban)/Journal of Xi'an Shiyou University*, *19*(February), 1155–1165. https://www.researchgate.net/publication/368646514_Potential_and_Challenges_in_Green_Synthesis_of_Nanoparticles_A_Review

Javed, R., Ain, N. ul, Gul, A., Arslan Ahmad, M., Guo, W., Ao, Q., and Tian, S. (2022). Diverse biotechnological applications of multifunctional titanium dioxide nanoparticles: An up-to-date review. *IET Nanobiotechnology*, *February*. https://doi.org/10.1049/nbt2.12085

JMP for Water Supply Sanitation and Hygiene. (2018). Core questions on water, sanitation and hygiene for household surveys-2018 update Core questions on water, sanitation and hygiene for household surveys WHO/UNICEF Joint Monitoring Programme for Water Supply, Sanitation and Hygiene 2018 UPDATE Core questions. 1–24. https://washdata.org

Joseph, A., and Vijayanandan, A. (2023). Review on support materials used for immobilization of nano-photocatalysts for water treatment applications. In *Inorganica Chimica Acta* (Vol. 545, p. 121284). Elsevier. https://doi.org/10.1016/j.ica.2022.121284

K. Balachandran, G. Vijayakumar, S. Mageswari, A. Preethi, and M.S. Viswak Senan. (2021). Synthesis and Characterization of Ag-Decorated TiO_2 Nanoparticles for Photocatalytic Application. *Journal of Environmental Nanotechnology*, *10*(4), 13–18. https://doi.org/10.13074/jent.2021.12.14446

Keane, D. A., Mcguigan, K. G., Fernandez Ibanez, P., Byrne, A. J., Da, K., Kg, M., Pf, I., Mi, B., Aj, D., Psm, O. ', Shea, K., Dd, D., and Solar, P. S. (2014). Solar photocatalysis for water disinfection: Materials and reactor design. *Catalysis Science & Technology*, *4*, 1211–1226. https://doi.org/https://doi.org/10.1039/C4CY00006D

Khan, F., Shariq, M., Asif, M., Siddiqui, M. A., Malan, P., and Ahmad, F. (2022). Green Nanotechnology: Plant-Mediated Nanoparticle Synthesis and Application. *Nanomaterials*, *12*(4). https://doi.org/10.3390/nano12040673

Khan, M., Khan, S. T., Khan, M., Adil, S. F., Musarrat, J., Al-Khedhairy, A. A., Al-Warthan, A., Siddiqui, M. R. H., and Alkhathlan, H. Z. (2014). Antibacterial properties of silver nanoparticles synthesized using *Pulicaria glutinosa* plant extract as a green bioreductant. *International Journal of Nanomedicine*, *9*(1), 3551–3565. https://doi.org/10.2147/IJN.S61983

Khokhra, R., and Kumar, R. (2015). Effect of Fe doping concentration on photocatalytic activity of ZnO nanosheets under natural sunlight. *AIP Conference Proceedings*, *1661*(Iccmp 2014), 1–8. https://doi.org/10.1063/1.4915405

Kitchener, B. G., Wainwright, J., and Parsons, A. J. (2017). A review of the principles of turbidity measurement. *Progress in Physical Geography*. https://doi.org/https://doi.org/10.1177/0309133317726540

KNBS. (2019). Distribution of Population by Administrative Units. In *2019 Kenya Population and Housing Census: Vol. II*. http://www.knbs.or.ke

Kobese, N. (2018). Synthesis of silver doped titanium dioxide nanocomposites using tea extract from Aspalathus linearis and evaluation of their antibacterial effects . By Nokubonga Kobese. September. http://hdl.handle.net/11394/6779

Kredy, H. M. (2018). The effect of pH, temperature on the green synthesis and biochemical activities of silver nanoparticles from *Lawsonia inermis* extract. *Journal of Pharmaceutical Sciences and Research*, *10*(8), 2022–2026. https://doi.org/https://www.researchgate.net/publication/327571058_The_effect_of_pH_temperature_on_the_green_synthesis_and_biochemical_activities_of_silver_nanoparticles_from_Lawsonia_inermis_extract

Kumar, B., Smita, K., Angulo, Y., and Cumbal, L. (2016). Valorization of rambutan peel for the synthesis of silver-doped titanium dioxide (Ag/TiO_2) nanoparticles. *Green Processing and Synthesis*, *5*(4), 371–377. https://doi.org/10.1515/gps-2016-0003

Lakshmanan, G., Sathiyaseelan, A., Kalaichelvan, P. T., and Murugesan, K. (2018). Plant-mediated synthesis of silver nanoparticles using fruit extract of *Cleome viscosa* L.: Assessment of their antibacterial and anticancer activity. *Karbala International Journal of Modern Science*, *4*(1), 61–68. https://doi.org/10.1016/j.kijoms.2017.10.007

Lars, M. R. H. and S. O. (2010). A Practical Method for Rapid Assessment of the Bacterial Quality of Water. https://www.google.com/url?sa=t&rct=j&q=&esrc=s&source=web&cd=&cad=rja&uact=8&ved=2ahUKEwj4-o2u0MaCAxUqUqQEHZvvA_UQFnoECAoQAQ&url=https%3A%2F%2Fissuu.com%2Funhabitat%2Fdocs%2Fa_practical_method_for_rapid_assessment&usg=AOvVaw0C9M8d3ep0Xl0Q4wEjupuZ&opi=899

Lawrie, K., Mills, A., Figueredo-Fernández, M., Gutiérrez-Alfaro, S., Manzano, M., & Saladin, M. (2015). UV dosimetry for solar water disinfection (SODIS) carried out in different plastic bottles and bags. *Sensors and Actuators, B: Chemical*, *208*, 608–615. https://doi.org/10.1016/j.snb.2014.11.031

Letema, S., van Vliet, B., and van Lier, J. B. (2014). Sanitation policy and spatial planning in urban East Africa: Diverging sanitation spaces and actor arrangements in Kampala and Kisumu. *Cities*, *36*, 1–9. https://doi.org/10.1016/j.cities.2013.08.003

Li, S., Shen, Y., Xie, A., Yu, X., Qiu, L., Zhang, L., and Zhang, Q. (2007). Green synthesis of silver nanoparticles using *Capsicum annuum* L. extract. *Green Chemistry*, *9*(8), 852–858. https://doi.org/10.1039/b615357g

Liu, G., Wang, L., Yang, H. G., Cheng, H. M., and Lu, G. Q. (2010). Titania-based photocatalysts - Crystal growth, doping and heterostructuring. *Journal of Materials Chemistry*, *20*(5), 831–843. https://doi.org/10.1039/b909930a

Liu, Y. S., Chang, Y. C., and Chen, H. H. (2018). Silver nanoparticle biosynthesis by using phenolic acids in rice husk extract as reducing agents and dispersants. *Journal of Food and Drug Analysis*, *26*(2), 649–656. https://doi.org/10.1016/j.jfda.2017.07.005

López-Lorente, Á. I., Pena-Pereira, F., Pedersen-Bjergaard, S., Zuin, V. G., Ozkan, S. A., and Psillakis, E. (2022). The ten principles of green sample preparation. In *TrAC - Trends in Analytical Chemistry* (Vol. 148, p. 116530). Elsevier. https://doi.org/10.1016/j.trac.2022.116530

Luzi, S., Tobler, M., Suter, F., and Meierhofer, R. (2016). SODIS manual. Guidance on solar water disinfection. (Issue January 2002). www.sodis.ch.

Ma, J., Xiong, Z., David Waite, T., Ng, W. J., and Zhao, X. S. (2011). Enhanced inactivation of bacteria with silver-modified mesoporous TiO_2 under weak ultraviolet irradiation. *Microporous and Mesoporous Materials*, *144*(1–3), 97–104. https://doi.org/10.1016/j.micromeso.2011.03.040

Mallikarjuna, K., Narasimha, G., Dillip, G. R., Praveen, B., Shreedhar, B., Sree Lakshmi, C., Reddy, B. V. S., and Deva Prasad Raju, B. (2011). Green synthesis of silver nanoparticles using Ocimum leaf extract and their characterization. *Digest Journal of Nanomaterials and Biostructures*, *6*(1), 181–186. https://api.semanticscholar.org/CorpusID:29059333

Maoulidi, M. (2010). A water and sanitation needs assessment for Kisumu City, Kenya. *MCI Social Sector Working Paper Series*, *September*, 1–32. https://doi.org/10.7916/D8SJ1TJ5

Maoulidi, M. (2012). Kisumu Millenium Development Goals Multi-Sector Household Survey. Decembe*r*, 1–46. https://doi.org/10.1007/s13398-014-0173-7.2

Martínez-García, A., Nahim-Granados, S., Berruti, I., Oller, I., and Polo-López, M. I. (2023). Assessment of solar water disinfection enhancement with H_2O_2 and dissolved oxygen on inactivating different waterborne pathogens. *Journal of Environmental Chemical Engineering*, *11*(6). https://doi.org/10.1016/j.jece.2023.111145

Martínez, N. N., Ribera, J. M., Hausmann-Muela, S., Cevallos, M., Hartinger, S. M., Christen, A., and Mäusezahl, D. (2020). The meanings of water: Socio-Cultural perceptions of solar disinfected (SODIS) drinking water in Bolivia and implications for its uptake. *Water (Switzerland)*, *12*(2), 442. https://doi.org/10.3390/w12020442

McGuigan, K. G., Conroy, R. M., Mosler, H. J., du Preez, M., Ubomba-Jaswa, E., and Fernandez-Ibañez, P. (2012). Solar water disinfection (SODIS): A review from bench-top to roof-top. In *Journal of Hazardous Materials* (Vols. 235–236, pp. 29–46). Elsevier. https://doi.org/10.1016/j.jhazmat.2012.07.053

McGuigan, K. G., Samaiyar, P., Du Preez, M., and Conroy, R. M. (2011). High compliance randomized controlled field trial of solar disinfection of drinking water and its impact on childhood diarrhea in rural Cambodia. *Environmental Science and Technology*, *45*(18), 7862–7867. https://doi.org/10.1021/es201313x

Mekprasart, W., Khumtong, T., Rattanarak, J., Techitdheera, W., and Pecharapa, W. (2013). Effect of nitrogen doping on optical and photocatalytic properties of TiO_2 thin film prepared by spin coating process. *Energy Procedia*, *34*, 746–750. https://doi.org/10.1016/j.egypro.2013.06.809

Méndez, D. A., Fabra, M. J., Gómez-Mascaraque, L., López-Rubio, A., and Martinez-Abad, A. (2021). Modelling the Extraction of Pectin towards the Valorisation of Watermelon Rind Waste. https://doi.org/10.3390/foods10040738

Mezbour, S., and Ghorab, M. F. (2019). Photoctalytic efficiency of silver doped TiO_2-PC500 for dyes removal from water under UV and solar radiations: Comparative study. *Journal of Water and Environment Technology*, *17*(4), 273–285. https://doi.org/10.2965/jwet.18-099

Mkhwanazi, F., Mazibuko, T., Mosoma, O., Rathebe, M., and Patel, M. (2024). Comparison of Petrifilm TM AC and pour plate techniques used for the heterotrophic aerobic bacterial count in water. *FEMS Microbiology Letters*, *371*, 29. https://doi.org/10.1093/femsle/fnae029

Motlagh, A. M., and Yang, Z. (2019). Detection and occurrence of indicator organisms and pathogens. In *Water Environment Research* (Vol. 91, Issue 10, pp. 1402–1408). https://doi.org/10.1002/wer.1238

Mushtaq, M., Sultana, B., Bhatti, H. N., and Asghar, M. (2015). RSM based optimized enzyme-assisted extraction of antioxidant phenolics from underutilized watermelon (*Citrullus lanatus* Thunb.) rind. *Journal of Food Science and Technology*, *52*(8), 5048–5056. https://doi.org/10.1007/s13197-014-1562-9

Nakada, L., and Urban, R. C. (2024). Uncorrected Proof Priority areas for the use of solar water disinfection (SODIS) in Brazil : a spatial approach Uncorrected Proof. *00*(0), 1–13. https://doi.org/10.2166/washdev.2024.129

Navarra, G., Moschetti, M., Guarrasi, V., Mangione, M. R., Militello, V., and Leone, M. (2017). Simultaneous determination of caffeine and chlorogenic acids in green coffee by UV/Vis spectroscopy. *Journal of Chemistry*, *2017*. https://doi.org/10.1155/2017/6435086

Ndikau, M. N. (2016). Green Synthesis Of Silver Nanoparticles Using *Citrullus Lanatus* Rind Extract As Reductant For Anti-Bacterial Applications Against Selected Bacteria.https://www.google.com/url?sa=t&rct=j&q=&esrc=s&source=web&cd=&cad=rja&uact=8&ved=2ahUKEwikkcSQ0caCAxWNVaQEHVLwCkEQFnoECAoQAQ&url=https%3A%2F%2Fir-library.ku.ac.ke%2Fbitstream%2Fhandle%2F123456789%2F18366%2FGreen%2520synthesis%2520of%2520silver%2520nanopa

Ndikau, M., Noah, N. M., Andala, D. M., and Masika, E. (2017). Green Synthesis and Characterization of Silver Nanoparticles Using *Citrullus lanatus* Fruit Rind Extract. *International Journal of Analytical Chemistry*, *2017*. https://doi.org/10.1155/2017/8108504

Niño-Martínez, N., Martínez-Castañón, G. A., Aragón-Piña, A., Martínez-Gutierrez, F., Martínez-Mendoza, J. R., and Ruiz, F. (2008). Silver nanoparticles synthesized on titanium dioxide fine particles. *Technical Proceedings of the 2008 NSTI Nanotechnology Conference and Trade Show, NSTI-Nanotech, Nanotechnology 2008*, *1*, 737–740. https://doi.org/10.1088/0957-4484/19/6/065711

Nwankwo, E. J., Agunwamba, J. C., Igwe, S. E., and Odenigbo, C. (2022). Regression models for predicting the die-off rate of *E. coli* in solar water disinfection. *Journal of Water Sanitation and Hygiene for Development*, *12*(8), 575–586. https://doi.org/10.2166/washdev.2022.056

Ohore, O. E., and Songhe, Z. (2019). Endocrine disrupting effects of bisphenol A exposure and recent advances on its removal by water treatment systems. A review. *Scientific African*, *5*. https://doi.org/10.1016/j.sciaf.2019.e00135

Oko, O. M. (2016). Evaluation of anti-nutrient contents of watermelon Citrullus lanatus. January.*2012*.https://www.researchgate.net/publication/259176462_Evaluation_of_anti-nutrient_contents_of_watermelon_Citrullus_lanatus

Ola, O., and Maroto-Valer, M. M. (2015). Review of material design and reactor engineering on TiO_2 photocatalysis for CO_2 reduction. *Journal of Photochemistry and Photobiology C: Photochemistry Reviews*, *24*(June), 16–42. https://doi.org/10.1016/j.jphotochemrev.2015.06.001

Olson, N. D., and Morrow, J. B. (2012). DNA extract characterization process for microbial detection methods development and validation. *BMC Research Notes*, *5*. https://doi.org/10.1186/1756-0500-5-668

Omar, H. H., Bahabri, F. S., and El-Gendy, A. M. (2017). Biopotential application of synthesis nanoparticles as antimicrobial agents by using *Laurencia papillosa*. *International Journal of Pharmacology*, *13*(3), 303–312. https://doi.org/10.3923/ijp.2017.303.312

ONU. (2022). The sustainable development goals report. *United Nations Publication Issued by the Department of Economic and Social Affairs*, 64. https://www.google.com/url?sa=t&rct=j&q=&esrc=s&source=web&cd=&cad=rja&uact=8&ved=2ahUKEwjX3IzX0caCAxVIRKQEHWhoBEwQFnoECAgQAw&url=https%3A%2F%2Funstats.un.org%2Fsdgs%2Freport%2F2022%2FThe-Sustainable-Development-Goals-Report-2022.pdf&usg=AOvVaw1RjsqrkXRXf

Opisa, S., Odiere, M. R., Jura, W. G. Z. O., Karanja, D. M. S., and Mwinzi, P. N. M. (2012). Faecal contamination of public water sources in informal settlements of Kisumu City, western Kenya. *Water Science and Technology*, *66*(12), 2674–2681. https://doi.org/10.2166/wst.2012.503

Oseni, O. A., and Okoye, V. I. (2013). Studies of Phytochemical and Antioxidant Properties of the Fruit of Watermelon (*Citrullus lanatus*). (Thunb.). *Journal of Pharmaceutical and Biomedical Sciences*, *27*(14), 508–514. https://doi.org/http://dx.doi.org/10.56093/ijas.v85i3.47179

Papyrakis, E. (2022). COVID-19 and International Development. In *COVID-19 and International Development*. https://doi.org/10.1007/978-3-030-82339-9

Peiris, S., de Silva, H. B., Ranasinghe, K. N., Bandara, S. V., and Perera, I. R. (2021). Recent development and future prospects of TiO_2 photocatalysis. In *Journal of the Chinese Chemical Society* (Vol. 68, Issue 5, pp. 738–769). John Wiley & Sons, Ltd. https://doi.org/10.1002/jccs.202000465

Pelaez, M., Nolan, N. T., Pillai, S. C., Seery, M. K., Falaras, P., Kontos, A. G., Dunlop, P. S. M., Hamilton, J. W. J., Byrne, J. A., O'Shea, K., Entezari, M. H., and Dionysiou, D. D. (2012). A review on the visible light active titanium dioxide photocatalysts for environmental applications. *Applied Catalysis B: Environmental*, *125*, 331–349. https://doi.org/10.1016/j.apcatb.2012.05.036

Petica, A., Florea, A., Gaidau, C., Balan, D., and Anicai, L. (2019). Synthesis and characterization of silver-titania nanocomposites prepared by electrochemical method with enhanced photocatalytic characteristics, antifungal and antimicrobial activity. *Journal of Materials Research and Technology*, *8*(1), 41–53. https://doi.org/10.1016/j.jmrt.2017.09.009

Pichel, N., Hymnô de Souza, F., Sabogal-Paz, L. P., Shah, P. K., Adhikari, N., Pandey, S., Shrestha, B. M., Gaihre, S., Pineda-Marulanda, D. A., Hincapie, M., Luwe, K., Kumwenda, S., Aguilar-Conde, J. C., Cortes, M. A. L. R. M., Hamilton, J. W. J., Byrne, J. A., and Fernandez-Ibañez, P. (2023). Field-testing solutions for drinking water quality monitoring in low- and middle-income regions and case studies from Latin American, African and Asian countries. *Journal of Environmental Chemical Engineering*, *11*(6). https://doi.org/10.1016/j.jece.2023.111180

Purnomo, F. O., Ningrum, S. S., and Kautsari, S. N. (2021). Synthesis and Characterization of Ag/TiO2 Nanoparticles using Mirabilis jalapa Plant Extract. *Jurnal Kimia Valensi*, *7*(1), 22–27. https://doi.org/10.15408/jkv.v7i1.18875

Rajoriya, P., Misra, P., Singh, V. K., Shukla, P. K., and Ramteke, P. W. (2017). Green Synthesis of Silver Nanoparticles. *Biotech Today : An International Journal of Biological Sciences*, *7*(1), 7. https://doi.org/10.5958/2322-0996.2017.00001.1

Ramasamy, P., Seo, D. M., Kim, S. H., and Kim, J. (2012). Effects of TiO_2 shells on optical and thermal properties of silver nanowires. *Journal of Materials Chemistry*, *22*(23), 11651–11657. https://doi.org/10.1039/c2jm00010e

Ramsden, J. J. (2013). The nanotechnology industry. *Nanotechnology Perceptions*, *9*(2), 102–118. https://doi.org/10.4024/N06RA13A.ntp.09.02

Ramteke, C., Chakrabarti, T., Sarangi, B. K., and Pandey, R. (2013). *Synthesis ofSilver Nanoparticles from the Aqueous Extract of Leaves of Ocimum sanctum for Enhanced Antibacterial Activity*. *2013*. https://doi.org/https://doi.org/10.1155/2013/278925

Rao, T. N., Riyazuddin, Babji, P., Ahmad, N., Khan, R. A., Hassan, I., Shahzad, S. A., and Husain, F. M. (2019). Green synthesis and structural classification of *Acacia nilotica* mediated-silver doped titanium oxide (Ag/TiO_2) spherical nanoparticles: Assessment of its antimicrobial and anticancer activity. *Saudi Journal of Biological Sciences*, *26*(7), 1385–1391. https://doi.org/10.1016/j.sjbs.2019.09.005

Rastogi, R. P. (2015). UV-Induced Oxidative Stress in Cyanobacteria: How Life is able to Survive? *Biochemistry & Analytical Biochemistry*, *04*(02). https://doi.org/10.4172/2161-1009.1000173

Rastogi, R. P., Richa, Kumar, A., Tyagi, M. B., and Sinha, R. P. (2010). Molecular mechanisms of ultraviolet radiation-induced DNA damage and repair. *Journal of Nucleic Acids*, *2010*. https://doi.org/10.4061/2010/592980

Renuga Devi, T. S., and Gayathri, S. (2010). FTIR And FT-Raman spectral analysis of Paclitaxel drugs. *International Journal of Pharmaceutical Sciences Review and Research*, *2*(2), 106–110.

Robinson, J., Majiwa, H., and Howland, O. (2022). Understanding Household Water Hygiene in Resource-Limited Settings in Kenya. In *Hygiene and Health in Developing Countries - Recent Advances*. IntechOpen. https://doi.org/10.5772/intechopen.108231

Roy, A., Lingampalli, S. R., Nassar, I. M., and Rao, C. N. R. (2016). Effectiveness of NiO in replacing Pt in the photochemical generation of hydrogen by $(TiO_2)1-x(NiO)x/Cd0.8Zn0.2S$ heterostructures *Solid State Communications*, *243*, 1–6. https://doi.org/10.1016/j.ssc.2016.05.018

Sahaya, P., Kumar, M., Francis, A. P., and Devasena, T. (2014). Biosynthesized and Chemically Synthesized Titania Nanoparticles: Comparative Analysis of Antibacterial Activity. *Journal of Environmental Nanotechnology*, *3*(3), 73–81. https://doi.org/10.13074/jent.2014.09.143098

Saladra, D., and Kopernik, M. (2016). Qualitative and quantitative interpretation of SEM image using digital image processing. *Journal of Microscopy*, *264*(1), 102–124. https://doi.org/10.1111/jmi.12431

Sambaza, S., Maity, A., and Pillay, K. (2019). Enhanced degradation of BPA in water by PANI supported Ag/TiO_2 nanocomposite under UV and visible light. *Journal of Environmental Chemical Engineering*, *7*(1), 102880. https://doi.org/10.1016/j.jece.2019.102880

Šamec, D., Karalija, E., Šola, I., Vujčić Bok, V., and Salopek-Sondi, B. (2021). The role of polyphenols in abiotic stress response: The influence of molecular structure. *Plants*, *10*(1), 1–24. https://doi.org/10.3390/plants10010118

Samoili, S., Farinelli, G., Moreno-SanSegundo, J. Á., McGuigan, K. G., Marugán, J., Pulgarín, C., and Giannakis, S. (2022). Predicting the bactericidal efficacy of solar disinfection (SODIS): from kinetic modeling of in vitro tests towards the in silico forecast of *E. coli* inactivation. *Chemical Engineering Journal*, *427*(February 2021). https://doi.org/10.1016/j.cej.2021.130866

Satterthwaite, D. (2016). Missing the Millennium Development Goal targets for water and sanitation in urban areas. *Environment and Urbanization*, *28*(1), 99–118. https://doi.org/10.1177/0956247816628435

Seo, S. W., Kim, D., Szubin, R., and Palsson, B. O. (2015). Genome-wide Reconstruction of OxyR and SoxRS Transcriptional Regulatory Networks under Oxidative Stress in *Escherichia coli* K-12 MG1655. *Cell Reports*, *12*(8), 1289–1299. https://doi.org/10.1016/j.celrep.2015.07.043

Shan, A. Y., Ghazi, T. I. M., and Rashid, S. A. (2010). Immobilisation of titanium dioxide onto supporting materials in heterogeneous photocatalysis: A review. *Applied Catalysis A: General*, *389*(1–2), 1–8. https://doi.org/10.1016/j.apcata.2010.08.053

Shanavas, S., Priyadharsan, A., Karthikeyan, S., Dharmaboopathi, K., Ragavan, I., Vidya, C., Acevedo, R., and Anbarasana, P. M. (2019). Green synthesis of titanium dioxide nanoparticles using *Phyllanthus niruri* leaf extract and study on its structural, optical and morphological properties. *Materials Today: Proceedings*, *26*(xxxx), 3531–3534. https://doi.org/10.1016/j.matpr.2019.06.715

Sharma, N. (2021). Self-organization of silver nanoparticles with femtosecond laser in TiO_2 matrix : Applications to plasmonic colours , multiple hidden images and Colour To cite this version : HAL Id : tel-03117138 Self-organization of silver nanoparticles with femtosecond. https://www.researchgate.net/publication/348740166_Self-organization_of_silver_nanoparticles_with_femtosecond_laser_in_TiO2_matrix_Applications_to_plasmonic_colours_multiple_hidden_images_and_Colour_Image-Multiplexing

Sharon, M., Modi, F., and Sharon, M. (2016). Titania based nanocomposites as a photocatalyst: A review. *AIMS Materials Science*, *3*(3), 1236–1254. https://doi.org/10.3934/matersci.2016.3.1236

Siddiqi, K. S., Husen, A., and Rao, R. A. K. (2018). A review on biosynthesis of silver nanoparticles and their biocidal properties. *Journal of Nanobiotechnology*, *16*(1). https://doi.org/10.1186/s12951-018-0334-5

Simiyu, S. (2016). Determinants of usage of communal sanitation facilities in informal settlements of Kisumu, Kenya. *Environment and Urbanization*, *28*(1), 241–258. https://doi.org/10.1177/0956247815616732

Singh, A., and Kumar, S. (2021). Effect of Ag doping on phase-change and photocatalytic performance of rutile–anatase mixed-phase titanium dioxide (TiO_2) nanoparticles. *Applied Physics A: Materials Science and Processing*, *127*(11), 1–14. https://doi.org/10.1007/s00339-021-04993-w

Sintubin, L., Awoke, A. A., Wang, Y., Van Der Ha, D., and Verstraete, W. (2012). Enhanced disinfection efficiencies of solar irradiation by biogenic silver. *Annals of Microbiology*, *62*(1), 187–191. https://doi.org/10.1007/s13213-011-0245-2

Siwila, S., and Brink, I. C. (2019). Low cost drinking water treatment using nonwoven engineered and woven cloth fabrics. *Journal of Water and Health*, *17*(1), 98–112. https://doi.org/10.2166/wh.2018.226

Skoog, D. A., Holler, J. F., and Crouch, S. R. (2018). An Introduction to Chromatographic Separations. In *Principles of Instrumental Analysis*. https://www.google.com/url?sa=t&rct=j&q=&esrc=s&source=web&cd=&cad=rja&uact=8&ved=2ahUKEwiBy-qB08aCAxUUUaQEHSwaBN8QFnoECA4QAQ&url=https%3A%2F%2Fimg1.wsimg.com%2Fblobby%2Fgo%2Feda849b5-0706-4fa4-8bc1-c28aaff08b58%2FPrinciples%2520of%2520Instrumental%2520An

Slavik, I., Oliveira, K. R., Cheung, P. B., and Uhl, W. (2020). Water quality aspects related to domestic drinking water storage tanks and consideration in current standards and guidelines throughout the world - A review. *Journal of Water and Health*, *18*(4), 439–463. https://doi.org/10.2166/wh.2020.052

Sorescu, A.-A., Nuţă, A., Ion, R.-M., and Ioana-Raluca, Ş.-B. (2016). *Green synthesis of silver nanoparticles using plant extracts*. *June*, 188–193. https://doi.org/10.18638/scieconf.2016.4.1.386

Stavinskaya, O., Laguta, I., Fesenko, T., and Krumova, M. (2019). Effect of temperature on green synthesis of silver nanoparticles using vitex agnus-castus extract. *Chemistry Journal of Moldova*, *14*(2), 117–121. https://doi.org/10.19261/cjm.2019.636

Strauss, A., Dobrowsky, P. H., Ndlovu, T., Reyneke, B., and Khan, W. (2016). Comparative analysis of solar pasteurization versus solar disinfection for the treatment of harvested rainwater. *BMC Microbiology*, *16*(1), 1–16. https://doi.org/10.1186/s12866-016-0909-y

Subagio, D. P., Srinivasan, M., Lim, M., and Lim, T. T. (2010). Photocatalytic degradation of bisphenol-A by nitrogen-doped TiO_2 hollow sphere in a vis-LED photoreactor. *Applied Catalysis B: Environmental*, *95*(3–4), 414–422. https://doi.org/10.1016/j.apcatb.2010.01.021

Tahir, M. N., Tremel, W., Al-warthan, A., Rafiq, M., Khan, M. M., Khan, M. M., Adil, S. F., Tahir, M. N., Tremel, W., Alkhathlan, H. Z., Al-warthan, A., and Siddiqui, M. R. H. (2013). Green synthesis of silver nanoparticles mediated by *Pulicaria glutinosa* extract. *International Journal of Nanomedicine*, *8*, 1507–1516. https://doi.org/10.2147/IJN.S43309

Tambi, A., Brighu, U., and Gupta, A. B. (2023). Methods for detection and enumeration of coliforms in drinking water: a review. *Water Supply*, *23*(10), 4047–4058. https://doi.org/10.2166/ws.2023.247

Tippayawat, P., Phromviyo, N., Boueroy, P., and Chompoosor, A. (2016). Green synthesis of silver nanoparticles in aloe vera plant extract prepared by a hydrothermal method and their synergistic antibacterial activity. *PeerJ*, *4*, e2589. https://doi.org/10.7717/peerj.2589

Tobaldi, D. M., Lajaunie, L., Seabra, M. P., and Arenal, R. (2020). TiO_2 surface hybridisation with noble metals (Ag and Cu x O) for solar de-NO x and VOC removal. *1*(x), 1–26. https://doi.org/https://doi.org/10.26434/chemrxiv.12198309.v1

UN-HABITAT. (2018). Adequate Housing and Slum Adequate Housing and Slum. 1–31. https://www.google.com/url?sa=t&source=web&rct=j&opi=89978449&url=https://unhabitat.org/sites/default/files/2020/06/indicator_11.1.1_training_module_adequate_housing_and_slum_upgrading.pdf&ved=2ahUKEwjRrrrl3bCJAxV_hv0HHV9XELUQFnoECBcQAQ&usg=AOvVaw2oo7F1-VqXNW2IB5mO0bm-

UNICEF & WHO. (2020). State of the World's Sanitation: An urgent call to transform sanitation for better health, environments, economies and societies. https://www.google.com/url?sa=t&rct=j&q=&esrc=s&source=web&cd=&cad=rja&uact=8&ved=2ahUKEwji0dXD1MaCAxVxU6QEHVGSD8kQFnoECAgQAQ&url=https%3A%2F%2Fwww.unicef.org%2Freports%2Fstate-worlds-sanitation-2020&usg=AOvVaw29eW1taGR1A61kIwl64GoS&opi=89978449

Venis, R. A. (2023). Behavior Change in Water, Sanitation, and Hygiene: A 100-Year Perspective. *International Studies Perspectives*, *24*(2), 169–188. https://doi.org/10.1093/isp/ekac016

Veronovski, N. (2018). TiO_2 Applications as a Function of Controlled Surface Treatment. *Titanium Dioxide - Material for a Sustainable Environment*. https://doi.org/10.5772/intechopen.72945

Vidhu, V. K., Aromal, S. A., and Philip, D. (2011). Green synthesis of silver nanoparticles using Macrotyloma uniflorum. *Spectrochimica Acta - Part A: Molecular and Biomolecular Spectroscopy*. https://doi.org/10.1016/j.saa.2011.08.051

Vijayaram, S., Razafindralambo, H., Sun, Y. Z., Vasantharaj, S., Ghafarifarsani, H., Hoseinifar, S. H., and Raeeszadeh, M. (2024). Applications of Green Synthesized Metal Nanoparticles — a Review. *Biological Trace Element Research*, *202*(1), 360–386. https://doi.org/10.1007/s12011-023-03645-9

Vrooman, I. (2016). A method for coating glass beads with TiO_2 and comparison of photocatalytic effectiveness for contaminant degradation A Major Qualifying Project Report. https://www.google.com/url?sa=t&rct=j&q=&esrc=s&source=web&cd=&ved=2ahUKEwiZn6P51MaCAxW-U6QEHSWAD_YQFnoECAoQAQ&url=https%3A%2F%2Fdigital.wpi.edu%2Fdownloads%2Fjs956h22x%3Flocale%3Den&usg=AOvVaw0XBzxBEo1LhOv8jbjAQpHJ&opi=89978449

Wang, Y., Jin, Y., Huang, Q., Zhu, L., Vivar, M., Qin, L., Sun, Y., Cui, Y., and Cui, L. (2016). Photovoltaic and disinfection performance study of a hybrid photovoltaic-solar water disinfection system. *Energy*, *106*, 757–764. https://doi.org/10.1016/j.energy.2016.03.112

Wang, Y., Yu, K., Yin, H., Song, C., Zhang, Z., Li, S., Shi, H., Zhang, Q., Zhao, B., Zhang, Y., and Zhu, Z. (2013). Facile synthesis, enhanced field emission and photocatalytic activities of Cu_2O-TiO_2-ZnO ternary hetero-nanostructures. *Journal of Physics D: Applied Physics*, *46*(17). https://doi.org/10.1088/0022-3727/46/17/175303

Wei, T., Liang, G., Chen, X., Qi, J., Lin, Q., Zhang, Y., and Yao, H. (2017). A functional applied material on recognition of metal ion zinc based on the double azine compound. *Tetrahedron*, *73*(20), 2938–2942. https://doi.org/10.1016/j.tet.2017.04.001

WHO. (2018). Core questions and indicators for monitoring WASH in health care facilities in the Sustainable Development Goals. https://www.google.com/url?sa=t&source=web&rct=j&opi=89978449&url=https://www.who.int/publications/i/item/9789241514545&ved=2ahUKEwiD4vG-3rCJAxXWgv0HHaPRHaEQFnoECBIQAQ&usg=AOvVaw2jHSmEeiYookAvMKURbz-F

Xu, J., Wang, W., Sun, S., and Wang, L. (2012). Enhancing visible-light-induced photocatalytic activity by coupling with wide-band-gap semiconductor: A case study on Bi 2WO 6/TiO 2. *Applied Catalysis B: Environmental*, *111–112*, 126–132. https://doi.org/10.1016/j.apcatb.2011.09.025

Zhao, Z. J., Hwang, S. H., Jeon, S., Hwang, B., Jung, J. Y., Lee, J., Park, S. H., and Jeong, J. H. (2017). Three-dimensional plasmonic Ag/TiO_2 nanocomposite architectures on flexible substrates for visible-light photocatalytic activity. *Scientific Reports*, *7*(1), 1–11. https://doi.org/10.1038/s41598-017-09401-z

APPENDICES

Appendix I: Survey

BASELINE SURVEY ON HOUSEHOLD WATER SUPPLY, SANITATION, HYGIENE AND ECONOMICS AT OBUNGA SLUM IN KISUMU-KENYA

Background

This survey aims at collecting baseline information on household water supply, sanitation and associated issues from residents of Obunga in the city of Kisumu, Kenya. The survey will randomly be administered to obtain the needed information to aid in analysing the various study questions. Respondents of this survey must be willing and voluntary participants who are adequately informed (*either directly or by proxy*) of their rights to refuse to answer any question(s) related to this survey as well as the discretion to bail-out of the entire process at any stage of the survey administration. Information collected will be treated in observation of the confidentiality required of scientific research. Respondent data will be kept confidential at all cost except in cases where the researcher is legally obligated to report research outcome. The survey does not aim at offering any direct benefits and/ or compensation to the respondents, though the results of the study will form a basis of improvement of water supply, sanitation and hygiene standards to the residents of Obunga.

ID:	**Date:**
(DD/MM/YYYY): _ _ /_ _ / _ _ _ _	

SECTION A: BACKGROUND INFORMATION

1. Gender: Male ( ) Female ( )

2. Age in years _____

3. Family member taking questionnaire

   Dad ( ) Mom ( ) Child ( ) Other ( ) _____ (indicate)

4. How many family members live in the household? _____

   1-5 people ( ) 6-10 people ( ) 11-15 People ( ) More than 15 People ( )

5. Classify members of your household by age group

   a) Adults (*including respondent*) > 15 years of age_____

   b) Children 5-14 years of age_____

   c) Infants 0-4 years of age_____

6. Respondents' highest level of education.

   Primary School ( ) High School ( ) Degree ( ) Post-graduate ( ) Other ( )

SECTION B: DATA ON WATER SOURCE AND COLLECTION METHODS

1. What is the main source of drinking water for members of your household?

   a) Piped water into the house

   b) Piped water to yard/ plot

c) Public tap water

d) Protected well

e) Unprotected well

f) Rain water

g) Bottled water

h) Cart with jerrycans

i) Surface water (rivers, dams, lake, pond)

j) Other _____

2. What is the main source of water by your household for other purposes besides drinking?

a) Piped water into the house

b) Piped water to yard/ plot

c) Public tap water

d) Protected well

e) Unprotected well

f) Rain water

g) Bottled water

h) Cart with jerrycans

i) Surface water (rivers, dams, lake, pond)

j) Other _____

3. What is the specific time you collect water for household drinking?
    a) Morning hours (5am-1pm)
    b) Afternoon hours (1pm- 9pm)
    c) Evening hours (9pm-5am)
    d) No specific time
4. What is the distance between the water source and the point of household use?

    Record approximate distance in Kilometres _____
5. Who goes to the water source to collect water for household use?
    a) Adult man
    b) Adult Woman
    c) Male Child <15 yrs. of age
    d) Female child <15 yrs. of age
    e) Don't know
6. Who is responsible for the decisions on household water source and collection times?
    a) Adult man in household
    b) Adult woman in household
    c) Children
    d) House-help
    e) Other relative
    f) No specific person is responsible for this.

7. How do you store your water after collection?
    a) In Pails without lids
    b) In Pails with lids
    c) in Jerrycans with lids
    d) In jerrycans without lids
    e) In big drum containers
    f) Mixed storage method of pails and Jerrycans
    g) Mixed storage method of pails and drums
    h) Mixed storage method of Jerrycans and drums
    i) Other _____
8. To the best of your knowledge, have there been any interruptions/breakdowns in the supply of household drinking water in the past 6 months?

    Yes ( ) No ( ) *Proceed to Q9 if answer is YES*
9. If YES is the answer to Q8 above, for what duration (in days) was the interruption experienced?..... days

SECTION C: DATA ON TREATMENT METHODS USED AND MODE OF USE

1. Do you treat your water in any way after collection to make it safe for household use?
    a) Yes
    b) No
    c) Sometimes
    d) I don't know

2. What water-treatment method do you use for your household drinking water?
    a) Boiling
    b) Cloth filtration
    c) Use of filters (Ceramic, Biofilters, sand, composite)
    d) Solar disinfection
    e) Chlorination/bleach
    f) Sedimentation
    g) Other _____

3. At what stage do you treat your water after collection?
    a) At the collection point
    b) During initial storage
    c) Prior to use
    d) No specific time of treatment

SECTION D: DATA ON DISEASE INCIDENCES CONSEQUENT TO POOR WATER SANITATION

1. Has any member of your household suffered from any waterborne disease(s) in the last year?
    a) Yes
    b) No
    c) Not sure

2. If YES in Q1 above, how frequent are the episodes of disease?
    a) Less than 3 times in the year
    b) More than 3 times in the year
    c) Can't recall the count of episodes

3. What type of toilet facilities do members of your family use?
    a) Pit latrine with cover on the pit
    b) Pit latrine without cover on the pit
    c) Piped sewer system
    d) Bucket and water for flushing toilet
    e) No toilet, bush or open defecation

4. How would you rate the cleanliness and sanitation of the toilet facility that you use?
    a) Very clean
    b) Clean
    c) Fairly clean
    d) Dirty
    e) Very dirty
    f) Don't know

5. Do you share this toilet facility(ies) with other members of the household?

   Yes ( ) No ( )

6. How many people in the household use this toilet facility?_____

7. How is the children's faecal matter discarded in this household?
   a) Children use toilets/ latrines by themselves
   b) Faecal matter is rinsed into toilets and/ or latrines
   c) Faecal matter is rinsed into drains or ditches
   d) Faecal matter is thrown in the garbage
   e) Faecal matter is buried in the ground
   f) Faecal matter in the open
   g) There are no children in this household.

SECTION E: DATA ON ECONOMICS OF WATER ACCESS METHOD OF WATER DISINFECTION

1. What is your monthly cost of purchase (If any), of water for household consumption in KShs …….

2. What is your monthly cost of purchase (If any), of water for other uses besides household use purpose in KShs …….

3. What is the cost of the water treatment method that you use?.....

4. What is the average gross monthly income of your family in KShs?.....

5. On grounds of cost, would you consider going for a cheaper source of household water use?

Y ( ) N ( )

6. To the best of your knowledge, what is the most efficient water treatment method?_____

Appendix II: Research Approval from Graduate School

KENYATTA UNIVERSITY
GRADUATE SCHOOL

E-mail: dean-graduate@ku.ac.ke
Website: www.ku.ac.ke

P.O. Box 43844, 00100
NAIROBI, KENYA
Tel. 020-8704150

Internal Memo

FROM: Dean, Graduate School
DATE: 4th June, 2021

TO: Ms. Gathiru Marylyn Mugure
C/o Department of Chemistry
REF: 156/37610/2017

SUBJECT: APPROVAL OF RESEARCH PROPOSAL

This is to inform you that Graduate School Board, at its meeting on 2nd June, 2021, approved your Research Proposal for the M.Sc. Degree entitled, **"Green Synthesis and Application of Nanostructured Composites for Modification of Solar Disinfection of Water for Obunga Slums Residents, Kisumu."**

You may now proceed with your Data collection, subject to clearance with the Director General, National Commission for Science, Technology & Innovation.

As you embark on your data collection, please note that you will be required to submit to Graduate School completed Supervision Tracking Form and Progress Report Forms per semester. The forms are available at the University's Website under Graduate School webpage downloads.

Thank you.

EDWIN OBUNGU
FOR: DEAN, GRADUATE SCHOOL

CC. Chairman, Chemistry Department
Supervisors:

1. Dr. Eric Masika
C/o Department of Chemistry
Kenyatta University

2. Dr. Naumih Noah
Department of Pharmacy and Health Sciences
United States International University Africa
C/o Department of Chemistry
Kenyatta University

3. Dr. Emilly Obuya
Department of Chemistry and Biochemistry
Rusell Sage College
C/o Department of Chemistry
Kenyatta University

Appendix III: Research Authorization from Graduate School

KENYATTA UNIVERSITY
GRADUATE SCHOOL

E-mail: dean-graduate@ku.ac.ke
Website: www.ku.ac.ke

P.O. Box 43844, 00100
NAIROBI, KENYA
Tel. 020-8704150

Our Ref: I56/37610/2017

DATE: 4th June, 2021

Director General,
National Commission for Science, Technology
and Innovation
P.O. Box 30623-00100
NAIROBI

Dear Sir/Madam,

RE: RESEARCH AUTHORIZATION FOR MS. GATHIRU MARYLYN MUGURE – REG. NO. 156/37610/17

I write to introduce Ms. Gathiru Marylyn Mugure who is a Postgraduate Student of this University. She is registered for M.Sc. degree programme in the Department of Chemistry.

Ms. Gathiru intends to conduct research for a M.Sc. thesis Proposal entitled, "Green Synthesis and Application of Nanostructured Composites for Modification of Solar Disinfection of Water for Obunga Slums Residents, Kisumu."

Any assistance given will be highly appreciated.

Yours faithfully,

PROF. ELISHIBA KIMANI
DEAN, GRADUATE SCHOOL

Appendix IV: Research Permit from NACOSTI

REPUBLIC OF KENYA

NATIONAL COMMISSION FOR SCIENCE,TECHNOLOGY & INNOVATION

Ref No: **313577**

Date of Issue: **14/July/2023**

RESEARCH LICENSE

This is to Certify that Miss.. Marylyn Mugure Gathiru of Kenyatta University, has been licensed to conduct research as per the provision of the Science, Technology and Innovation Act, 2013 (Rev.2014) in Kisumu, Nairobi on the topic: Green synthesis and Application of Nanostructured Composites for modification of solar disinfection of water for Obunga slums residents, Kisumu for the period ending : 14/July/2024.

License No: **NACOSTI/P/23/27075**

313577

Applicant Identification Number

Director General
NATIONAL COMMISSION FOR SCIENCE,TECHNOLOGY & INNOVATION

Verification QR Code

NOTE: This is a computer generated License. To verify the authenticity of this document, Scan the QR Code using QR scanner application.

See overleaf for conditions

THE SCIENCE, TECHNOLOGY AND INNOVATION ACT, 2013 (Rev. 2014)

Legal Notice No. 108: The Science, Technology and Innovation (Research Licensing) Regulations, 2014

The National Commission for Science, Technology and Innovation, hereafter referred to as the Commission, was the established under the Science, Technology and Innovation Act 2013 (Revised 2014) herein after referred to as the Act. The objective of the Commission shall be to regulate and assure quality in the science, technology and innovation sector and advise the Government in matters related thereto.

CONDITIONS OF THE RESEARCH LICENSE

1. The License is granted subject to provisions of the Constitution of Kenya, the Science, Technology and Innovation Act, and other relevant laws, policies and regulations. Accordingly, the licensee shall adhere to such procedures, standards, code of ethics and guidelines as may be prescribed by regulations made under the Act, or prescribed by provisions of International treaties of which Kenya is a signatory to
2. The research and its related activities as well as outcomes shall be beneficial to the country and shall not in any way;
    i. Endanger national security
    ii. Adversely affect the lives of Kenyans
    iii. Be in contravention of Kenya's international obligations including Biological Weapons Convention (BWC), Comprehensive Nuclear-Test-Ban Treaty Organization (CTBTO), Chemical, Biological, Radiological and Nuclear (CBRN).
    iv. Result in exploitation of intellectual property rights of communities in Kenya
    v. Adversely affect the environment
    vi. Adversely affect the rights of communities
    vii. Endanger public safety and national cohesion
    viii. Plagiarize someone else's work
3. The License is valid for the proposed research, location and specified period.
4. The license any rights thereunder are non-transferable
5. The Commission reserves the right to cancel the research at any time during the research period if in the opinion of the Commission the research is not implemented in conformity with the provisions of the Act or any other written law.
6. The Licensee shall inform the relevant County Director of Education, County Commissioner and County Governor before commencement of the research.
7. Excavation, filming, movement, and collection of specimens are subject to further necessary clearance from relevant Government Agencies.
8. The License does not give authority to transfer research materials.
9. The Commission may monitor and evaluate the licensed research project for the purpose of assessing and evaluating compliance with the conditions of the License.
10. The Licensee shall submit one hard copy, and upload a soft copy of their final report (thesis) onto a platform designated by the Commission within one year of completion of the research.
11. The Commission reserves the right to modify the conditions of the License including cancellation without prior notice.
12. Research, findings and information regarding research systems shall be stored or disseminated, utilized or applied in such a manner as may be prescribed by the Commission from time to time.
13. The Licensee shall disclose to the Commission, the relevant Institutional Scientific and Ethical Review Committee, and the relevant national agencies any inventions and discoveries that are of National strategic importance.
14. The Commission shall have powers to acquire from any person the right in, or to, any scientific innovation, invention or patent of strategic importance to the country.
15. Relevant Institutional Scientific and Ethical Review Committee shall monitor and evaluate the research periodically, and make a report of its findings to the Commission for necessary action.

National Commission for Science, Technology and
Innovation(NACOSTI),
Off Waiyaki Way, Upper Kabete,
P. O. Box 30623 - 00100 Nairobi, KENYA
Telephone: 020 4007000, 0713788787, 0735404245
E-mail: dg@nacosti.go.ke
Website: www.nacosti.go.ke